SMART PITCH CONTROL STRATEGY FOR WIND GENERATION SYSTEM USING DOUBLY FED INDUCTION GENERATOR

BY

SYED AHMED RAZA

A Thesis Presented to the

DEANSHIP OF GRADUATE STUDIES

KING FAHD UNIVERSITY OF PETROLEUM & MINERALS

DHAHRAN, SAUDI ARABIA

In Partial Fulfillment of the
Requirements for the Degree of

MASTER OF SCIENCE

In

ELECTRICAL ENGINEERING

MAY, 2012

KING FAHD UNIVERSITY OF PETROLEUM & MINERALS
DHAHRAN 31261, SAUDI ARABIA

DEANSHIP OF GRADUATE STUDIES

This thesis, written by **SYED AHMED RAZA** under the direction of his thesis adviser and approved by his thesis committee, has been presented to and accepted by the Dean of Graduate Studies, in partial fulfillment of the requirements for the degree of **MASTER OF SCIENCE IN ELECTRICAL ENGINEERING**.

Thesis Committee

A. H. Rahim

Dr. A.H.M.A. Rahim
(Adviser)

Dr. Mohammad A. Abido
(Member)

Dr. Ibrahim M. ElAmin
(Member)

Dr. Ali A. Al-Shaikhi
(Department Chairman)

Dr. Salam A. Zummo
(Dean of Graduate Studies)

27/5/12

Date

Dedication

This thesis is dedicated to my father, who taught me one thing; to try and excel in your field. It is also dedicated to my mother, who prayed for my success even in the most challenging times.

ACKNOWLEDGMENTS

All praise and glory to Allah who has given me the strength and courage to complete this thesis as without His help I cannot even imagine that this would have been possible.

Firstly, I would like to thank KFUPM for providing the excellent research facilities at the university and encouraging students to take part in active research. I would like to acknowledge my thesis adviser Dr. A.H.M.A. Rahim for his constant guidance during the course of this thesis and the time he has spent in reviewing it. I would also like to thank him for not getting upset at me, when I used to take his guidance besides his office hours. His hospitable way of welcoming his students and kind and gentle way of explaining concepts will always be the things that I will cherish for the rest of my life. I am also deeply thankful to my committee members, Dr. M.A. Abido and Dr. Ibrahim Al-Ameen for their involvement in this thesis.

I am also sincerely grateful to my parents and brothers, who have been there for me when I was down and out. Their relentless support and encouragement will always be a shining light for me.

Here, I ,must mention my friends and colleagues at KFUPM and in Pakistan, for their moral support and motivation. I will never forget their support in the completion of this thesis.

TABLE OF CONTENTS

LIST OF FIGURES viii

LIST OF TABLES xiii

ABSTRACT (ENGLISH) xiv

ABSTRACT (ARABIC) xvii

CHAPTER 1 INTRODUCTION 1

1.1 Wind Generators 2

1.2 Controls for Wind Generators 3

1.3 Intelligent Controls 4

1.4 Problem Formation 5

1.5 Thesis Objectives 5

1.6 Thesis Organization 7

CHAPTER 2 LITERATURE REVIEW 9

2.1 Wind Turbine Basics 10

2.2 Wind Turbine Classifications 12

2.3 Operating Regions 14
2.4 Blade Pitch Control 16
2.4.1 Fuzzy Logic Controllers 17
2.4.2 Robust Controllers 19
2.4.3 Generalized Predictive Control 20
2.4.4 Neural Network Based Controllers 20
2.4.5 Adaptive Neural Networks 22
2.4.6 Adaptive Controllers 23
2.4.7 Non-Linear Controllers 24
2.4.8 Linear Controllers 25
2.5 Doubly Fed Induction Generator Based WECS 25

CHAPTER 3 SYSTEM MODELING 27

3.1 Induction Generator Model 27
3.2 Wind Turbine Aerodynamics 31
3.3 Drive Train Modeling 32
3.4 The Converter Model 33
3.5 Pitch Angle Control 35
3.6 Linearized Model 37
3.6.1 Generator model 37
3.6.2 Wind Turbine Aerodynamics 39
3.6.3 Drive Train Modeling 41
3.6.4 The Converter Model 42

3.6.5 Pitch Angle Control 42
3.6.6 Formation of closed loop system matrix 43
3.6.7 Initial Conditions 45

CHAPTER 4 THE SMART CONTROL ALGORITHMS 48

4.1 Differential Evolution 49
4.1.1 Overview 49
4.1.2 DE Algorithm 50
4.1.2.1 Initialization 50
4.1.2.2 Evaluation and finding the best solution 51
4.1.2.3 Mutation 52
4.1.2.4 Crossover 52
4.1.2.5 Selection 53
4.1.2.6 Stopping Criteria 53
4.1.3 Differential Evolution Applied to Pitch Control 54
4.2 Artificial Neural Network 57
4.2.1 Back Propagation Algorithm Applied to Pitch Control 57
4.3 Adaptive Neural Network 60
4.3.1 μ-LMS Algorithm 61

CHAPTER 5 TESTING THE SMART PITCH CONTROLLER 64

5.1 Generation of adaptive controller parameters 66
5.2 Eigenvalues of the closed loop system 70
5.3 Test Case I 71

5.4 Test Case II 78

5.5 Test Case III 84

5.6 Test Case IV 91

CHAPTER 6 CONCLUSION AND FUTURE WORK 98

6.1 Conclusion 98

6.2 Future Work 100

APPENDICES 101

NOMENCLATURE 130

BIBLIOGRAPHY 135

List of Publications 150

Vita 151

LIST OF FIGURES

2.1 Operating regions for a wind turbine 14

3.1 DFIG system configuration equipped with pitch controller 28

3.2 Mechanical Power for various pitch angles at wind speed of $12m/s$ 32

3.3 The shaft system representation with the use of two-mass model 33

3.4 Pitch control strategy using generator power 36

3.5 Pitch control strategy using rotor speed 36

3.6 Single line diagram of DFIG to find the initial conditions 45

4.1 Adaptive neural network based pitch controller 49

4.2 Crossover process 54

4.3 Flowchart of Differential Evolution 56

4.4 Flowchart of Neural Network to be employed for pitch controller 59

5.1 DFIG system configuration equipped with pitch controller 65

5.2 Cost function vs. no. of iterations for optimization at v=$12m/s$ 68

5.3 Convergence of K_P vs. no. of iterations for optimization at v=$12m/s$ . . . 68

5.4 Convergence of K_I vs. no. of iterations for optimization at v=$12m/s$ . . . 69

5.5 Test case wind speed 72

5.6 Mechanical Power for various pitch angles at wind speed of 12 m/s 73

5.7 Output power with a step change in wind speed from 12m/s to 11m/s at t=1sec (a) With adaptive neural network and (b) Nominal control scenario 73

5.8 Generator speed with a step change in wind speed from 12m/s to 11m/s at t=1sec (a) With adaptive neural network and (b) Nominal control scenario . 74

5.9 Change in slip with a step change in wind speed from 12m/s to 11m/s at t=1sec (a) With adaptive neural network and (b) Nominal control scenario . 74

5.10 Terminal voltage with a step change in wind speed from 12m/s to 11m/s at t=1sec (a) With adaptive neural network and (b) Nominal control scenario . 75

5.11 Response of stator current with a step change in wind speed from 12m/s to 11m/s at t=1sec (a) With adaptive neural network and (b) Nominal control scenario 75

5.12 Response of rotor current with a step change in wind speed from 12m/s to 11m/s at t=1sec (a) With adaptive neural network and (b) Nominal control scenario 76

5.13 DC link voltage with a step change in wind speed from 12m/s to 11m/s at t=1sec (a) With adaptive neural network and (b) Nominal control scenario 76

5.14 Variation of K_P with a step change in wind speed from 12m/s to 11m/s at t=1sec while K_P=1 for nominal control 77

5.15 Variation of K_I with a step change in wind speed from 12m/s to 11m/s at t=1sec while K_I=0 for nominal control 77

5.16 Test case wind speed 79

5.17 Output power with a step change in wind speed from 12m/s to 14m/s at t=1sec (a) With adaptive neural network and (b) Nominal control scenario 79

5.18 Generator speed with a step change in wind speed from 12m/s to 14m/s at t=1sec (a) With adaptive neural network and (b) Nominal control scenario . 80

5.19 Change in slip with a step change in wind speed from 12m/s to 14m/s at t=1sec (a) With adaptive neural network and (b) Nominal control scenario . 80

5.20 Terminal voltage with a step change in wind speed from 12m/s to 14m/s at t=1sec (a) With adaptive neural network and (b) Nominal control scenario 81

5.21 Response of stator current with a step change in wind speed from 12m/s to 14m/s at t=1sec (a) With adaptive neural network and (b) Nominal control scenario 81

5.22 Response of rotor current with a step change in wind speed from 12m/s to 14m/s at t=1sec (a) With adaptive neural network and (b) Nominal control scenario 82

5.23 DC link voltage with a step change in wind speed from 12m/s to 14m/s at t=1sec (a) With adaptive neural network and (b) Nominal control scenario 82

5.24 Variation of K_P with a step change in wind speed from 12m/s to 14m/s at t=1sec while K_P=1 for nominal control 83

5.25 Variation of K_I with a step change in wind speed from 12m/s to 14m/s at t=1sec while K_I=0 for nominal control 83

5.26 Test case wind speed 85

5.27 Output power with a sinusoidal change in wind speed at t=1sec (a) With adaptive neural network and (b) Nominal control scenario 86

5.28 Generator speed with a sinusoidal change in wind speed at t=1sec (a) With adaptive neural network and (b) Nominal control scenario 86

5.29 Change in slip with a sinusoidal change in wind speed at t=1sec (a) With adaptive neural network and (b) Nominal control scenario 87

5.30 Terminal voltage with a sinusoidal change in wind speed at t=1sec (a) With adaptive neural network and (b) Nominal control scenario 87

5.31 Response of stator current with a sinusoidal change in wind speed at t=1sec (a) With adaptive neural network and (b) Nominal control scenario 88

5.32 Response of rotor current with a sinusoidal change in wind speed at t=1sec (a) With adaptive neural network and (b) Nominal control scenario 88

5.33 DC link capacitor voltage with a sinusoidal change in wind speed at t=1sec (a) With adaptive neural network and (b) Nominal control scenario 89

5.34 Pitch angle variation with a sinusoidal change in wind speed at t=1sec while $\beta = 11^0$ in nominal control scenario 89

5.35 Variation of K_P with a sinusoidal change in wind speed at t=1sec while $K_P = 1$ in nominal control scenario 90

5.36 Variation of K_I with a sinusoidal change in wind speed at t=1sec while $K_I = 0$ in nominal control scenario 90

5.37 Scaled wind speeds as taken from KFUPM beach front 92

5.38 Mechanical power available from wind and the resultant electrical power from (a) With adaptive neural network and (b) Nominal control scenario . . 93

5.39 Generator speed with real wind data in (a) With adaptive neural network and (b) Nominal control scenario 93

5.40 Change in slip with real wind data in (a) With adaptive neural network and (b) Nominal control scenario 94

5.41 Variation in terminal voltage with real wind data (a) With adaptive neural network and (b) Nominal control scenario 94

5.42 Response of stator current with real wind data in (a) With adaptive neural and (b) Nominal control scenario network 95

5.43 Response of rotor current with real wind data in (a) With adaptive neural network and (b) Nominal control scenario 95

5.44 Response of rotor current with real wind data in (a) With adaptive neural network and (b) Nominal control scenario 96

5.45 Variation of pitch angle β while $\beta = 11^0$ in nominal control scenario 96

5.46 Variation of K_P while $K_P = 1$ in nominal control scenario 97

5.47 Variation of K_I while $K_I = 0$ in nominal control scenario 97

1 Single line diagram of DFIG to find the initial conditions 107

LIST OF TABLES

4.1 Adaptive Neural Network Algorithm for pitch control 63

5.1 System Data 66

5.2 Optimum controller parameters for 12 m/s wind speed 69

5.3 Eigenvalues of the system at $9m/s$ wind speed for the optimal PI controller compared with nominal control scenario 70

1 System Data 101

THESIS ABSTRACT

NAME: Syed Ahmed Raza

TITLE OF STUDY: **Smart Pitch Control Strategy for Wind Generation System using Doubly Fed Induction Generator**

MAJOR FIELD: Electrical Engineering

DATE OF DEGREE: May, 2012

A smart pitch control strategy for a variable speed doubly fed wind generation system is presented in this thesis. A complete dynamic model of DFIG system is developed. The model consists of the generator, wind turbine, aerodynamic and the converter system. The strategy proposed includes the use of adaptive neural network to generate optimized controller gains for pitch control. This involves the generation of controller parameters of pitch controller making use of differential evolution intelligent technique. Training of the back propagation neural network has been carried out for the development of an adaptive neural network. This tunes the weights of the network according to the system states in a variable wind speed environment. Four cases have been taken to test the pitch controller which includes step and sinusoidal changes in

wind speeds. The step change is composed of both step up and step down changes in wind speeds. The last case makes use of scaled wind data collected from the wind turbine installed at King Fahd University beach front. Simulation studies show that the differential evolution based adaptive neural network is capable of generating the appropriate control to deliver the maximum possible aerodynamic power available from wind to the generator in an efficient manner by minimizing the transients.

MASTER OF SCIENCE DEGREE

KING FAHD UNIVERSITY OF PETROLEUM AND MINERALS,

DHAHRAN

MAY 2012

خلاصة

الاسم: **سيد أحمد رضا**

عنوانالرسالة :استراتيجية التحكم الانحرافى الذكى لنظام مولدات الرياح باستخدام مولد الرياح مزدوج التغذية

التخصص :الهندسةالكهربائية

تاريخالتخرج :مايو 2012

فى هذه الرسلة تم تقديم استراتيجية طريقة الانحراف الذكى لنظام التحكم المتغير لمولد الرياح المزدوج التغذية. تم بناء النموذج الديناميكى المتكامل لمولد الرياح المزدوج التغذية. ويتكون النظام من المولد , توربينة الرياح , النظام الهوائى و نظام التحول. وتضمن الأستراتيجية المقترحة استخدام الشبكة العصبية المكيفة لأنتاج معاملات التحكم الأمثل للانحراف الذكى. ويتضمن هذاتوليد معاملات التحكم للمحكم الانحرافى باستخدام التقنية الذكية للتطور الفرقى. وتم تدريب الشبكة الذكية من النوع اعادة الانتشار وذلك لبناءالشبكة العصبية المكيفة. وهذا يؤدى الى ضبط اوزان الشبكة طبقا لمعاملات النظام فى نظام الرياح المتغير السرعة. تم اختبار النظام لأربع حالات مختلفة وهى التغير الدرجى والتغير الجيبى فى سرعة الرياح. وتم التغير الدرجى بزيادة سرعة الرياحوكذلكبتقليلها. اما الحالة الأخيرة فتم استخدام معلومات الرياح المجمعة من توربينة الرياح فى شاطىء جامعة الملك فهد.ودلت نتائج المحاكاة للدراسات على ان التطور الفرقى المبنى على الشبكة العصبية المكيفة قادر على توليد التحكم المناسب لنقل اقصى طاقة رياح ممكنة من التوربينة الى المولد بكفاءة عالية مع تقليل الظواهر العابرة.

درجة الماجستير في العلوم

جامعة الملك فهد للبترول والمعادن

مايو 2012

CHAPTER 1

INTRODUCTION

Over the last twenty years, renewable energy sources have attracted great attention due to the cost increase, limited reserves and adverse environmental impact of fossil fuels. In the meantime, technological advancements, cost reduction, and governmental incentives have made some renewable energy sources more competitive in the market. Among them, wind energy is one of the fastest growing renewable energy sources.

Besides environmental problems in other forms of electricity production, the world's oil reserves are also diminishing, and oil prices are soaring in the global market so the governments all around the world are being attracted by the concept of renewable energy and more so because of the Kyoto protocol bounding nations to green energy. The renewable energy reserves like wind and solar energy are increasingly becoming popular. Wind energy in itself encompasses various engineering fields and is rapidly developing into a multi-disciplinary area of research and experimentation [1].

According to the American Wind Energy Association, there was an annual increase of 29% in the installed capacity of Wind Energy Conversion Systems (WECS) from

2002-2007. This inexhaustible resource of energy has a bright future as a study reveals that if only 10% of raw wind potential could be utilized; the energy demand of the world could be met. At the end of year 2007, only in US the installed capacity had reached 17,000 MW [1] and by 2012, it has increased to about 48,900 MW. At present, the amount of electricity produced from wind energy in Western Denmark is so significant that it can alone meet the demand of the country [2]. With the bright prospects of wind energy some ambitious targets have already been laid for the year 2020. The European Union is targeting to achieve 20% renewable energy contribution by 2020 [3].

1.1 Wind Generators

Early wind farms were dependent on squirrel induction generators and so they were fixed speed wind turbines. This considerably reduces the overall efficiency of these wind turbines. These days emphasis are being laid on variable speed wind turbines (VSWT). Amongst the VSWT, the important ones are permanent magnet synchronous generators (PMSG) and doubly fed induction generators (DFIG). The variable speed turbine generators are connected to the grid through power electronic devices, which convert variable frequency power to DC and then invert it back to fixed frequency AC power suitable for the grid connections.

The PMSG has the capability of direct connection (direct-drive) to wind turbines, with no gearbox [4–13]. The advantages of the permanent magnet synchronous generator are their lifetime and maintenance. The rotor of these machines are either electri-

cally excited or make use of permanent magnet [10]. The PM and electrically-excited synchronous generators differ from the induction generator, in that the magnetization is provided by a permanent magnet pole system or a dc supply on the rotor, while the induction generator makes use of a self-excitation property. This allows the PM synchronous generators to work at higher power factors and efficiencies.

The DFIG equipped wind turbines are becoming popular. When compared with permanent magnet synchronous generators, the DFIG has several advantages in terms of control of reactive power and support grid voltage and the decoupled control of active and reactive power, efficiency, size, etc [14, 15]. Also the DFIGs come in larger sizes of up to 10 MW as compared to PMSGs, which has a maximum size of 2 MW at this time. Considering all the above, DFIGs are best suited for pitch controlled variable speed wind turbines.

1.2 Controls for Wind Generators

Wind turbines in general have two main controls. The mechanical control which includes the blade pitch control and the electrical control covers the control of the power converters and the load side control. The blade pitch angle control is a necessary part of variable speed wind turbines as by controlling the pitch angle, the aerodynamic power that flows through to the generator can be controlled [16]. By carefully controlling the pitch angle, maximum power delivered to the generator at a particular wind speed can be affected [17].

Wind speed is stochastic since it varies randomly throughout the day. Even in

the same wind farm not all the turbines connected in that farm may be getting the same wind speed all the time. This causes the generated power to fluctuate. Besides pitch control, there is also a need that the overall generator output has minimal fluctuations [18].

The mechanical and electrical controls that are employed in the system must provide stability to the system in case of disturbances. The disturbances can be either wind gusts on the mechanical side or changes in electrical variables on the generator side. The controls must be robust enough to cope with these disturbances.

This thesis relates to smart pitch control for variable speed wind turbines and for this purpose intelligent control techniques have been incorporated. With the use of such techniques, it is guaranteed that the controller parameters obtained are optimized by minimizing or maximizing a particular cost function.

1.3 Intelligent Controls

Intelligent control is envisioned as emulating the human abilities of learning, adapting, coping with large amount of data in order to effectively control complex processes. The uncertainity with wind speeds makes the use of intelligent control techniques justifiable in wind power systems. Control algorithms employing neural network learning technique have the ability to adapt to a variety of scenarios such as unexpected change of wind speeds [19, 20].

The training of neural networks are often carried out using some heuristic techniques like genetic algorithm, particle swarm optimization, differential evolution,

etc [21, 22]. These evolution based techniques that try to locate the optimum minima or maxima, depending upon the objective function, through systematic search procedure. Networks are taught to learn from the trained data and apply this learning to actual scenarios. The weighting functions are normally determined from a huge amount of data presented to the network. To apply the neural network to physical systems online, the effort should be directed towards adapting the weighting functions depending on the data presented to the network.

1.4 Problem Formation

Fixed pitch wind turbines are gradually becoming obsolete and variable pitch wind turbines are taking their place. The objective should be to extract maximum power from wind. At the same time the turbine should have higher efficiency to transfer maximum power to the grid. In such circumstances, pitch control of wind turbines becomes an important area of research. In this work, a variable speed DFIG system will be investigated for pitch control. Pitch controller parameters are to be found using an adaptive intelligent control for maximum power transfer from wind. The proposed work will involve the following steps,

1.5 Thesis Objectives

In summary, the objectives of the proposed work are:

1. Dynamic modeling of double fed induction generator (DFIG).

This includes forming the non-linear model, incorporating the converter circuitry and pitch controller. It also includes the mechanical power modeling, depending upon the wind speed, pitch angle and the tip speed ratio. The available mechanical power from wind will make use of highly non-linear expression of power coefficient C_p. The non-linear model including the wind model is then linearized around an operating point and eigenvalues are found to identify the dominant eigen poles of the system.

2. Data collection

   Incorporation of wind data from the wind generator at the KFUPM beach front. The research institute at KFUPM, keeps logs of wind speed data for the small 5kW wind turbine installed at the KFUPM beach.

3. Controller design

   The control design has to be performed in the following stages,

   - Use of PI controller in the pitch control system.
   - Use of back propagation neural network algorithm to determine the PI gains for the variable wind speed.
   - Obtain the test data for neural network through differential evolution technique
   - Implementation of an adaptive neural network for the pitch controller.

4. Testing

The controller performance has to be analyzed by applying various types changes in wind speeds to the system. The system states have to be plotted for each of these types of disturbances. The last case to be assessed is when the real wind data is applied as a wind gust to the system.

5. Evaluating the system performance

   The system performance with the proposed adaptive intelligent control has to be compared with a nominal control scenario and the enhanced damping provided by the controller has to be examined.

1.6 Thesis Organization

A comprehensive literature review is provided in chapter 2. It encompasses, basic ideas about wind turbines, operating regions and the various control schemes reported in the literature.

Chapter 3 involves the system modeling. A 12th order non-linear model of the DFIG system is developed, which includes models for the turbine, aerodynamics, induction generator, converters and the pitch controller. A linear model is derived for the control design.

Chapter 4 presents the proposed approach for developing a smart pitch control. An expert system is developed making use of differential evolution (DE) and adaptive neural network.

Chapter 5 presents the simulation results. Results are also included for the real system data collected.

Conclusion and future work is presented in chapter 6. This is followed by the various appendices of the thesis.

CHAPTER 2

LITERATURE REVIEW

Since 1990, there have been marked developments that have taken place in renewable energy field especially in the domain of the wind energy. Three major trends have dominated the development of grid connected wind turbines. They have been summarized below:

- Turbines have become larger - the average size of turbines sold in the market has increased substantially.
- The efficiency of turbine production has increased steadily.
- Generally, the amount of capital invested per kW has decreased.

It has been observed that the average size of the wind turbines has increased over the last 10-15 years. In 1990, the size of wind turbines was 200 kW which increased to 2 MW in 2007. The current size of wind turbines is about 5 MW [23].

The power production from the turbines is associated with the selected site of the turbine, the hub height and the efficiency of power production. It is observed that

by just increasing the height of the turbines, the power production can be increased. In recent years, wind speed evaluation at a site have significantly improved and thus site selection for new turbines has drastically improved [24]. With this rapid increase in wind power capacity in Germany and Denmark, the best wind sites in these countries have already been occupied and in order to erect new turbines, they have to be deployed in areas with a marginally lower average wind speed [1]. In Germany and Denmark, which are extensively involved in wind energy, are now replacing older smaller turbines with modern versions. Today, in Germany around 5% of electricity is already being provided by wind turbines, while in Denmark this figure is more than 30% [2]. However, in Germany, more power is being supplied by wind energy than by hydroelectric plants.

The electricity production efficiency, due to better equipment, which is measured as annual energy production per square meter of swept rotor area (kWh/m^2) at a specific site, has correspondingly improved significantly in recent years. With improved equipment efficiency, turbine siting and higher hub height, the overall production efficiency has increased by 2-3 per cent annually over the last 15 years [25].

2.1 Wind Turbine Basics

The conversion of kinetic energy from the wind for technical applications is effected by means of a variety of turbine types. Wind Turbines are basically of two types i.e. horizontal-axis wind turbines (HAWTs) and vertical axis wind turbines (VAWTs). Depending on the way in which energy is extracted from the wind, wide variations are

discernible between converters, on the fact whether these wind turbines use the drag developed at the surface of the moving parts or the lift exerted on the blades. The turbines are constructed so that they can utilize the force of lift [26]. Lift originates in the flow of air past the rotor blade, which causes an overpressure on the underside of the blade and an under pressure on the top. The tangential component of the lifting forces causes the rotor blade to rotate [16, 27].

In horizontal axis wind turbines, the orientation of the spin axis is parallel to the ground. The tower elevates the nacelle to provide sufficient space for the rotor blade rotation and to reach better wind conditions. The nacelle supports the rotor hub that holds the rotor blades and also houses the gear box, generator, and in some designs power converters. The industry standard ,HAWT, uses a three blade rotor positioned in front of the nacelle, which is known as upwind configuration [24]. In vertical axis wind turbines, the orientation of the spin axis is perpendicular to the ground. The turbine rotor uses curved vertically mounted airfoils. The generator and gear box are normally placed in the base of the turbine on the ground. The rotor blades of the VAWT have a variety of designs with different shapes and number of blades. The VAWT normally needs guide wires to keep the rotor shaft in a fixed position and minimize possible mechanical vibrations [1]

In essence the HAWTs have higher wind energy conversion efficiency, access to stronger wind due to high tower and possess power regulation by stall and pitch angle control at high wind speeds. But as compared to VAWTs, HAWTS have a higher installation cost mainly because of the construction of a stronger tower to

support heavy weight of the nacelle and longer cable from the top of the tower to the ground [2]. On the other hand, VAWTs have lower installation cost. Their operation is independent of wind direction and they are mainly suitable for rooftops. But these turbines are inferior to HAWTs because of lower wind energy conversions, higher torque fluctuations and prone to mechanical vibrations and limited options for power regulation at high wind speeds [28].

The visible components of a wind turbine are its tower, nacelle and the rotor. The nacelle holds the generator, which is connected to the rotor through a gear box. The inclusion of the gear box depends upon the type of generator being used. Switchgear and protection system is required for supplying the end user or power storage systems.

This has been observed earlier that permanent magnet synchronous generators (PMSGs) do not have to be installed with a gear box, while other generators including doubly fed induction generators (DFIGs) do have to be connected with a gear box. The function of the gear box is that it connects the low speed shaft of the rotor with the high speed shaft of the generator. The rotor of the wind turbine captures the kinetic energy of the wind, converts it into the kinetic energy of the rotor and finally into the kinetic energy of the generator [29].

2.2 Wind Turbine Classifications

Wind Turbines are further categorized into two types i.e. variable pitch or fixed pitch. The role of pitching is that it allows the movement of the blades of the wind turbines to move in the longitudinal axis, depending upon the control command. A fixed pitch

differs from variable pitch in the manner that its blades are already positioned in a certain direction and in such machines maximum power could be delivered at a certain wind speed which corresponds to that particular pitch. But since they are unable to change the aerodynamic torque, such machines are becoming less common. On the other hand variable pitched wind turbines may allow all or part of their blades to rotate along the pitch angle [30, 31].

There are further divisions of wind turbines. These can be variable speed or fixed speed. As the name suggests, fixed speed wind turbines rotate at almost a constant speed which is determined by the gear ratio, the grid frequency and the number of poles of the generator. The maximum conversion efficiency can be achieved only at a given wind speed, and the system efficiency degrades at other wind speeds [14]. The turbine is protected by aerodynamic control of blades from possible damage caused by high wind gusts. The fixed speed turbine generates highly fluctuating output power to the grid, causing disturbances to the power system. This type of turbine also requires a sturdy mechanical design to absorb high mechanical stresses [32].

On the other hand, variable speed wind turbines can achieve maximum energy conversion efficiency over a wide range of wind speeds. The turbine can continuously adjust its rotational speed according to the wind speed. In doing so, the tip speed ratio, which is the ratio of the blade tip speed to the wind speed, can be kept at an optimal value to achieve the maximum power conversion efficiency at different wind speeds [33].

To make the turbine speed adjustable, the wind turbine generator is normally

connected to the utility grid through a power converter system. The converter system enables the control of the speed of the generator that is mechanically coupled to the rotor blades of the wind turbine. The main advantages of the variable speed turbine include increased wind energy output, improved power quality, and reduced mechanical stresses [34]. The main drawbacks are the increased manufacturing cost and power losses due to the use of power converters. Nevertheless, the additional cost and power losses are compensated for by the higher energy production.

2.3 Operating Regions

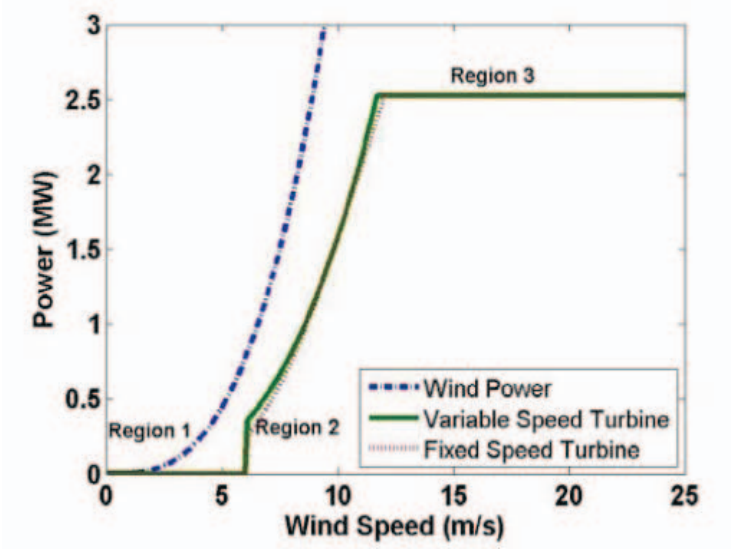

Figure 2.1: Operating regions for a wind turbine

The power characteristics of a wind turbine are defined by the power curve, which relates the mechanical power of the turbine to the wind speed. The three operating regions i.e. cut-in wind speed, rated wind speed and cut-out speed have been highlighted in [1]. The cut-in wind speed, as the name suggests, is the wind speed at which

the turbine starts to operate and deliver power. The blade should be able to capture enough power to compensate for the turbine power losses. The rated wind speed is the speed at which the system produces nominal power, which is also the rated output power of the generator. The cut-out wind speed gives us the highest wind speed at which the turbine is allowed to operate before it is shut down. For wind speeds above the cut-out speed, the turbine must be stopped, preventing damage from excessive wind [24].

As it can be seen from figure 2.1, the wind turbine starts to capture power at the cut-in speed. The power captured by the blades is a cubic function of the wind speed until the wind speed reaches its rated value. To deliver captured power to the grid at different wind speeds, the wind generator should be properly controlled with variable speed operation. As the wind speed increases beyond the rated speed, aerodynamic power control of the blades is required to keep the power at the rated value. This task is performed by stalling the blades.

For both the fixed speed and the variable speed wind turbines, when the speed is low i.e. below 6 m/s, the power available from the wind is very low and there are considerable losses. The 6 m/s speed of wind is sometimes known as the cut in speed for the turbine. The two types of turbines actually differ in operation in region 2 with wind speeds ranging from 6 m/s to 11.7 m/s. As is the case with the fixed speed wind turbines, which are designed for one operating speed in this region 2, the variable speed wind turbines captures more power than the former. The region 3 is the cut out speed for the turbines.

2.4 Blade Pitch Control

In order to control the aerodynamic torque of the wind turbine, the most widely used control methodology is the blade pitch control [35]. Rotating the blades about their longitudinal axes facilitates swift and active modification of the drive power to the rotor. The pitch mechanism can change the angle of attack of the blades with respect to the wind, by which aerodynamic characteristics of the blade can be adjusted [36]. This provides a degree of control over the captured power to improve conversion efficiency or to protect the turbine. When the wind speed is at or below its rated speed, the angle of attack of the blades is kept at an optimal value, at which the turbine can capture the maximum power available from the wind. When the wind speed exceeds the rated value, the blade angle is stalled i.e. the blades are completely pitched out of wind, to reduce the mechanical stresses on the tower [37].

The pitch mechanism is usually placed in the rotor hub together with a backup energy storage system for safety purposes. A pitch variation mechanism must apply the necessary moment to the blade. Adjusting the pitch of the rotor blades provides an effective means of regulating or limiting turbine performance in high wind speeds or storm conditions, or changing the speed of rotation. To put the blades into the necessary position, various mechanisms are employed. These may allow repositioning of the entire blade or just its tip [29].

In order to control the aerodynamic torque of the wind turbine, the most widely used control methodology is the blade pitch control. Conventional pitch control strategy has been described in [37]. This type of control strategy makes use of PI controller

for the pitch control. The system dynamics using the PI controller have been described in [26, 38–40]. In [37], a comparison has been made between the PI controller based pitch control with the system incorporating fuzzy logic based pitch control. Advantages and disadvantages of such type of controllers have been described in [41, 42]

2.4.1 Fuzzy Logic Controllers

Fuzzy logic based pitch control has been a popular technique in literature. In [43], this technique was used to find out the parameters of the PI controller for the pitch control. The model was prepared in Simulink and the results were compared with the conventional PI controller. From the results it was clear that fuzzy logic based pitch controller's performance was more efficient than the conventional based PI controller. In [44] another method of employing fuzzy logic into pitch control but the paper describes a more thorough approach by taking into account the stochastic behavior of wind, air masses complex dynamics, the turbine and the generator's non-linear model. The result of this control system permits a smooth and stable operation to the turbine under the regions of operations. In contrast to the proposed work, it considers situations where the wind speed exceeds the rating of the wind turbine. In such cases, the wind turbine must be able to produce constant rated power by varying the pitch angle. For wind speeds below the rated wind speeds, the blade angle has been kept at 0 degrees, without catering for the safety limit of the wind turbines.

In [31] a self tuning fuzzy-PID controller has been proposed, whose PID parameters can be adjusted on-line. The controller designed does not require a precise mathe-

matical model of the plant. According to the authors, such a controller takes into account various disturbances and suppresses them. The generator taken into account in this paper was PMSG and also the simulations were performed in simulink. The results show that the control has a fast response to any disturbances that happen in the system.

The references quoted up till now employ fuzzy logic for the pitch control only but in [45] three fuzzy logic based controllers have been developed. One controller tracks the generator speed with the wind velocity to extract the maximum power, second controller is used for light load efficiency improvement while the third controller acts against wind gusts and sudden mechanical torque changes of the turbine. A full working algorithm of the system has been provided by the authors explaining each of the three fuzzy logic controllers and when each of these controllers are going to be activated. One of the advantages of this system is the way the second controller works. The generator flux programming control reduces the machine rotor flux to reduce the core loss and this increases the torque current. The overall system loss decreases and hence increases the total generator power. This search is continued until the system finds the maximum power point. One of the differences from the work that has been proposed and this paper is the type of generator that is being used. The generator being used in this paper is squirrel cage induction generator (SCIG) and includes control of the back to back connected converters. The 3 different fuzzy logic controllers added to the system in this work for pitch control adds to the complexity and cost.

A new technique of pitch control has been described in [46]. In this the authors have come up a new type of fuzzy logic based PI controller by placing it in the feed forward loop. According to the authors, this method is going to improve the performance of controller. The signal given to the controller in the feed forward path is the wind speed variation. From the results of the paper, it was observed that the system stabilized in less time and the interference capability of the system was enhanced. This works takes into account only a second order system, ignoring the stator and rotor dynamics. Also the wind speeds taken to test the system vary slightly about the mean speed of $12m/s$.

2.4.2 Robust Controllers

Several others methods have been proposed for pitch control of wind turbines. These include the use of robust control, gain-scheduling control and other non-linear controllers. Robust controllers for output power leveling of variable speed variable pitch wind turbine generator systems have been discussed in [16]. The controller developed in the text can be applicable in a wide wind speed range subjected to large parametric and non-parametric disturbances. This work takes into account ramp changes in wind speeds only and evaluates the performance of the robust controller for pitch control.

Other works of robust control include the use of less conservative robust control [36]. It has been observed previously also that the dynamics of the wind turbine system vary according to the wind speed and also the generator speed. Again they use the "bladed" software. The same technique has been proposed in [47] also. The main

concept of this method is that the control bandwidth is restricted by the magnitude of the multiplicative perturbations in the low frequency band, so the perturbations in the low frequency band should be re-represented as the feedback perturbations. The control performance was then evaluated using "bladed". Other robust controllers have been discussed in [48]. The use of "bladed" software in these works, make use of ready-to-use models for the system and applying the robust controller for pitch control.

2.4.3 Generalized Predictive Control

Some new techniques include the use of generalized predictive control (GPC). This has been recorded in [49–53]. The proposed method presents a control strategy based on the average wind speed and standard deviation of wind speed and the pitch angle control, using GPC in all operating regions for WTG. The standard deviation of wind speed is then corrected using fuzzy reasoning as found in [54]. These controllers apply fuzzy reasoning when there are only wind speed changes irrespective of how the system is reacting to the changes.

2.4.4 Neural Network Based Controllers

The pitch controller based on neural network alone has also been proposed in the literature. An adaptive neural network capable of self tuning during different operating conditions has been reported in [19]. The proposed controller consists of neural networks inverse and forward identifiers, used for modeling the dynamics of the system.

The neural controller is used to generate the command signal for the pitch. In [19] authors have used the different transfer functions for the transducer, actuator and the drive train and generator. According to [55], neural networks have the capability of dealing effectively with the process control systems. Initially the authors in [19] tried the system without the controller, only to find it unstable. Then with the neural network, they first trained the inverse system using offline techniques with a sufficiently large data set that can give details for the plant. After the inverse identification has been performed, then both the neuro- controller and the plant forward identifier are then trained online. As seen from the results, it takes a large number of iteration or epochs for the neural network backward identifier to completely recognize the system but the results show that power stability and torque gets stabilized within 5 seconds of the disturbance. Besides the power requirement, the pitch also changes to cope up with the disturbance in the wind speed.

By controlling the pitch using the neural network, another work using an improved elman neural network (IENN) based algorithm has been reported in [56]. This paper presents an improved elman neural network (IENN)-based algorithm for optimal wind-energy control with maximum power point tracking. In [56], an online training method known as IENN controller with back propagation has been designed with a modified optimization technique known as MPSO (modified particle swarm optimization) [57]. It has been noted that PSO has least computation, fast convergence and easy code and implementation [58]. Elman neural network (ENN) is a partial recurrent network model first proposed by Elman in 1990 [59]. But according to the author, ENN has

a disadvantage that it can only work well for single order dynamic systems, so the basic ENN was modified to work with higher order systems. In the implementation part, the reference speed of the rotor is obtained for each particular wind speeds. The control scheme proposed was compared with the PI controller as well as the fuzzy based algorithm and the average power is compared. The system was implemented on real time workshop (RTW). It was found that the best results of power tracking and efficiency comes from the proposed IENN method with MPSO. Later in [56], the IENN method was developed with other optimization techniques like simple PSO, GA, with simple IENN and with simple ENN. The number of iterations, the mean square error, CPU usage time and accuracy was compared for each of these methods. The best results were coming for IENN with MPSO.

The neural networks used for pitch control described in the literature, do not cater for the adaptively tuning the weights of the network as the system states change. This thesis investigates as to tune the controller parameters and the weights of the neural network with changes in wind speeds and system states.

2.4.5 Adaptive Neural Networks

In determining the best neural network for the system, a few optimization parameters are taken into account like the weights of the network, the learning parameter, the number of hidden layers, number of nodes and number of input variables. The weights of the neural network are trained using some prior knowledge using the offline data available. Other techniques involve making use of adaptive neural networks, where

the neural network is adapted as the system data changes online. Adaptive neural networks have been applied to a wide variety of engineering fields including the coordination of PSSs and FACTS devices in multi-machine power system [60]. The paper deals with a new procedure for online control coordination which leads to adaptive PSS and supplementary damping controllers of FACTS.

Besides this, adaptive neural networks have also been discussed in prediction model for energy consumption [61].In this paper, various methods have been described for updating weights including the use of sliding window. Other methods include the use of adaptive wavelet neural networks as discussed in [62]. Adaptive neural networks for non-linear systems by state and output feedback have been discussed in [63]. This makes use of time derivatives of the states that are available for feedback. By constructing a high gain observer to estimate the derivatives of the system output, an adaptive output feedback NN controller is proposed in the paper.

It is observed from the literature, that adaptive neural networks for pitch control have not been implemented for pitch control of wind turbines. This area as been investigated in this particular thesis.

2.4.6 Adaptive Controllers

Adaptive controllers have been observed in [64, 65]. Tuning methods of PID using Ziegler Nichols is also found in the literature [66]. In [64], the PID parameters are tuned using actor critic learning method which can solve the deficiency of realizing effective control for complex and time varying systems by conventional PID controllers.

Actor-critic learning is time delay method, the transfer functions of which are found in [67, 68], that has a separate memory structure to clearly represent the policy independent of the value function. The actor plays a role of policy and value function is used to the critic. The critic evaluates the action made by the actor. Learning is always on policy i.e. the critic must learn and evaluate whatever policy is currently supplied by the actor. The literature making use of these controllers, assume transfer functions for the wind turbine system, emphasizing more on the controller performance. The wind speed changes taken for the simulations are either ramp or step changes.

2.4.7 Non-Linear Controllers

Other types of pitch controllers observed in literature make use of non-linear controllers. Such non-linear controllers have been studied in [69, 70]. In the domain of non-linear controllers, is the prevailing approach of non-linear model predictive control (NMPC) with neural network covered in [71, 72]. This approach was applied in [73] for fixed pitch variable speed wind turbines. NMPC promises to be advanced control algorithms and it is applicable to systems where the system dynamics are much faster and which requires continuous real-time input. One of the drawbacks that has been reported of such algorithms is the enhanced computational time mainly because of the extensive mathematics involved.

2.4.8 Linear Controllers

The last type of controllers that has been studied is the linear quadratic controllers. This type of controller depends upon the linearization of the system around different operating points corresponding to the sub-systems of the multimodal base and a state feedback for the control commands. The objective function is developed which requires solving the ricatti equation to get the control for the system in order to get a solution of an LQR problem [74]. In [75–77], multi-model approach is used in the modeling making use of several linear models, all of them valid around an operating point. The equivalent instantaneous model is formed by the fusion of successful models. The choice of these models depends upon the wind speed. This approach promises the electrical power transmission with a high performance behaviour for all the state variables. The works quoted, all make use of a 4th order model for the system but these linear controllers guarantee that optimized controller parameters around one operating point.

2.5 Doubly Fed Induction Generator Based WECS

Different models have been used for DFIG modeling [78–80]. In most of the models in the literature simplified control loops are implemented. Decoupled P-Q model is usually implemented as far as the modeling of the DFIG is concerned. In offshore wind farms, HVDC is often used; therefore the corresponding controller design is essential for power system dynamics. The small-signal stability of the DFIG has been examined in papers, either for open-loop [81] or with control loops [82] without

considering pitch control. The impact of variable-speed wind turbines on power system oscillations has been treated in [83] with a constant power model for variable-speed wind turbines. Modeling with back to back PWM converters and their applications to variable speed wind-energy generation has been observed in [84]. Comparison between fixed speed and doubly fed induction wind turbines was studied in [14]. Some of the other control aspects of DFIG were seen in [85, 86]. In both of these articles, PI controllers were used in the control loop for controlling the rotor speed and reactive power. It is concluded that wind power tends to increase the damping of oscillations of a synchronous generator against a strong system and of inter-area oscillations, while the impact on intra-area oscillations is not significant.

Overall, DFIG is a complex machine, which requires a great deal of efficient control methodology for steady state as well as dynamic operation. With VSWTs becoming more popular, DFIGs are preferred over conventional induction generators.

CHAPTER 3

SYSTEM MODELING

The non-linear and linear modeling of the doubly fed induction generator including the pitch controller is developed in this chapter. The non-linear model consists of the induction generator model, drive train modeling, the wind turbine aerodynamics, the converter model and the pitch angle control. The linearized model is used for the optimization of the controller parameters in the subsequent chapters.

3.1 Induction Generator Model

A schematic diagram of the DFIG system connected to the power grid equipped with pitch controller is shown in figure 3.1. The induction generator is driven by a horizontal axis wind turbine through its gear boxes. The converters are located between the rotor terminals and the grid. The dynamic model of the system includes the wind turbine, pitch controller and the generator with its converters. The voltage

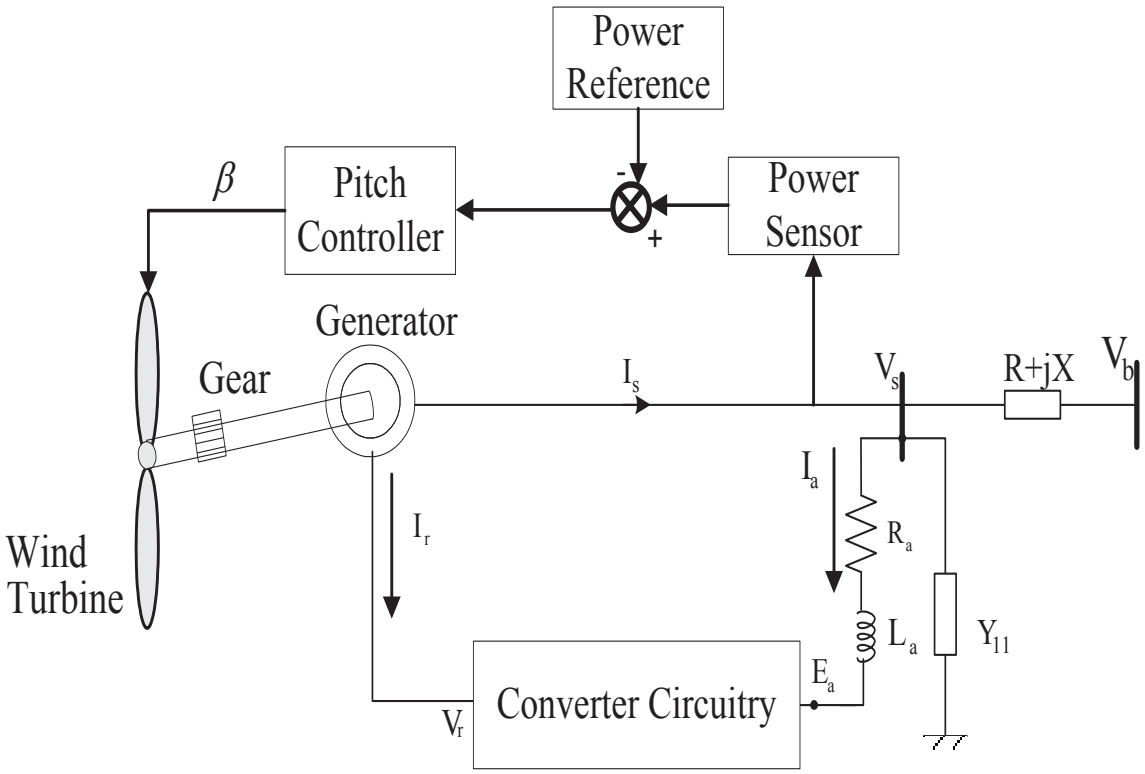

Figure 3.1: DFIG system configuration equipped with pitch controller

current relationships along the d-q axis, as derived in [87], are given by,

$$\begin{aligned} \frac{1}{\omega_0}\dot{\Psi}_{ds} - \frac{\omega_e}{\omega_0}\Psi_{qs} - R_s i_{ds} &= v_{ds} \\ \frac{1}{\omega_0}\dot{\Psi}_{qs} + \frac{\omega_e}{\omega_0}\Psi_{ds} - R_s i_{qs} &= v_{qs} \end{aligned} \tag{3.1}$$

$$\begin{aligned} \frac{1}{\omega_0}\dot{\Psi}_{dr} - s\Psi_{qr} - R_r i_{dr} &= v_{dr} \\ \frac{1}{\omega_0}\dot{\Psi}_{qr} + s\Psi_{dr} - R_s i_{qr} &= v_{qr} \end{aligned} \tag{3.2}$$

The above equations are in per unit (pu) system. Recognizing that in pu system the inductances and the reactances are the same, the stator and rotor flux linkages

and currents are expanded through the following set of equations,

$$\begin{aligned}\Psi_{ds} &= -x_s i_{ds} - x_m i_{dr} \\ \Psi_{qs} &= -x_s i_{qs} - x_m i_{qr}\end{aligned} \tag{3.3}$$

$$\begin{aligned}\Psi_{dr} &= -x_r i_{dr} - x_m i_{ds} \\ \Psi_{qr} &= -x_r i_{qr} - x_m i_{qs}\end{aligned} \tag{3.4}$$

By substituting set of eq.3.3 and 3.4 in 3.1 and 3.2, we have,

$$\begin{bmatrix} \dot{i}_{ds} \\ \dot{i}_{dr} \end{bmatrix} = \frac{1}{x_s x_r - {x_m}^2} \begin{bmatrix} -\omega_0 R_s x_r & \omega_0 \left(x_r x_s - s{x_m}^2\right) & \omega_0 R_r x_m & \omega_0 x_m x_r \left(1-s\right) \\ \omega_0 R_s x_m & \omega_0 x_s x_m \left(s-1\right) & -\omega_0 x_s R_r & \omega_0 \left(s x_r x_s - {x_m}^2\right) \end{bmatrix} \cdot \begin{bmatrix} i_{ds} \\ i_{qs} \\ i_{dr} \\ i_{qr} \end{bmatrix} + \frac{1}{x_s x_r - {x_m}^2} \begin{bmatrix} -\omega_0 x_r v_{ds} + \omega_0 x_m v_{dr} \\ \omega_0 x_m v_{ds} - \omega_0 x_s v_{dr} \end{bmatrix} \tag{3.5}$$

$$\begin{bmatrix} \dot{i}_{qs} \\ \dot{i}_{qr} \end{bmatrix} = \frac{1}{x_s x_r - {x_m}^2} \begin{bmatrix} \omega_0 \left(s{x_m}^2 - x_s x_r\right) & -\omega_0 R_s x_r & \omega_0 x_m x_r \left(s-1\right) & \omega_0 R_r x_m \\ \omega_0 x_s x_m \left(1-s\right) & \omega_0 x_m R_s & \omega_0 \left({x_m}^2 - s x_r x_s\right) & -\omega_0 R_r x_s \end{bmatrix} \cdot \begin{bmatrix} i_{ds} \\ i_{qs} \\ i_{dr} \\ i_{qr} \end{bmatrix} + \frac{1}{x_s x_r - {x_m}^2} \begin{bmatrix} -\omega_0 x_r v_{qs} + \omega_0 x_m v_{qr} \\ \omega_0 x_m v_{qs} - \omega_0 x_s v_{qr} \end{bmatrix} \tag{3.6}$$

By combining the state equations for the stator and rotor currents from eq.3.5 and 3.6, we can write them in matrix form as shown in eq.3.7

$$\begin{bmatrix} \dot{i_{ds}} \\ \dot{i_{qs}} \\ \dot{i_{dr}} \\ \dot{i_{qr}} \end{bmatrix} = \begin{bmatrix} a(1,1) & a(1,2) & a(1,3) & a(1,4) \\ a(2,1) & a(2,2) & a(2,3) & a(2,4) \\ a(3,1) & a(3,2) & a(3,3) & a(3,4) \\ a(4,1) & a(4,2) & a(4,3) & a(4,4) \end{bmatrix} \begin{bmatrix} i_{ds} \\ i_{qs} \\ i_{dr} \\ i_{qr} \end{bmatrix} + \begin{bmatrix} b(1,1) & 0 & b(1,3) & 0 \\ 0 & b(2,2) & 0 & b(2,4) \\ b(3,1) & 0 & b(3,3) & 0 \\ 0 & b(4,2) & 0 & b(4,4) \end{bmatrix} \begin{bmatrix} v_{ds} \\ v_{qs} \\ v_{dr} \\ v_{qr} \end{bmatrix} \quad (3.7)$$

Eq.3.7 gives the non-linear relationship of the stator and rotor currents. The matrix elements i.e. $(a(1,1)...a(4,4))$ and $(b(1,1)...b(4,4))$ are specified in Appendix A.

where the electrical power is given by,

$$P_e = \Psi_{qr} i_{dr} - \Psi_{dr} i_{qr} \quad (3.8)$$

and the slip of the machine is determined by,

$$s = \frac{\omega_s - \omega_r}{\omega_s} \quad (3.9)$$

3.2 Wind Turbine Aerodynamics

The amount of power extracted from wind is a function of the cube of wind speed as is represented by eq.3.10 ,

$$P_m = \frac{1}{2}\rho\pi R^2 V_w^3 C_p(\lambda, \beta) \tag{3.10}$$

Here, V_w is the wind velocity, R is the radius of the rotor blades and C_p is the power coefficient that is dependent upon the tip speed ratio λ and the pitch angle β.

The rotor mechanical power can be computed with the use of power coefficient curves. Such curves are given by the wind turbine manufacturer power as C_p characteristics, where C_p denotes the power coefficient and is a non-linear function of λ and β given by eq.3.11 [15],

$$\begin{aligned} C_p(\lambda, \beta) &= 0.5176\left[\frac{116}{\lambda_i} - 0.4\beta - 5\right] e^{\frac{-21}{\lambda_i}} + 0.0068\lambda \\ \frac{1}{\lambda_i} &= \frac{1}{\lambda + 0.08\beta} - \frac{0.035}{\beta^3 + 1} \end{aligned} \tag{3.11}$$

The tip speed ratio is related to wind speed through,

$$\lambda = \frac{\omega_t R}{V_w} \tag{3.12}$$

The variation of mechanical power with respect to the rotor speed for a particular wind speed for different values of pitch angle is given in figure 3.2.

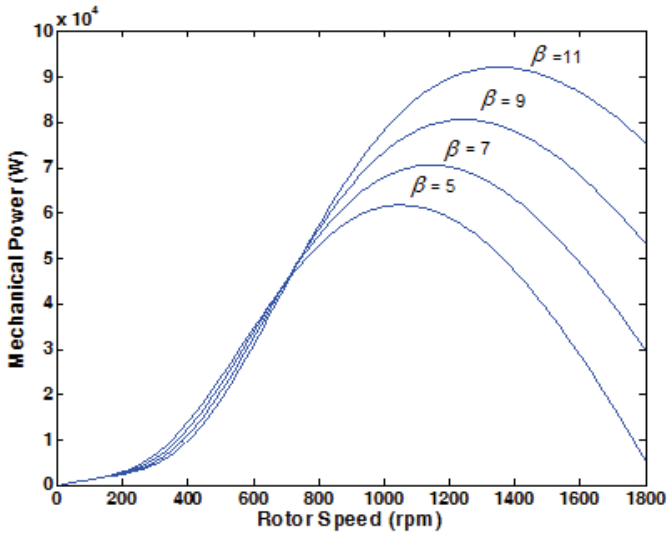

Figure 3.2: Mechanical Power for various pitch angles at wind speed of $12m/s$

3.3 Drive Train Modeling

A sketch of the shaft system is shown in figure 3.3. At the rotor end, the shaft system of the grid connected wind turbine is subject to mechanical torque T_M. At the generator end, the shaft system is subject to electrical torque, T_E, generated by the electromagnetic field of the generator. Therefore the shaft system will be subjected to torsion θ_s. At varying electrical torque T_E, the shaft twist θ_s will also vary. The shaft system will either twist more or relax according to the variations of the electrical torque T_E.

When the dynamic wind turbine model is applied in investigations of power system stability, the shaft system can be represented as a two mass model. In this model, rotor inertia is connected to the generator rotor inertia through the shaft system. The connection provided by the shaft is relatively soft. The state equations in drive train model include the turbine speed, w_t, the torsion twist angle, θ_s, and the generator

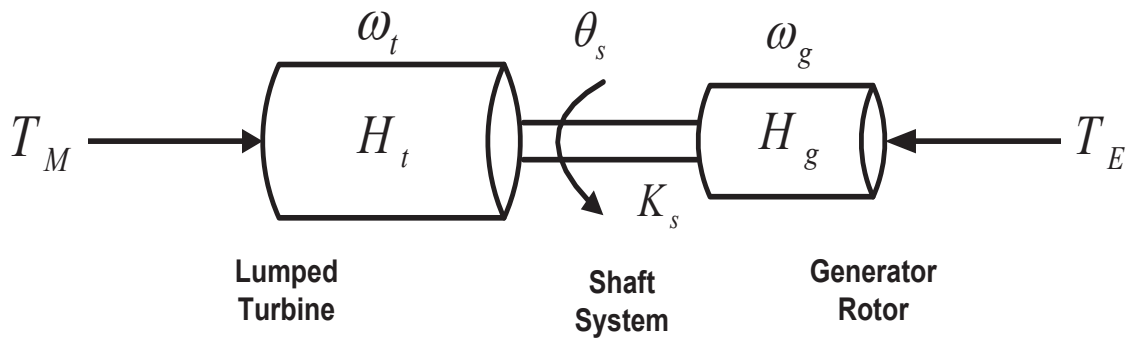

Figure 3.3: The shaft system representation with the use of two-mass model

rotor speed, w_g.

$$\dot{\omega}_t = \frac{P_m - K_s\theta_s}{2H_t} \tag{3.13}$$

$$\dot{\theta}_s = \omega_e\left(\omega_t - \omega_r\right) \tag{3.14}$$

$$\Delta\dot{s} = \frac{K_s\theta_s - P_e}{2H_g} \tag{3.15}$$

3.4 The Converter Model

Two back-to-back converters, one at the grid side and the other at the rotor side are connected through a common DC link. From Fig.1, R_a and L_a are the resistor and inductor per phase of the grid side converter. The state equations for the converter currents can then be written as,

$$\frac{d}{dt}\begin{bmatrix} i_{da} \\ i_{qa} \end{bmatrix} = \frac{\omega_0}{L_a}\begin{bmatrix} -R_a & X_a \\ -X_a & R_a \end{bmatrix} + \frac{\omega_0}{L_a}\begin{bmatrix} v_{ds} - E_{qa} \\ v_{qs} - E_{qa} \end{bmatrix} \tag{3.16}$$

Here, $I_a = i_{da} + ji_{qa}$, $V_s = v_{ds} + jv_{qs}$, and $E_a = E_{da} + jE_{qa}$, $\omega_0 = \omega_s$ is the base

frequency. The AC voltages are linked to capacitor voltage by,

$$E_{da} = m_1 V_c \cos \alpha_1$$
$$E_{qa} = m_1 V_c \sin \alpha_1 \tag{3.17}$$

where, α_1 is the phase angle of E_a while m_1 is the modulation index. Similarly for the rotor side we have $V_r = v_{dr} + jv_{qr}$ and its relationship to DC link capacitor voltage is given by,

$$v_{dr} = m_2 V_c \cos \alpha_2$$
$$v_{qr} = m_2 V_c \sin \alpha_2 \tag{3.18}$$

Where, α_2 is the phase angle of V_r, while m_2 is the modulation index. The AC power relationships at the two ends of the converters are given by,

$$P_{AC1} = E_{da} i_{da} + E_{qa} i_{qa}$$
$$P_{AC2} = v_{dr} i_{da} + v_{qr} i_{qr} \tag{3.19}$$

The DC power through the capacitor is given by,

$$P_{DC} = V_c C \frac{dV_c}{dt} \tag{3.20}$$

The converters are considered to be lossless and hence the total power has the

relationship,

$$P_{DC} = P_{AC1} + P_{AC2} \tag{3.21}$$

Using the set (8)-(11) and substituting in (12) gives the state equation for the DC link capacitor voltage,

$$\frac{dV_c}{dt} = \frac{1}{C}[m_1 \cos\alpha_1 i_{da} + m_1 \sin\alpha_1 i_{qa} + m_2 \cos\alpha_2 i_{dr} + m_2 \sin\alpha_2 i_{qr}] \tag{3.22}$$

3.5 Pitch Angle Control

As can be observed from figure 3.2, control of pitch angle β provides an effective means for controlling the power input to the generator under varying wind speeds. The dynamic blade angle control can be organized in a generic way and, in the case of the pitch control as shown in figures 3.4 and 3.5. In these two types of control systems, the blade angle β, is controlled by,

- An electrical value. For instance, the active power, P_g.
- A mechanical value. For instance, the generator rotor speed, ${\omega_m}^{ref}$.

To put the blades into the necessary position, pitch servos are employed, which may be hydraulic or electrical systems. Conventional pitch angle control use PI controllers to generate the appropriate β. The pitch servo system compares the measured angle of β to the reference and corrects the error. Usually a first order servo model is sufficient in investigations of power system stability. However, more detailed pitch servo models may be used also.

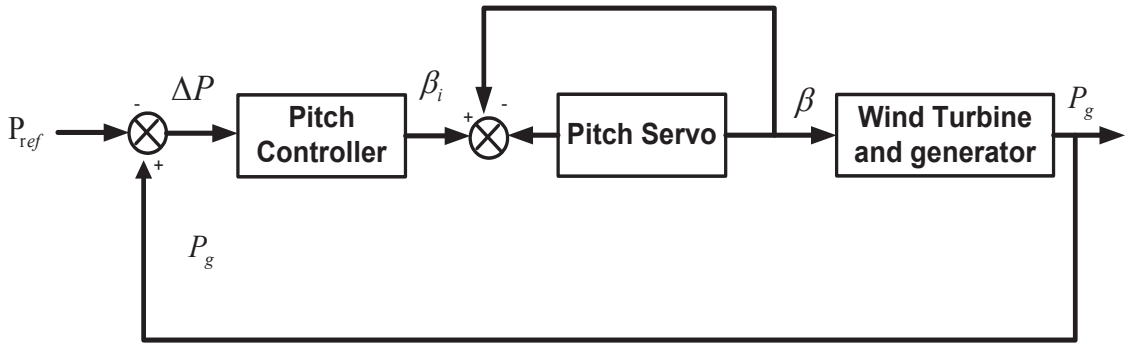

Figure 3.4: Pitch control strategy using generator power

In order to get more realistic response of the generic, regular pitch control a number of delay mechanisms must be implemented in control system models. Such delays represent sampling and filters, damping natural frequencies in wind turbine construction.

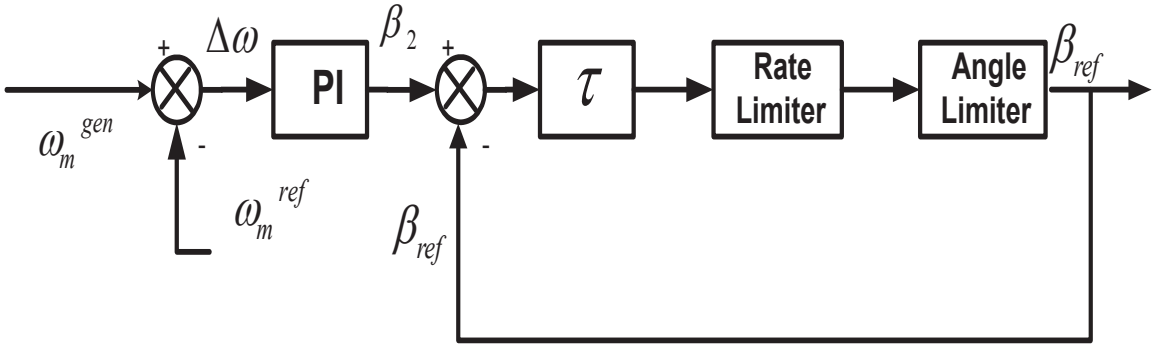

Figure 3.5: Pitch control strategy using rotor speed

Figure 3.4 shows a popular method of employing the pitch control which makes use of the generator power as a feedback signal compared with the reference mechanical power available from wind. This method has been incorporated as the pitch control strategy in this thesis. Here P_g represented the electrical power output from the system. The controller equations can be derived as,

$$\dot{\beta}_i = K_I \left(P_e - P_{e,ref} \right) \tag{3.23}$$

where β_i is an intermediate state because of the integral gain and $P_{e,ref}$ is the reference mechanical power obtained from figure 3.2 and K_I is the integral gain.

and

$$\dot{\beta} = K_a \left(K_P \left(P_e - P_{e,ref} \right) + \beta_i \right) - K_a \beta_i \tag{3.24}$$

where K_a represents the pitch servo gain and K_P is the proportional gain

Combine the equations (3.7), (3.13-3.15), (3.16), (3.22), (3.23-3.24) to get the complete system dynamic model,

$$\dot{x} = f\left[x, u\right] \tag{3.25}$$

where $x = [i_{ds}, i_{qs}, i_{dr}, i_{qr}, \omega_t, \theta_s, \omega_r, i_{da}, i_{qa}, V_c, \beta_i]$ and control $u = \beta$.

3.6 Linearized Model

From the non-linear model given in sections 3.1-3.5, the linearized equations are obtained for a specific operating point. The individual models are combined to a give a composite system.

3.6.1 Generator model

The stator d-axis current as found from eq. 3.7 is,

$$\dot{i_{ds}} = a(1,1) i_{ds} + a(1,2) i_{qs} + a(1,3) i_{dr} + a(1,4) i_{qr} + b(1,1) v_{ds} + b(1,3) v_{dr} \tag{3.26}$$

Linearizing this equation gives us,

$$\begin{aligned}\Delta\dot{i}_{ds} = \frac{1}{x_s x_r - {x_m}^2}\Big\{ & \left(-\omega R_s x_r\right)\Delta i_{ds} + \left(\omega x_s x_r - \omega s_0 {x_m}^2\right)\Delta i_{qs} \\ & - \left({x_m}^2 \omega i_{qs0} - \omega x_r x_m i_{qr0}\right)\Delta\omega_g + \left(\omega x_r x_m - \omega x_r x_m s_0\right)\Delta i_{qr} \\ & + \left(\omega x_r\right) z_{11}\Delta i_{ad} + \left(\omega x_r\right) z_{12}\Delta i_{aq} + \left(\omega x_m\right)\left(m_2 \cos\alpha_2\right)\Delta V_c \\ & + \left(\omega x_r\right) z_{11}\Delta i_{dg} + \left(\omega x_r\right) z_{12}\Delta i_{qg}\Big\}\end{aligned} \tag{3.27}$$

Similarly, the non-linear q-axis stator current as given in eq. was found out to be,

$$\dot{i_{qs}} = a(2,1)i_{ds} + a(2,2)i_{qs} + a(2,3)i_{dr} + a(2,4)i_{qr} + b(2,2)v_{qs} + b(2,4)v_{qr} \tag{3.28}$$

Linearizing eq.3.28,

$$\begin{aligned}\Delta\dot{i}_{qs} = \frac{1}{x_s x_r - {x_m}^2}\Big\{ & \omega\left(s_0 {x_m}^2 - x_r x_s\right)\Delta i_{ds} - \left(\omega R_s x_r\right)\Delta i_{qs} \\ & + \left(\omega {x_m}^2 i_{ds0} + \omega x_r x_m i_{dr0}\right)\Delta\omega_g + \left(\omega x_r x_m\left(s_0 - 1\right)\right)\Delta i_{dr} \\ & + \left(\omega R_r x_m\right)\Delta i_{qr} - \left(\omega x_r\right) z_{21}\Delta i_{ds} - \left(\omega x_r\right) z_{22}\Delta i_{qs} \\ & + \left(\omega x_r\right) z_{21}\Delta i_{ad} + \left(\omega x_r\right) z_{22}\Delta i_{aq} + \left(\omega x_m\right)\left(m_2 \sin\alpha_2\right)\Delta V_c\Big\}\end{aligned} \tag{3.29}$$

The rotor d-axis current is given by,

$$\dot{i_{dr}} = a(3,1)i_{ds} + a(3,2)i_{qs} + a(3,3)i_{dr} + a(3,4)i_{qr} + b(3,1)v_{ds} + b(3,3)v_{dr} \tag{3.30}$$

By linearizing eq.3.30,

$$\begin{aligned}\Delta\dot{i}_{dr} = \frac{1}{x_s x_r - {x_m}^2}\Big\{ & \left(\omega R_s x_m\right)\Delta i_{ds} + \left(\omega x_m x_s\left(s_0 - 1\right)\right)\Delta i_{qs} \\ & - \left(\omega R_r x_s\right)\Delta i_{dr} + \left(\omega\left(s_0 x_r x_s - {x_m}^2\right)\right)\Delta i_{qr} \\ & + \left(\omega x_m x_s i_{qs0} + \omega x_r x_s i_{qr0}\right)\Delta\omega_g + \left(\omega x_m\right) z_{11}\Delta i_{ds} \\ & + \left(\omega x_m\right) z_{12}\Delta i_{qs} + \left(\omega x_s\right) z_{11}\Delta i_{ad} + \left(\omega x_s\right) z_{12}\Delta i_{aq} \\ & - \left(\omega x_s m_2 \cos\alpha_2\right)\Delta V_c\Big\}\end{aligned} \tag{3.31}$$

The rotor q-axis current is given by,

$$\dot{i_{qr}} = a(4,1)i_{ds} + a(4,2)i_{qs} + a(4,3)i_{dr} + a(4,4)i_{qr} + b(4,2)v_{qs} + b(4,4)v_{qr} \tag{3.32}$$

By linearizing eq.3.32,

$$\begin{aligned}\Delta\dot{i}_{qr} = \frac{1}{X_s X_r - {X_m}^2}\Big\{ & \left(\omega X_s X_m\left(1 - s_0\right)\right)\Delta i_{ds} + \left(\omega R_s X_m\right)\Delta i_{qs} \\ & + \left(\omega\left({X_m}^2 - s_0 X_r X_s\right)\right)\Delta i_{dr} - \left(\omega R_r X_s\right)\Delta i_{qr} \\ & - \left(\omega X_s X_m i_{ds0} + \omega\left(X_r X_s\right) i_{dr0}\right)\Delta\omega_g - \left(\omega X_m\right) z_{21}\Delta i_{ad} \\ & - \left(\omega X_m\right) z_{22}\Delta i_{aq} - \left(\omega X_s m_2 \sin\alpha_2\right)\Delta V_c\Big\}\end{aligned} \tag{3.33}$$

3.6.2 Wind Turbine Aerodynamics

The mechanical power that was stated in eq.3.10 consists of the power coefficient expression which is highly non-linear and hence needs to be linearized. By substituting

the tip speed ratio expression, given in eq.3.12, in eq.3.11 we have,

$$C_p\left(\lambda,\beta\right)=0.5176\left[\frac{116}{\frac{\omega_t R}{V}+0.08\beta}-\frac{4.06}{\beta^3+1}\right]\mathrm{e}^{\left[-\frac{21}{\frac{\omega_t R}{V}+0.08\beta}+\frac{0.735}{\beta^3+1}\right]}+0.0068\frac{\omega_t R}{V} \quad (3.34)$$

Eq.3.34 now contains the terms ω_t and β. It is now possible to evaluate the partial derivatives of C_p with respect to these two terms.

Taking partial derivative first w.r.t. ω_t

$$\begin{aligned}\frac{\partial C_p\left(\lambda,\beta\right)}{\partial\omega_t}=0.5176\Bigg\{&\left[116\left(\frac{\omega_t R}{V}+0.08\beta\right)^{-1}-\frac{4.06}{\beta^3+1}\right]\\&\cdot\mathrm{e}^{\left[-21\left(\frac{\omega_t R}{V}+0.08\beta\right)^{-1}+0.735\left(\beta^3+1\right)^{-1}\right]}\cdot\left(\frac{21}{\frac{\omega_t R}{V}}\cdot\frac{R}{V}\right)\Bigg\}\\&+0.5176\Bigg\{\mathrm{e}^{\left[-21\left(\frac{\omega_t R}{V}+0.08\beta\right)^{-1}+0.735\left(\beta^3+1\right)^{-1}\right]}\cdot\\&-116\left(\left(\frac{\omega_t R}{V}+0.08\beta\right)^{-2}\cdot\frac{R}{V}\right)\Bigg\}\end{aligned} \quad (3.35)$$

Now w.r.t. β

$$\begin{aligned}\frac{\partial C_p\left(\lambda,\beta\right)}{\partial\beta}=0.5176\Bigg\{&\left[\frac{116}{\left(\frac{\omega_{t0}R}{V}+0.08\beta_0\right)}-\frac{0.035}{\left(\beta_0^3+1\right)}-0.4\beta_0-5\right]\cdot\\&\mathrm{e}^{-21\left[\left(\frac{\omega_{t0}R}{V}+0.08\beta_0\right)^{-1}-0.035\left(\beta_0^3+1\right)^{-1}\right]}\cdot\\&\left[1.68\left(\frac{\omega_{t0}R}{V}+0.08\beta_0\right)^{-2}-2.205\beta_0^2\left(\beta_0^3+1\right)^{-2}\right]\Bigg\}\\&+0.5176\left[\mathrm{e}^{-21\left(\frac{\omega_{t0}R}{V}+0.08\beta_0\right)^{-1}-0.035\left(\beta_0^3+1\right)^{-1}}\right]\cdot\\&166\left[\left(-0.08\left(\frac{\omega_{t0}R}{V}+0.08\beta_0\right)^{-2}+\frac{0.105\beta_0^2}{\left(\beta_0^3+1\right)^2}\right)-0.4\right]\end{aligned} \quad (3.36)$$

Finally, the mechanical power as found in eq.3.10 can be written in its linearized

as,

$$\begin{aligned}\Delta P_m =& \frac{\partial C_p\left(\lambda,\beta\right)}{\partial \omega_T}\Delta\omega_t + \frac{\partial C_p\left(\lambda,\beta\right)}{\partial \beta}\Delta\beta \\ =& \mathcal{K}_1\Delta\omega_t + \mathcal{K}_2\Delta\beta\end{aligned} \tag{3.37}$$

Where, $\mathcal{K}_1$ aand $\mathcal{K}_2$ are linearization constants.

3.6.3 Drive Train Modeling

After the linearization of mechanical power, available from wind, the set of equations 3.13-3.15 can now linearized by making use of eq.3.37.

The three states in the drive train modeling i.e. turbine speed, ω_t, torsional twist angle, θ_s, and generator speed, ω_g, is linearized as,

$$\Delta\dot{\omega}_t = \frac{1}{2H_t}\left(\mathcal{K}_1\Delta\omega_t + \mathcal{K}_2\Delta\beta - K_s\Delta\theta_s\right) \tag{3.38}$$

ω_g is linearized when P_e is substituted as,

$$P_e = x_m i_{ds} i_{qr} - x_m i_{qs} i_{dr} \tag{3.39}$$

$$\begin{aligned}\Delta\dot{\omega}_g =& \frac{1}{2H_g}\Big\{ K_s\Delta\theta_s - x_m i_{qr0}\Delta i_{ds} + x_m i_{dr0}\Delta i_{qs} \\ & - x_m i_{ds0}\Delta i_{qr} + x_m i_{qs0}\Delta i_{dr}\Big\}\end{aligned} \tag{3.40}$$

Finally, the linearized form θ_s can be written as,

$$\Delta\dot{\theta}_s = \omega_e\left(\Delta\omega_t - \Delta\omega_g\right) \tag{3.41}$$

3.6.4 The Converter Model

The converter currents as well as the DC link capacitor voltage equations found in the non-linear model are linearized at this stage.

Initially, the d-axis converter current is linearized as,

$$\begin{aligned}\Delta \dot{i_{ad}} =& \frac{\omega_e}{X_a} z_{11} \Delta i_{ds} + \frac{\omega_e}{X_a} z_{12} \Delta i_{qs} - \frac{\omega_e}{X_a} \left(R_a + z_{11}\right) \Delta i_{ad} \\ &+ \left(\omega_e - \frac{\omega_e}{X_a} z_{12}\right) \Delta i_{aq} - \frac{\omega_e}{X_a} m_1 \cos\alpha_1 \Delta V_c\end{aligned} \tag{3.42}$$

For the q-axis converter current we get,

$$\begin{aligned}\Delta \dot{i_{aq}} =& \frac{\omega_e}{X_a} z_{21} \Delta i_{ds} + \frac{\omega_e}{X_a} z_{22} \Delta i_{qs} - \frac{\omega_e}{X_a} \left(R_a + z_{22}\right) \Delta i_{aq} \\ &+ \left(-\omega_e - \frac{\omega_e}{X_a} z_{21}\right) \Delta i_{ad} - \frac{\omega_e}{X_a} m_1 \sin\alpha_1 \Delta V_c\end{aligned} \tag{3.43}$$

The DC link capacitor voltage found in eq.3.22 is linearized as,

$$\begin{aligned}\Delta \dot{V}_c =& \frac{1}{C} \Big[\left(m_1 \cos\alpha_1\right) \Delta i_{ad} + \left(m_1 \sin\alpha_1\right) \Delta i_{aq} + \left(m_2 \cos\alpha_2\right) \Delta i_{dr} \\ &+ \left(m_2 \sin\alpha_2\right) \Delta i_{qr} \Big]\end{aligned} \tag{3.44}$$

3.6.5 Pitch Angle Control

Finally, with the controller equations, as defined in the previous section, can now be linearized to complete the 12th order model for the system.

The intermediate integral gain state β_i can be linearized as shown in eq.3.45,

$$\Delta \dot{\beta}_i = K_I \Big[x_m i_{qr0} \Delta i_{ds} - x_m i_{dr0} \Delta i_{qs} - x_m i_{qs0} \Delta i_{dr} + x_m i_{ds0} \Delta i_{qr} \Big] \tag{3.45}$$

while the pitch angle, β, coming from the pitch servo transfer function is linearized as,

$$\begin{aligned}\Delta\dot{\beta} =& K_a K_P \left(x_m i_{qr0}\Delta i_{ds} - x_m i_{dr0}\Delta i_{qs} - x_m i_{qs0}\Delta i_{dr} + x_m i_{ds0}\Delta i_{qr}\right) \\ &+ K_a\Delta\beta_i - K_a\Delta\beta\end{aligned} \tag{3.46}$$

3.6.6 Formation of closed loop system matrix

Combining equations (3.27), (3.29), (3.31), (3.33), (3.38), (3.40), (3.41), (3.42), (3.43), (3.44), (3.45) and (3.46), the perturbed states found in the previous section are used to form the over all closed loop A_c matrix in the form,

$$\dot{Z} = A_c Z \tag{3.47}$$

The A_c matrix is given by eq.3.48. Where, Z will contain all the perturbed states. The constants in the A_c matrix i.e. $a_{(1,1)}...a_{(12,12)}$ are given in Appendix B.

$$
\begin{bmatrix}
\Delta\dot{i}_{ds} \\ \Delta\dot{i}_{qs} \\ \Delta\dot{i}_{dr} \\ \Delta\dot{i}_{qr} \\ \Delta\dot{\omega}_t \\ \Delta\dot{\omega}_g \\ \Delta\dot{\theta}_s \\ \Delta\dot{i}_{ad} \\ \Delta\dot{i}_{aq} \\ \Delta\dot{V}_c \\ \Delta\dot{\beta}_i \\ \Delta\dot{\beta}
\end{bmatrix}
=
\begin{bmatrix}
a_{(1,1)} & a_{(1,2)} & a_{(1,3)} & a_{(1,4)} & 0 & a_{(1,6)} & 0 & a_{(1,8)} & a_{(1,9)} & a_{(1,10)} & 0 & 0 \\
a_{(2,1)} & a_{(2,2)} & a_{(2,3)} & a_{(2,4)} & 0 & a_{(2,6)} & 0 & a_{(2,8)} & a_{(2,9)} & a_{(2,10)} & 0 & 0 \\
a_{(3,1)} & a_{(3,2)} & a_{(3,3)} & a_{(3,4)} & 0 & a_{(3,6)} & 0 & a_{(3,8)} & a_{(3,9)} & a_{(3,10)} & 0 & 0 \\
a_{(4,1)} & a_{(4,2)} & a_{(4,3)} & a_{(4,4)} & 0 & a_{(4,6)} & 0 & a_{(4,8)} & a_{(4,9)} & a_{(4,10)} & 0 & 0 \\
0 & 0 & 0 & 0 & a_{(5,5)} & 0 & a_{(5,7)} & 0 & 0 & 0 & 0 & a_{(5,12)} \\
a_{(6,1)} & a_{(6,2)} & a_{(6,3)} & a_{(6,4)} & 0 & 0 & a_{(6,7)} & 0 & 0 & 0 & 0 & 0 \\
0 & 0 & 0 & 0 & a_{(7,5)} & a_{(7,6)} & 0 & 0 & 0 & 0 & 0 & 0 \\
a_{(8,1)} & a_{(8,2)} & 0 & 0 & 0 & 0 & 0 & a_{(8,8)} & a_{(8,9)} & a_{(8,10)} & 0 & 0 \\
a_{(9,1)} & a_{(9,2)} & 0 & 0 & 0 & 0 & 0 & a_{(9,8)} & a_{(9,9)} & a_{(9,10)} & 0 & 0 \\
0 & 0 & a_{(10,3)} & a_{(10,4)} & 0 & 0 & 0 & a_{(10,8)} & a_{(10,9)} & 0 & 0 & 0 \\
a_{(11,1)} & a_{(11,2)} & a_{(11,3)} & a_{(11,4)} & 0 & 0 & 0 & 0 & 0 & 0 & 0 & 0 \\
a_{(12,1)} & a_{(12,2)} & a_{(12,3)} & a_{(12,4)} & 0 & 0 & 0 & 0 & 0 & 0 & a_{(12,11)} & a_{(12,12)}
\end{bmatrix}
\begin{bmatrix}
\Delta i_{ds} \\ \Delta i_{qs} \\ \Delta i_{dr} \\ \Delta i_{qr} \\ \Delta\omega_t \\ \Delta\omega_g \\ \Delta\theta_s \\ \Delta i_{ad} \\ \Delta i_{aq} \\ \Delta V_c \\ \Delta\beta_i \\ \Delta\beta
\end{bmatrix}
\tag{3.48}
$$

3.6.7 Initial Conditions

From figure 1 we find the intial conditions of the system. This is done by writing the stator current I_s in terms of the converter current I_a, load current I_c and the transmission line current I_{Line} in terms of the load Y_{11}, the terminal bus voltage V_s and the infinite bus voltage V_b. The load Y_{11} can be decomped into g_{11} and b_{11}, while the lumped transmission line impedance can be written in the form $R + jX$. This shown by eq.3.49-3.50.

Now by decomposing the terminal bus voltage into its d-q components and writing them in terms of the converter currents we have,

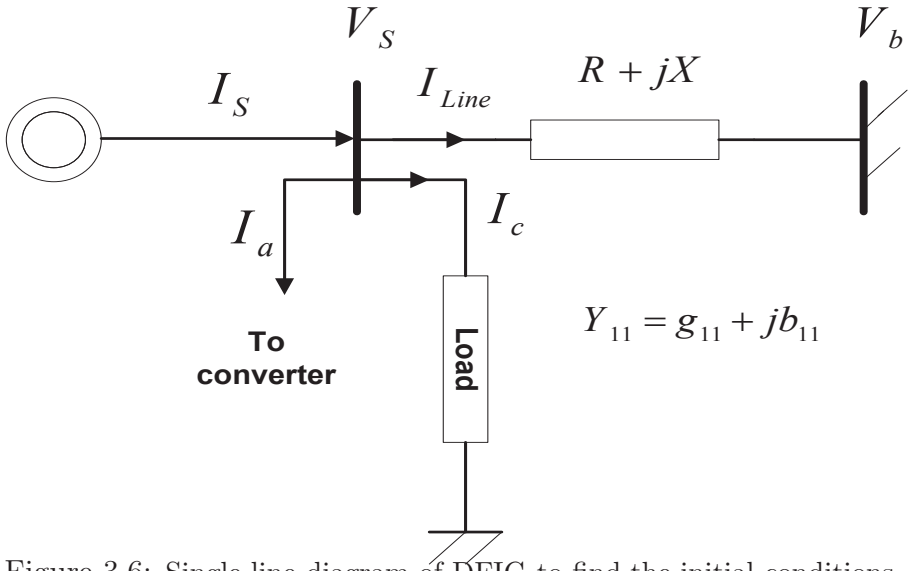

Figure 3.6: Single line diagram of DFIG to find the initial conditions

$$
\begin{aligned}
I_s &= I_a + I_c + I_{Line} \qquad (3.49)\\
I_s - I_a &= V_s\, Y_{11} + I_{Line}\\
I_s - I_a &= V_s\, Y_{11} + [(V_s - V_b)\, Y_{12}]
\end{aligned}
$$

$$I_s - I_a = V_s\,[Y_{11} + Y_{12}] - V_b\,Y_{12} \tag{3.50}$$

$$\begin{bmatrix} (g_{11} + g_{12}) & -(b_{11} + b_{12}) \\ (b_{11} + b_{12}) & (g_{11} + g_{12}) \end{bmatrix} \begin{bmatrix} v_{ds} \\ v_{qs} \end{bmatrix} = \begin{bmatrix} g_{12} \\ b_{12} \end{bmatrix} V_b + \begin{bmatrix} i_{ds} - i_{ad} \\ i_{qs} - i_{aq} \end{bmatrix} \tag{3.51}$$

Making v_{ds} and v_{qs} as the subject of the equation gives,

$$\begin{bmatrix} v_{ds} \\ v_{qs} \end{bmatrix} = \begin{bmatrix} z_{11} & z_{12} \\ z_{21} & z_{22} \end{bmatrix} \begin{bmatrix} g_{12} \\ b_{12} \end{bmatrix} V_b + \begin{bmatrix} z_{11} & z_{12} \\ z_{21} & z_{22} \end{bmatrix} \begin{bmatrix} i_{ds} - i_{ad} \\ i_{qs} - i_{aq} \end{bmatrix} \tag{3.52}$$

where impedance matrix, $\begin{bmatrix} z_{11} & z_{12} \\ z_{21} & z_{22} \end{bmatrix}$ is given by the inverse of $\begin{bmatrix} (g_{11} + g_{12}) & -(b_{11} + b_{12}) \\ (b_{11} + b_{12}) & (g_{11} + g_{12}) \end{bmatrix}$. The individual elements of the impedance matrix are given in Appendix A.

For the stator and the rotor currents initial conditions we have to make use of the induction generator model which when substituted in eq.3.52 results in,

$$\begin{bmatrix} -(R_s + z_{11}) & (X_s + z_{12}) & 0 & X_m \\ -(X_{ss} + z_{21}) & -(R_s + z_{22}) & -X_m & 0 \\ 0 & sX_m & -R_r & sX_{rr} \\ -sX_m & 0 & -sX_{rr} & -R_r \end{bmatrix} \begin{bmatrix} i_{ds} \\ i_{qs} \\ i_{dr} \\ i_{qr} \end{bmatrix} = \begin{bmatrix} z_{11}\, g_{12} + z_{12}\, b_{12} \\ z_{21}\, g_{12} + z_{22}\, b_{12} \\ v_{dr} \\ v_{qr} \end{bmatrix} V_b - \begin{bmatrix} z_{11}\, i_{ad} + z_{12}\, i_{aq} \\ z_{21}\, i_{ad} + z_{22}\, i_{aq} \\ 0 \\ 0 \end{bmatrix} \quad (3.53)$$

CHAPTER 4

THE SMART CONTROL ALGORITHMS

The wind generation system including the pitch controller configuration is shown in figure 3.1. The control design has to cater for variable wind speed. The proposed control strategy involves determination of optimum control parameters for different wind speeds, the optimization being carried out through a differential evolution technique. The differential evolution technique maximizing the system damping. A neural network is employed to select the control parameters for actual wind speed and operating scenario. A strategy is presented which will adapt the weights of the neural network providing a smart control strategy. The differential evolution algorithm, back propagation neural network and adaptive algorithm is presented in this chapter briefly.

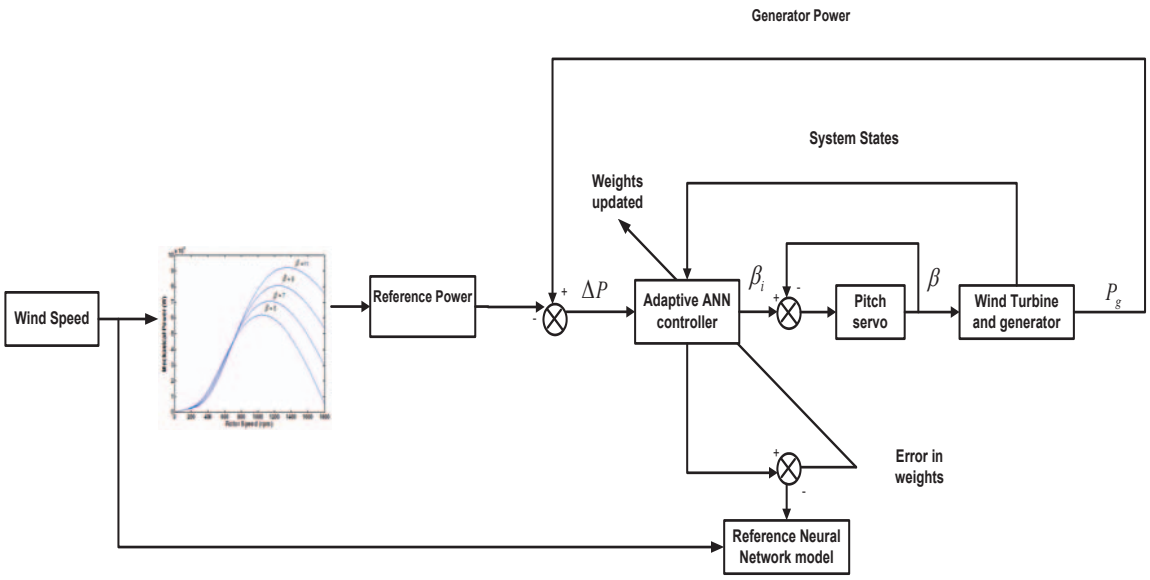

Figure 4.1: Adaptive neural network based pitch controller

4.1 Differential Evolution

4.1.1 Overview

Intelligent control is composed of a variety heuristic techniques like genetic algorithm, particle swarm optimization, simulated annealing, tabu search, differential evolution etc. The differential evolution algorithm covers up for the disadvantages of other techniques because of its ease of use, efficient memory utilization, lower computational complexity, lower computational effort due to its fast convergence and above all its robustness to get to optimal solutions even in non-differentiable optimization problems. More details about this technique follow up in this chapter.

The DE is a population based optimization technique and is suited for solving non-linear and non-differentiable optimization problems. DE is a kind of searching technique and requires number (NP) of candidate solutions (X_n^i) to form a population (G^i), where each solution consists of certain number of parameters x_{nj} depending on

the problem dimension [88].

$$G^i = [X_1, X_2, ..., X_{NP}] \qquad i : \text{Generation}, NP : \text{Population size} \tag{4.1}$$

$$X_n^i = [x_{n1}, x_{n2}, ..., x_{nj}] \qquad n : \text{Problem dimension} \tag{4.2}$$

The main idea in any search technique relies in how to generate a variant (offspring) vector solution, on which the decision will be made, in order to choose the best (parent or variant). The strategy applied in this technique is to use the difference between randomly selected vectors to generate a new solution. For each solution in the original population, a trail solution is generated by performing process of mutation, recombination and selection operators. The old and new solutions are compared and the best solutions are emerged in the next generation. Initially the DE was developed to solve single objective optimization problem.

The DE, as an evolutionary technique, generally performs three steps: initialization, creating new trail generation and selection.

4.1.2 DE Algorithm

4.1.2.1 Initialization

As a preparation for the optimization process, the following requirements should be specified:

- D: Problem dimension which defines the number of control variables. Also, the range of each control element should be defined. This range is required during

the process.

- Minimum and maximum values of the parameters to be optimized.
- NP: Population size
- The number of iterations for which the algorithm is going to run
- $\mathcal{F}$: Mutation factor, which is helpful in finding the optimal solution in the entire search space by mutating the control parameters.
- $\mathcal{CR}$: Crossover factor, which determines probability for offspring parameters for each control vector.

The first step in order to perform optimization using DE, is to generate an initial population composed of NP vectors (solutions). Each vector includes the values of the various control variables which represent a candidate solution to the problem. This is done by assigning random values for each parameter of solution x_i, within the range of the corresponding control variable [89].

$$x_{i,j} = x_{j,min} + rand\,(0,1)\,(x_{j,max} - x_{j,min}) \quad i = 1, NP, j = 1, D \tag{4.3}$$

4.1.2.2 Evaluation and finding the best solution

Once the initial population is formed, the objective value for each vector is calculated and then compared to get the best solution achieving the optimal objective. This value is stored externally and updated by comparison with all solutions in every generation.

4.1.2.3 Mutation

The mutation operation is considered as the first step towards the generation of new solutions. At this stage, for every solution (individual) in the population in generation-i: $X_i^{(G)}$ i=1,...,NP, a mutant vector $V_i^{(G+1)}$ is generated using one of the equations given by eq.4.4-4.7 [90]:

$$V_i^{(G+1)} = X_{r1}^{(G)} + \mathcal{F}\left(X_{r2}^{(G)} - X_{r3}^{(G)}\right) \tag{4.4}$$

$$V_i^{(G+1)} = X_{best}^{(G)} + \mathcal{F}\left(X_{r1}^{(G)} - X_{r2}^{(G)}\right) \tag{4.5}$$

$$V_i^{(G+1)} = X_{best}^{(G)} + \mathcal{F}\left(X_{best}^{(G)} - X_i^{(G)}\right) + \mathcal{F}\left(X_{r1}^{(G)} - X_{r2}^{(G)}\right) \tag{4.6}$$

$$V_i^{(G+1)} = X_{r1}^{(G)} + \mathcal{F}\left(X_{r2}^{(G)} - X_{r3}^{(G)}+\right) + \mathcal{F}\left(X_{r4}^{(G)} - X_{r5}^{(G)}\right) \tag{4.7}$$

Where, $X_{r1}^{(G)}, X_{r2}^{(G)}, X_{r3}^{(G)}, X_{r4}^{(G)}, X_{r5}^{(G)}$ are randomly selected solution vectors from the current generation (different from each other and the corresponding X_i) and X_{best}^{G} is the solution achieving best value. F is a mutation constant and it takes values between 1 and 0. The factor F plays a role in controlling the speed of convergence.

4.1.2.4 Crossover

To further perturb the generated solutions and enhance the diversity, a crossover operation is applied by the DE. In this step the parameters of the generated mutant vector and its corresponding vector i in the original population are copied to a trial solution according to a certain crossover factor CR between 0 and 1. For each parameter, a random number in the range 0 and 1 is generated and compared with CR, and

if its value is less than or equal to CR, the parameter value is taken from the mutant vector, otherwise, it will be taken from the parent. The crossover process is shown in figure 4.2. However, in case CR was defined to be zero, then all the parameters of the trial vector are copied from the parent vector X_i, except one value (randomly chosen) of the trial vector is set equal to the corresponding parameter in the mutant vector. On the other hand, if CR is set equal to one then all parameters will be copied from the mutant vector, except one value (randomly chosen) of the trial vector is set equal to the corresponding parameter in the parent vector. The factor CR plays a role in controlling the smoothness of the convergence. As CR becomes very small, it becomes very probable that the trial solutions would have characteristic of their parent vectors and therefore, slow the convergence [89, 90].

4.1.2.5 Selection

The last step towards generation of a new population is to compare the solutions in old population and their corresponding trail solutions and then select the better one. For this, the objective value corresponding to each trail solution is calculated and compared with the value of the parent. If the new solution performed better it replaces the parent, otherwise the old solution is retained [89].

4.1.2.6 Stopping Criteria

Once, a new generation is produced, the problem updates the global best. The user defined criteria would also be checked. In most cases a maximum number of iterations

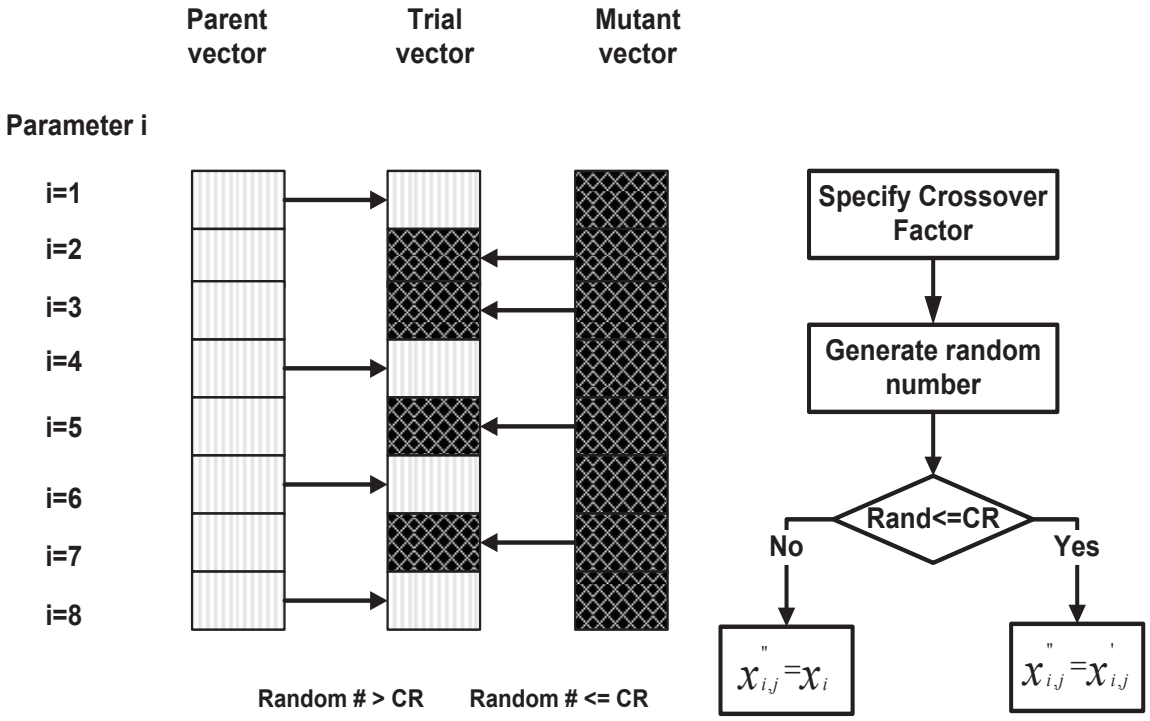

Figure 4.2: Crossover process

is defined and selected as stopping criteria. In practice, the user can check the results and verify the change and can determine when to stop [89].

4.1.3 Differential Evolution Applied to Pitch Control

A flowchart of DE algorithm, pertaining to pitch control problem is shown in figure 4.3. The algorithm begins by taking wind speed as input. The parameters to be optimized are the PI controller gains. Therefore 'D' is set to be equal to 2. An initial population with NP=100 by taking random values of K_P and K_I defined between the minimum and maximum values for these control parameters using eq.4.3.

In order to diversify the search for the optimal solution mutation and crossover

functions are applied. Objective function is then evaluated. The selected values of controller parameters are used to evaluated the eigenvalues of the closed loop matrix developed in chapter 3. DE will try to push all those eigenvalues that have damping ratio less than the preselected one to have the desired damping.

Trial and mutated vectors are formed using the crossover process illustrated in figure 4.2. The new population formed through this process is arranged in an ascending order of their objective function values. A check is carried out to see whether the objective function is minimized or not. If it is then the resultant control parameters constitute an optimal solution otherwise the algorithm continues until the desired parameters are achieved.

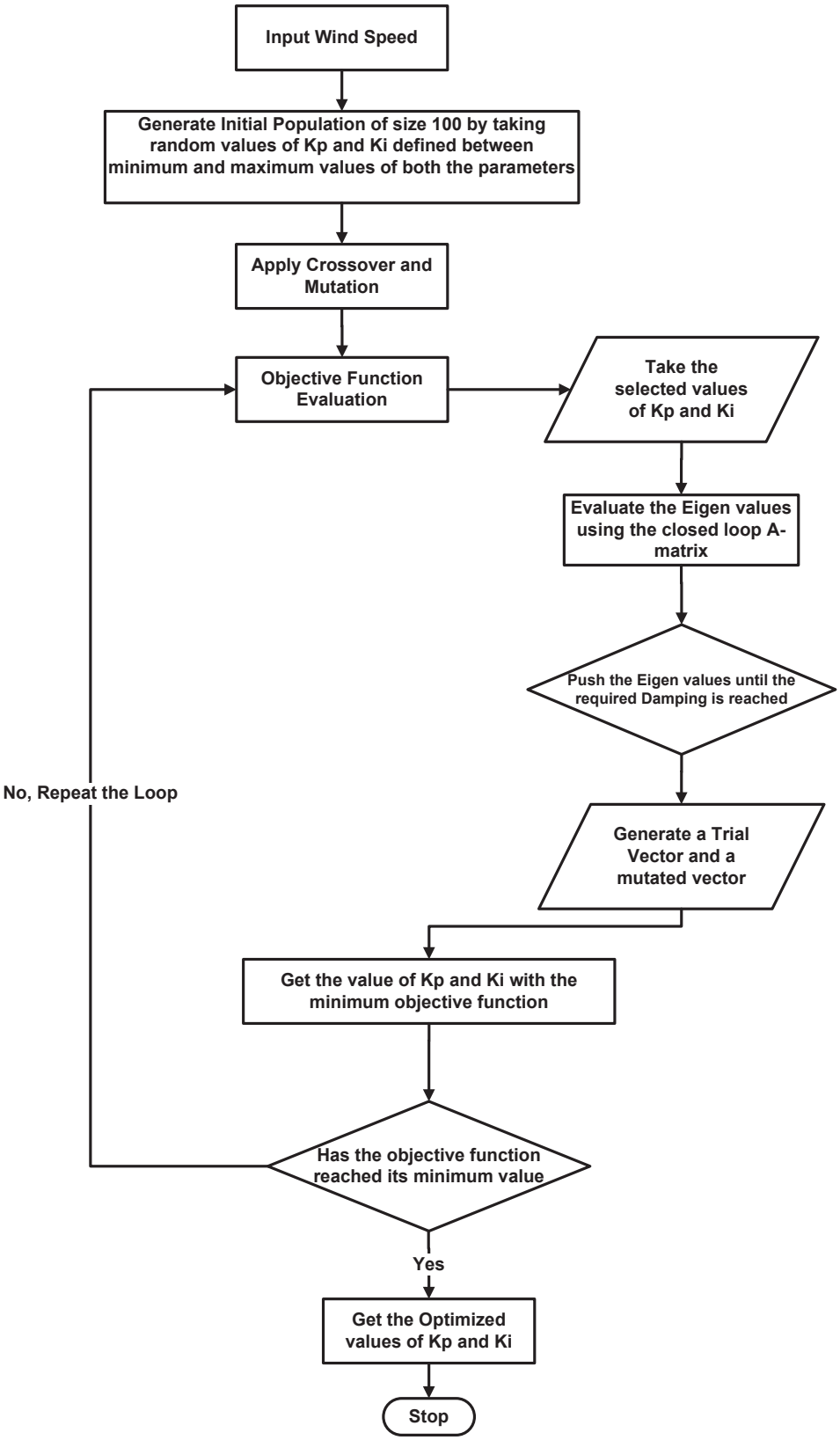

Figure 4.3: Flowchart of Differential Evolution

4.2 Artificial Neural Network

The back propagation algorithm represents one of the most classical examples of an artificial neural network (ANN), being also one of the simplest in the overall design. The network consists of several layers of neurons. The first layer of neurons is known as a sensory layer - each neuron receives just one component of the input vector. This gets distributed to all the neurons from the input layer.The last layer is known as the output layer, which processes the data presented from the input layer into relevant outputs [91]. The intermediate layers in the network are known as hidden layers.

4.2.1 Back Propagation Algorithm Applied to Pitch Control

For the pitch control problem, figure 4.4 shows the flowchart that is used. It makes use of differential evolution as the back end program to generate optimum control parameters for particular wind speed.

The training data for the back propagation neural network is achieved by taking random values of wind speeds between $5m/s$ and $15m/s$. These wind speeds are saved into an input vector while the resultant controller gains for a particular wind speed is saved into an output vector. These two vectors serve as inputs and targets for the back propagation algorithm. The weights in the hidden layer are trained using this algorithm. A large training data is taken so that 500 data sets could be used for the training of the data while the remaining could be used for its validation. The training of the network continues until the total sum-of-squares function [60], given by eq.4.8 is minimized. For an input vector X_i and the associated target T , the sum of squares

error function $E(W)$, E is dependent on the weights of the network and is defined as,

$$E(W) = \frac{1}{2}\sum_{q=1}^{N_L}[z_{Lq}X_i - T_qX_i]^2 \tag{4.8}$$

where z_{Lq} is the output of neuron q from the output layer. The network once trained is saved to be recalled later for time domain simulations. This trained neural network will be used as a reference model once an adaptive neural network is developed. The details are discussed in the next section.

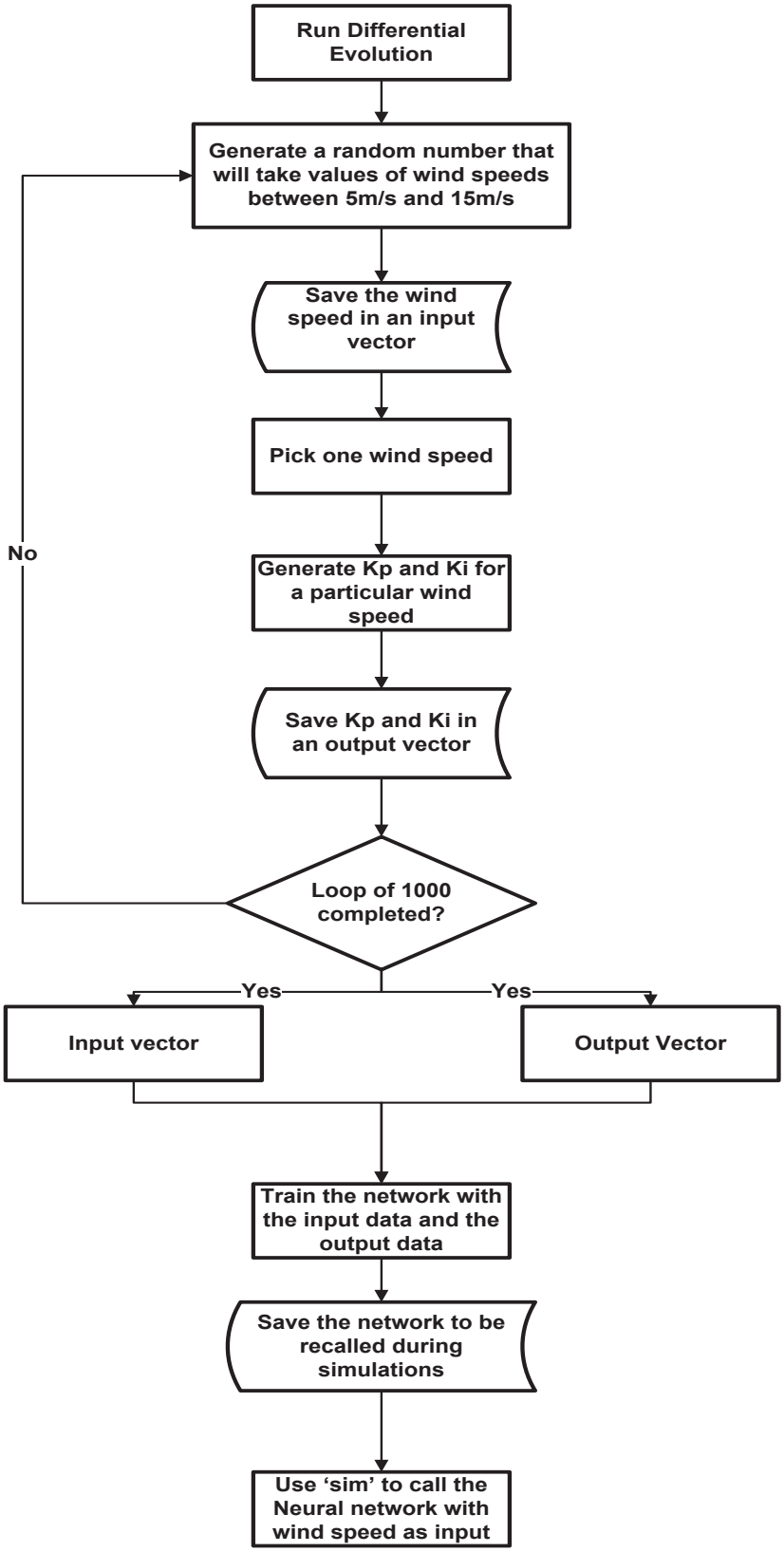

Figure 4.4: Flowchart of Neural Network to be employed for pitch controller

4.3 Adaptive Neural Network

With the evolution in adaptive neural networks, two kinds of error correction rules for online weight updates have come to forefront. They are error correction rules and gradient rules. Error correction rules alter the weights of a network to correct error in the output response to the present input pattern. Gradient rules, following up from the back propagation neural network discussed in the previous section, alter the weights of the network during each pattern presentation by gradient descent with the objective of reducing mean square error, averaged over all training patterns [91].

In back propagation algorithm, the weights are updated by making use of eq.4.9,

$$W(t+1) = W(t) - \mu \nabla E \tag{4.9}$$

where ∇E represents the rate of change of error of weights in *lth* layer and N number of neurons, given by eq.4.10,

$$\nabla E_l = \begin{pmatrix} \frac{\partial E}{\partial w_{l11}} & \cdots & \frac{\partial E}{\partial w_{l1N_{l-1}}} \\ \vdots & \ddots & \vdots \\ \frac{\partial E}{\partial w_{lN_l1}} & \cdots & \frac{\partial E}{\partial w_{l_{N_l}N_{l-1}}} \end{pmatrix} \tag{4.10}$$

In adaptive neural networks, the weight update is carried out by making use of μ-LMS algorithm.

4.3.1 μ-LMS Algorithm

The μ-LMS algorithm works by performing approximate steepest descent on the weights [91]. Since mean square error is a quadratic function of the weights. An instantaneous gradient based upon the square of the instantaneous linear error is,

$$\hat{\nabla} E_t = \frac{\partial \epsilon_t^2}{\partial W(t)} = \begin{bmatrix} \frac{\partial \epsilon_t^2}{\partial w_{0t}} \\ \vdots \\ \frac{\partial \epsilon_t^2}{\partial w_{Nt}} \end{bmatrix} \tag{4.11}$$

LMS works by using this crude gradient estimate in place of the true gradient ∇E as in eq.4.10. Making this replacement in eq.4.9 yields,

$$\begin{aligned} W(t+1) &= W(t) - \mu \hat{\nabla} E_t \\ &= W(t) - \mu \frac{\partial \epsilon_t^2}{\partial W_t} \end{aligned} \tag{4.12}$$

The instantaneous gradient is used because it is readily available from a single data sample. The true gradient is generally difficult to obtain. Computing it would involve averaging the instantaneous gradient associated with all patterns in the training set. Applying differentiation on eq.4.12 gives,

$$W(t+1) = W(t) - 2\mu \epsilon_t \frac{\partial \epsilon_t}{\partial W_t} \tag{4.13}$$

Now assuming that ϵ_t gives the linear difference between the desired response at any stage d_t and the output $W_t^T x_t$. Replacing ϵ_t in eq.4.13 results in,

$$W(t+1) = W(t) - 2\mu\epsilon_t \frac{\partial \left(d_t - W_t^T x_t\right)}{\partial W_t} \tag{4.14}$$

Noting that d_t and x_t are independent of the current instant of weight value W_t yields,

$$W(t+1) = W(t) + 2\mu\epsilon_t x_t \tag{4.15}$$

The learning constant μ determines the stability and the convergence rate as discussed in the previous section. In this algorithm, and other iterative steepest descent procedures, use of the instantaneous gradient is perfectly justified if the step size is small.

Figure 3.4 once incorporates the adaptive neural network can be visualized as illustrated by figure 4.1. The algorithm followed by the adaptive neural network for the pitch control is summarized below,

Adaptive Neural Network for Pitch Control

At initial conditions operating at one wind speed do,

1. Find out the reference power from figure 3.2 at an initial pitch angle β and rotor speed.
2. The reference neural network model computes the optimum K_P and K_I for the PI controller at that wind speed according to figure 4.4. This is done by making use of the back propagation algorithm. The weights of this neural network are fixed.
3. Evaluate the system states from the linearized model given in eq.3.48. This involves making use of the initial conditions highlighted in chapter 3.

Adapting weights in case of wind speed disturbance

1. The reference model generates new optimum K_P and K_I.
2. The system states vary according to the disturbance.
3. By setting the new optimum K_P and K_I as the targets and also making use of limits for generator speed and terminal voltage variation, the weights of the adaptive neural network are adapted by making use of eq.4.10-4.15.
4. The new generated K_P and K_I are applied to the system to come with an optimized value for the pitch control β.

Table 4.1: Adaptive Neural Network Algorithm for pitch control

CHAPTER 5

TESTING THE SMART PITCH CONTROLLER

The intelligent control based algorithm generated for the DFIG system is tested in this section. Results are presented for different wind speed scenarios and compared with the nominal system operation. Controller design is carried out for a range of wind speeds and tuned for optimum parameter values. The control design involves,

- Simulation results of the DE optimization procedure
- Neural network based training and testing of the parameter
- Determination of adaptive weights for the neural network

Simulation of the DFIG system with the pitch controller was followed by the four test cases i.e.

- Step change in wind speed from 12 m/s to 11 m/s

- Step change in wind speed from 12 m/s to 14 m/s
- Sinusoidal change in wind speed with the addition of white noise
- With scaled real wind data as a disturbance

The DFIG configuration with pitch control is shown in figure 5.1. The optimally tuned adaptive back propagation weights were used in the testing phase. The system data is tabulated in table 5.1.

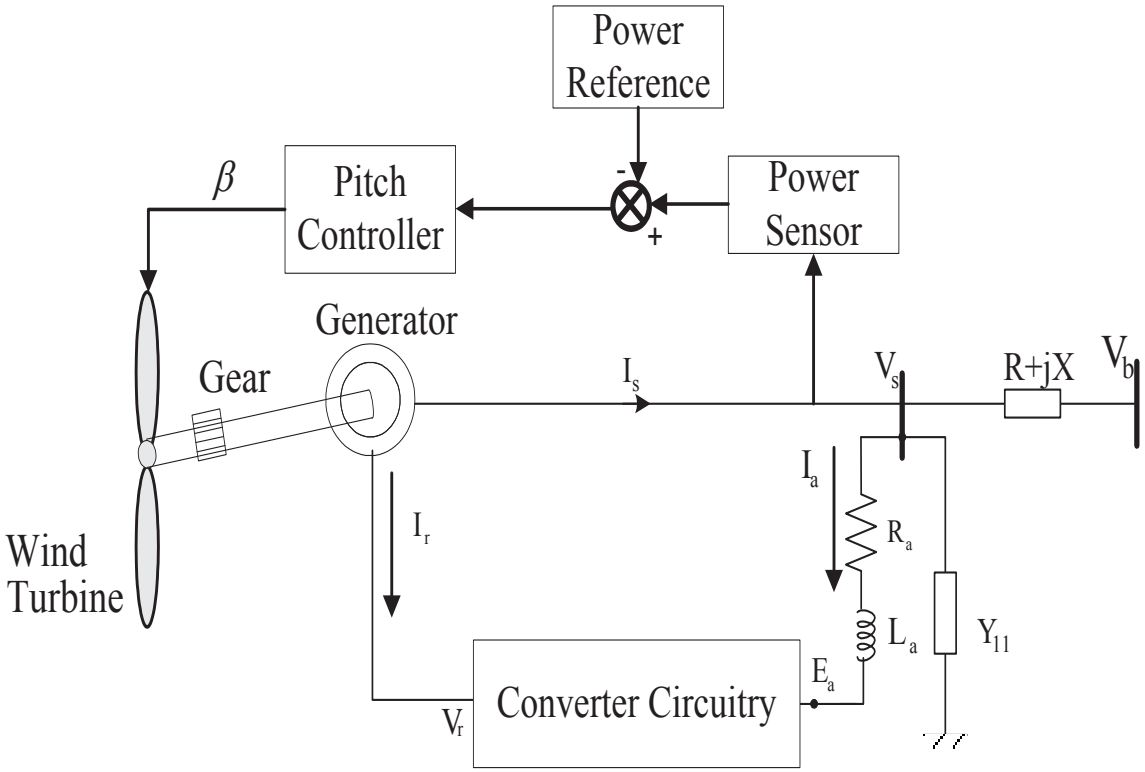

Figure 5.1: DFIG system configuration equipped with pitch controller

Mean wind speed (V_w)	12 m/s
Radius of the blades (R)	13.5 m
Density of air (ρ)	1.225 kg/m^2
Turbine intertia (H_t)	2 s
Generator intertia (H_g)	0.5 s
Shaft stiffness (K_s)	0.3 p.u/el.rad
Stator reactance (x_s)	0.09241 p.u
Stator resistance (R_s)	0.00488 p.u
Rotor reactance (x_r)	0.2 p.u
Rotor resistance (R_r)	0.0059 p.u
Mutual inductance (x_m)	3.95379 p.u
Grid side converter circuit resistance (R_a)	0.001 p.u
Grid side converter circuit reactance (L_a)	0.1 p.u
Transmission line resistance (R)	0.02 p.u
Transmission line reactance (X)	0.15 p.u
Capacitor (C)	1.0 p.u
Load (Y_{11})	0.402-j0.0389 p.u

Table 5.1: System Data

5.1 Generation of adaptive controller parameters

The training data for the adaptive neural network is obtained from the differential evolution expert system. A differential evolution program was used to generate the controller gains for various wind speeds. DE uses dominant eigenvalues of the linearized system and finds the controller parameters so as to make the damping ratio less than the preselected value ζ_0. The objective function to be minimized is written as,

$$J = \sum_{i=1}^{n} (\zeta - \zeta_0)^2 \tag{5.1}$$

The values for crossover and mutation in this study are taken to be 0.8 and 0.4 respectively. The DE algorithm is supplied with a set of maximum and minimum

values of parameters as,

$$\begin{aligned} -15 \leq K_P \leq 7 \\ -7 \leq K_I \leq 10 \end{aligned} \tag{5.2}$$

The differential evolution will try to find out the optimized parameters of the PI controller under given initial conditions. The algorithm begins with wind speed as input and generating an initial population of size 100 by taking random values for K_P and K_I. The DE will try to search for the optimum values of K_P and K_I within the range,

In order to search for optimal values, procedures such as crossover and mutation are then applied. For a wind speed of 12 m/s, the DE converged to the optimal value in about 25 iterations as shown in figure 5.2. It is observed that the differential evolution algorithm tries to search for global optima as the number of iterations increase. There are regions where the cost function does not change. These areas can be identified as local minimas and in order to avoid these, crossover and mutations are applied until there is no further changes in the cost function. The cost function does not change after about 25 iterations onwards.

The convergence characteristics of the PI gains as functions of iteration numbers are shown in figures 5.3 and 5.4. Similar to the cost function plotted for the DE, the PI controller gains converge after about 25 iterations. It is observed that again there are regions where the gains do not change. These are regions of local minimas. By the use of heuristic processes of crossover and mutation, global optimas of gains are obtained until there they converge. The optimized controller parameters, for wind speed of 12 m/s, are tabulated in table 5.2.

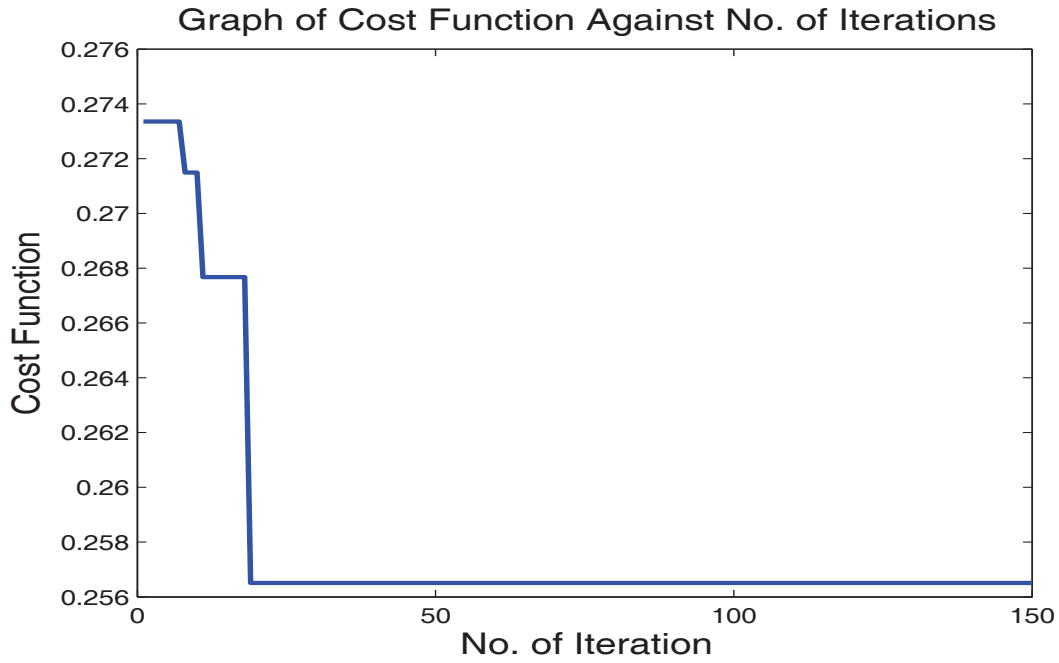

Figure 5.2: Cost function vs. no. of iterations for optimization at v=12m/s

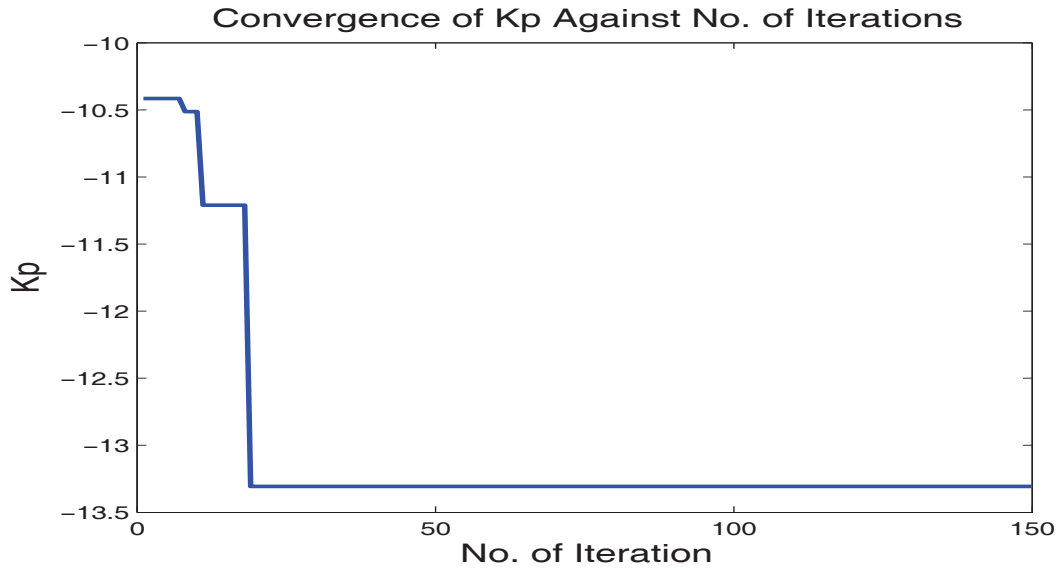

Figure 5.3: Convergence of K_P vs. no. of iterations for optimization at v=12m/s

The output of the DE program was used to train the back propagation neural networks for a range of wind speed inputs. The input vector of the reference model consists of wind speeds while the output vector consists of optimized controller pa-

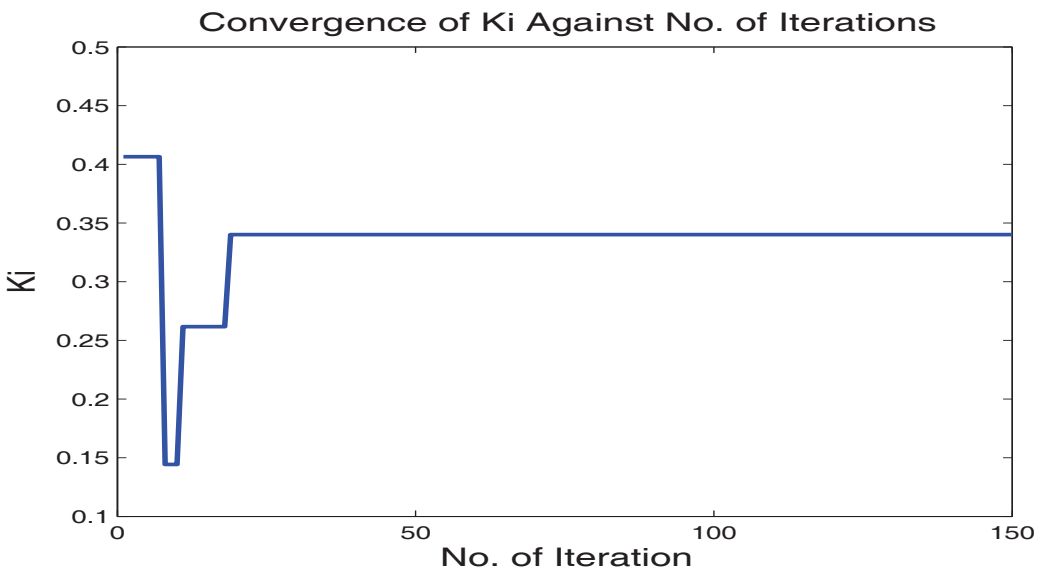

Figure 5.4: Convergence of K_I vs. no. of iterations for optimization at v=12m/s

	$K_{P,opt}$	$K_{I,opt}$
v=12m/s	-13.3061	0.3401

Table 5.2: Optimum controller parameters for 12 m/s wind speed

rameters. This reference model is compared with the network that is trained with the states of the system as input and the corresponding optimized parameters. Since the system makes use of a neural network that depends upon the system states, the targets set for this system to adapt comes from the reference neural network. The converged weighting function obtained after adapting the system for 3 layers and 20 neurons neural network was.

$$W_{(3\times 20)} = \begin{bmatrix} -0.2906 & -3.6181 & 0.1279 & \cdots & 0.5319 & -0.1234 & -0.1896 \\ 0.3457 & 3.6770 & -0.3672 & \cdots & -0.5104 & -0.0340 & 0.0433 \\ -0.0657 & -1.0036 & 0.3063 & \cdots & -0.0370 & 0.3468 & -0.0131 \end{bmatrix} \quad (5.3)$$

These values are further adapted after changing operating conditions and are shown in individual test cases.

5.2 Eigenvalues of the closed loop system

The eigenvalues of the linearized for the controller gains obtained for wind speed of $9m/s$ are compared with nominal control i.e. with K_P=1 and K_I=0. These are tabulated in table 5.3. It can be observed that the optimized PI controller gains improve the system stability.

The dominant eigenvalue in the case of nominal control was found out to be $-0.207 \pm 1.072j$. By making use of the differential evolution algorithm, the eigenvalues having damping ratio less than preselected value ζ_0 are pushed so that the desired damping ratio could be achieved. For the case of optimal PI controller, all the eigenvalues have damping ratio at least greater than or equal to the ζ_0 and hence the resultant controller gains found are optimal parameters that minimize the objective function defined in eq.5.1.

Nominal Control	**With Optimal PI Controller**
$-327.719 \pm 1346.361j$	$-327.719 \pm 1346.361j$
$-5.837 \pm 378.403j$	$-5.837 \pm 378.403j$
$-5.818 \pm 39.975j$	$-5.799 \pm 39.971j$
$-0.409 + 7.589j$	$-0.643 \pm 7.362j$
$-0.207 \pm 1.072j$	-9.623
-0.027	$-0.525 \pm 2.316j$
0	-0.25

Table 5.3: Eigenvalues of the system at $9m/s$ wind speed for the optimal PI controller compared with nominal control scenario

5.3 Test Case I

A step change from $12m/s$ to $11m/s$ is applied to the system as shown in figure 5.5. Initially, the system was working at 0.902 p.u power loading as is evident from figure 5.7. The disturbance is applied at time t=1 sec and the response of the system states is observed. As the wind speed changes to $11m/s$, the pitch controller must adjust the pitch of the turbine blades so that maximum possible aerodynamic power could be extracted from the wind. Using the wind model developed in chapter 3 and extracting reference settings for mechanical power from figure 5.6, it is observed that the new mechanical power reference is set to about 0.82 p.u. This power is sent to the wind conversion system and from figure 5.7, it is evident that the generator is able to achieve the new mechanical power settings in about 5 seconds after the disturbance was applied. With the reduction in mechanical power, the generator speed and slip decreases from an initial value to adjust to the change noticeable from figures 5.8 and 5.9.

The control parameters shown in figures 5.14 and 5.15 make use of the adaptive neural network to adjust the gains and achieve the reference power. The adaptive neural network, as discussed previously, makes use of the system states like generator speed, stator and rotor current, terminal voltage and DC link voltage to provide the optimum controller gains to damp the transients. From figures 5.8-5.13, it is observed that as the system states vary, the controller parameters also adjust themselves until they are able to stabilise the system. As the system achieves the set reference power, there is minimal variation in the K_P and K_I, which is expected.

Contrary to adaptive neural network based controller, it is concluded that in nominal control scenario, the system damping is insufficient and there are transients available in the system states. The states are unable to stabilise within the simulation time and hence has a poor performance as compared to the adaptive neural network based controller.

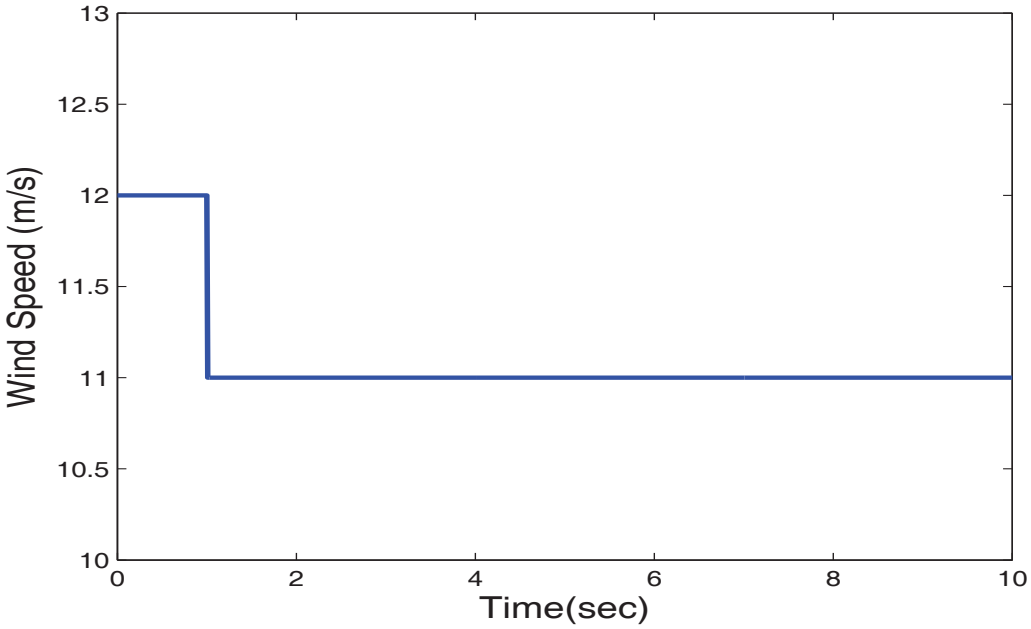

Figure 5.5: Test case wind speed

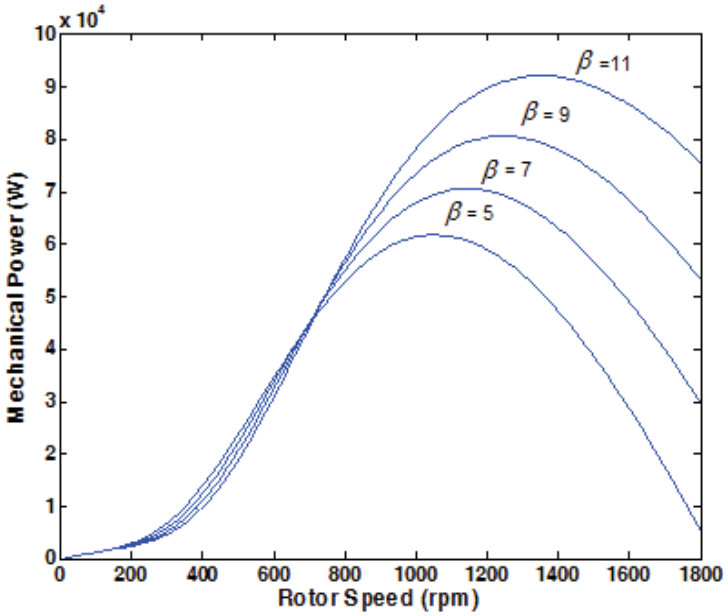

Figure 5.6: Mechanical Power for various pitch angles at wind speed of 12 m/s

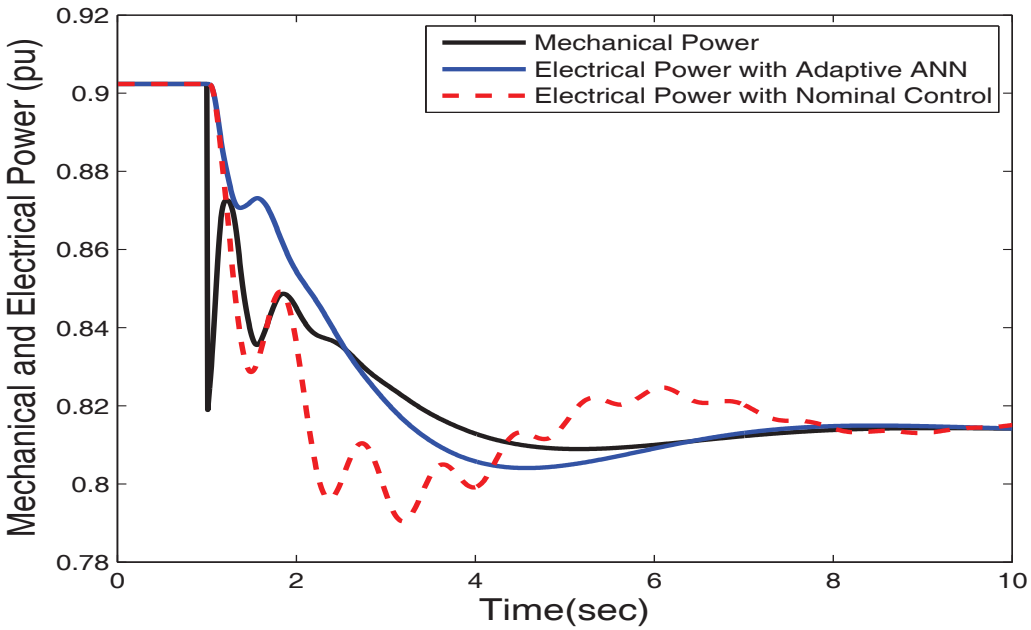

Figure 5.7: Output power with a step change in wind speed from 12m/s to 11m/s at t=1sec (a) With adaptive neural network and (b) Nominal control scenario

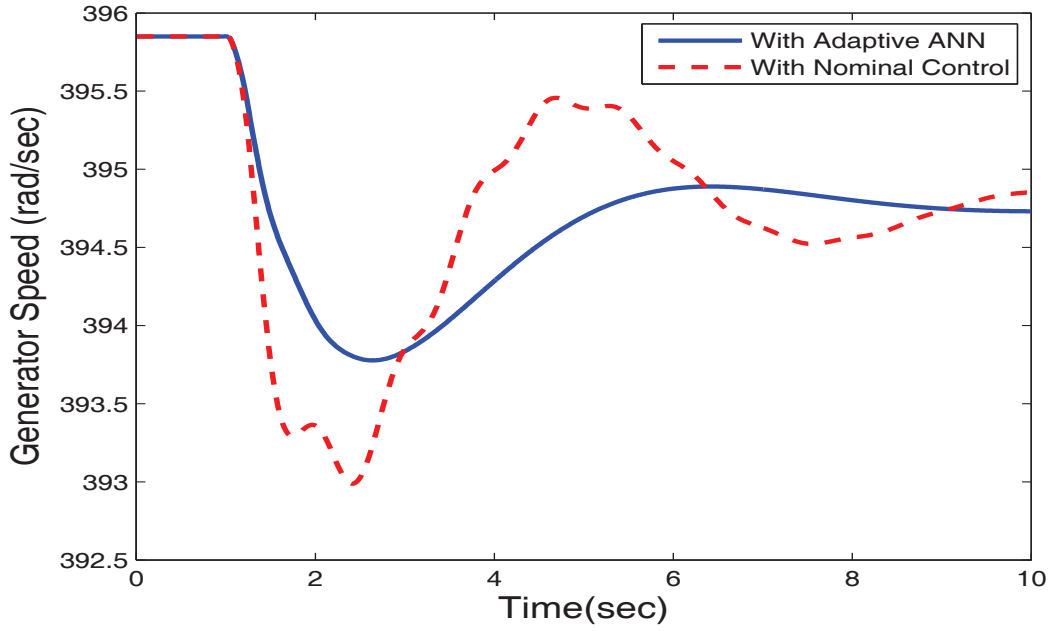

Figure 5.8: Generator speed with a step change in wind speed from 12m/s to 11m/s at t=1sec (a) With adaptive neural network and (b) Nominal control scenario

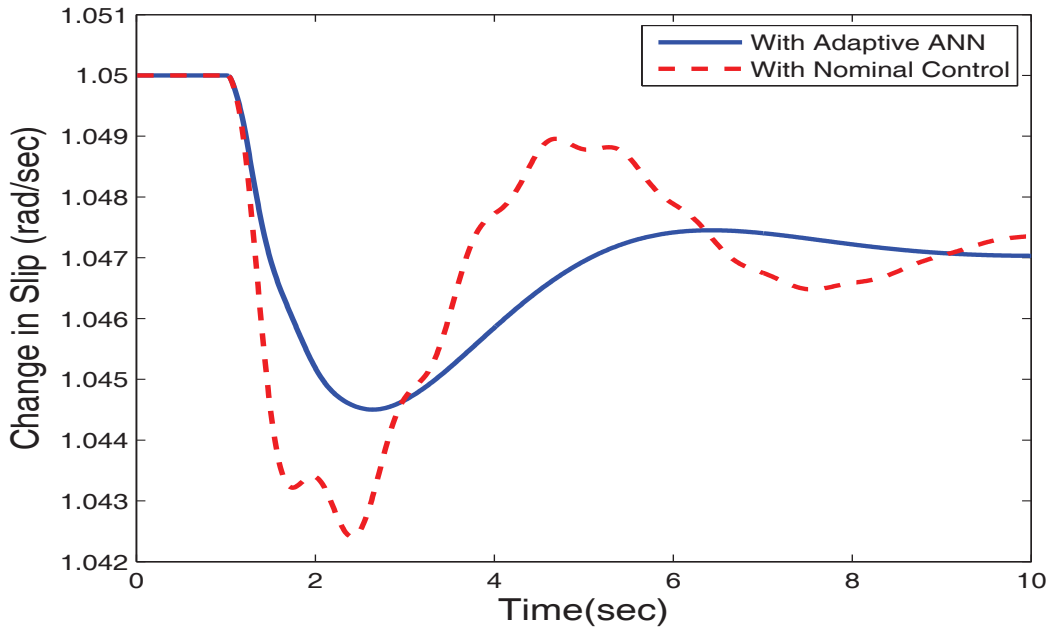

Figure 5.9: Change in slip with a step change in wind speed from 12m/s to 11m/s at t=1sec (a) With adaptive neural network and (b) Nominal control scenario

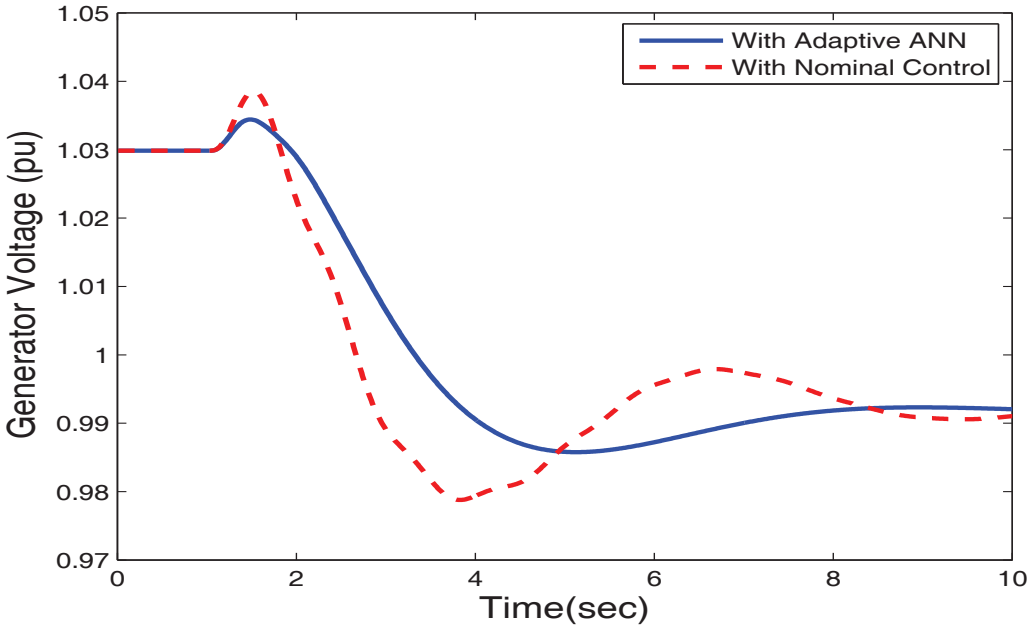

Figure 5.10: Terminal voltage with a step change in wind speed from 12m/s to 11m/s at t=1sec (a) With adaptive neural network and (b) Nominal control scenario

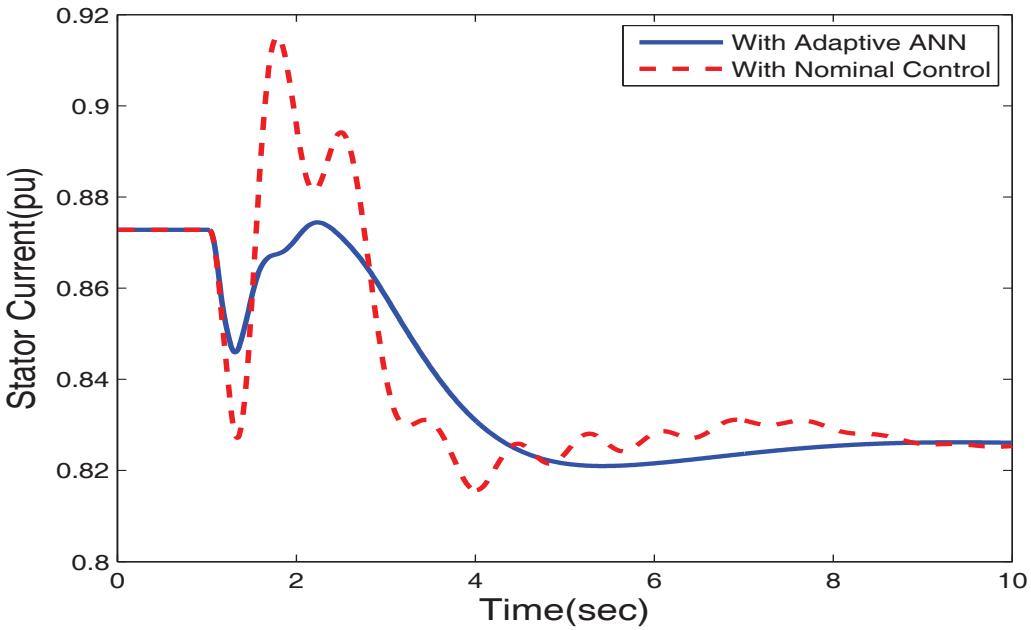

Figure 5.11: Response of stator current with a step change in wind speed from 12m/s to 11m/s at t=1sec (a) With adaptive neural network and (b) Nominal control scenario

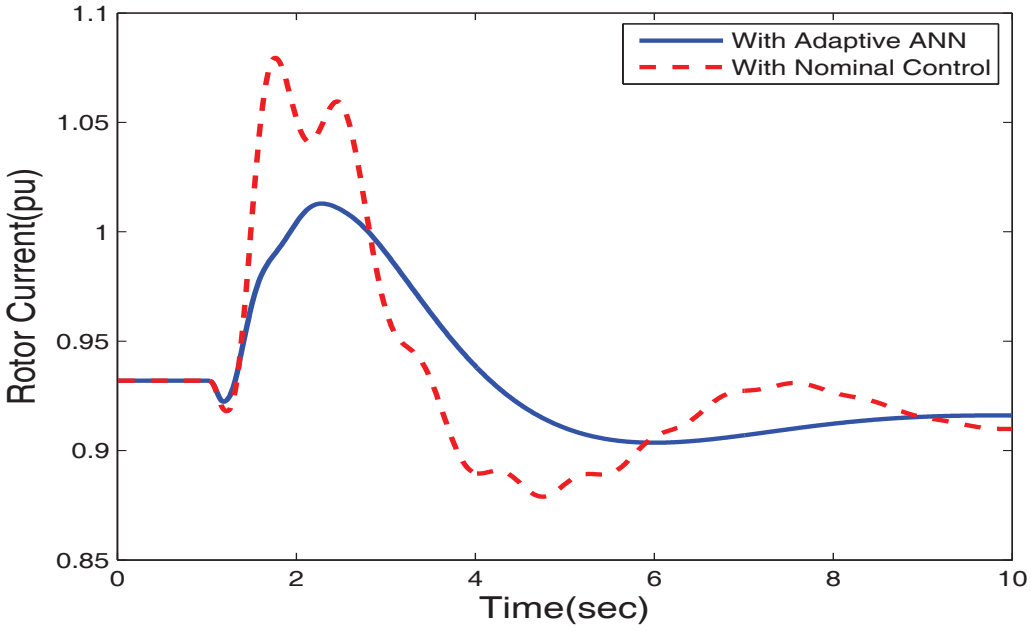

Figure 5.12: Response of rotor current with a step change in wind speed from 12m/s to 11m/s at t=1sec (a) With adaptive neural network and (b) Nominal control scenario

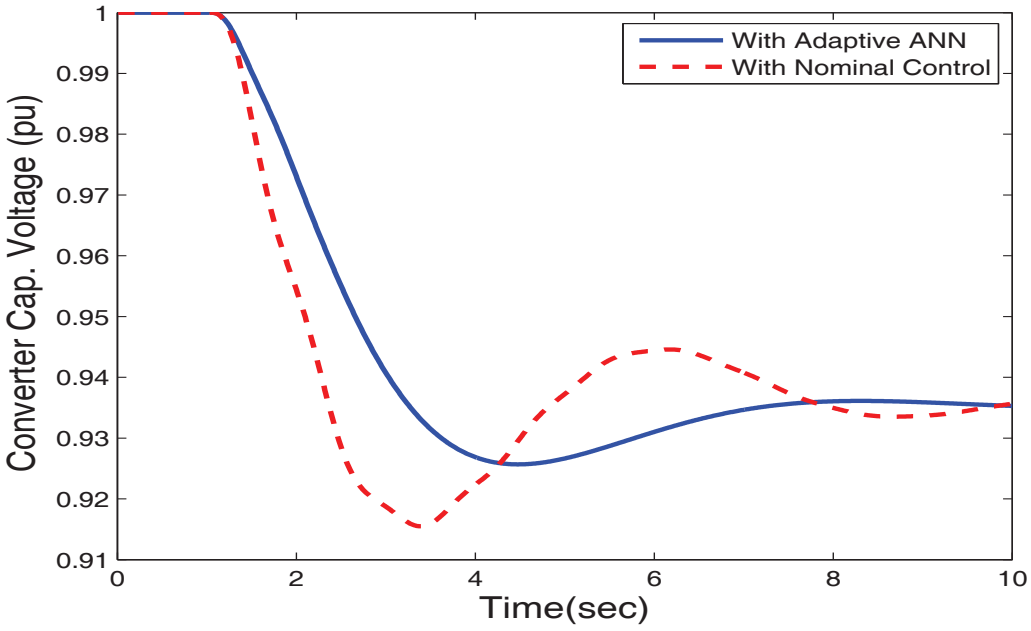

Figure 5.13: DC link voltage with a step change in wind speed from 12m/s to 11m/s at t=1sec (a) With adaptive neural network and (b) Nominal control scenario

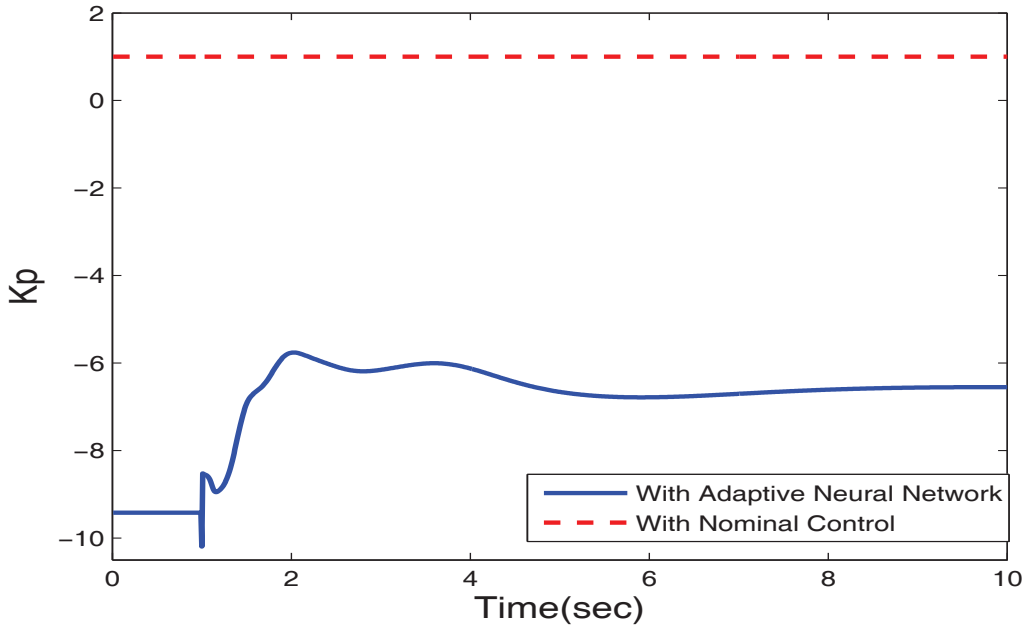

Figure 5.14: Variation of K_P with a step change in wind speed from 12m/s to 11m/s at t=1sec while K_P=1 for nominal control

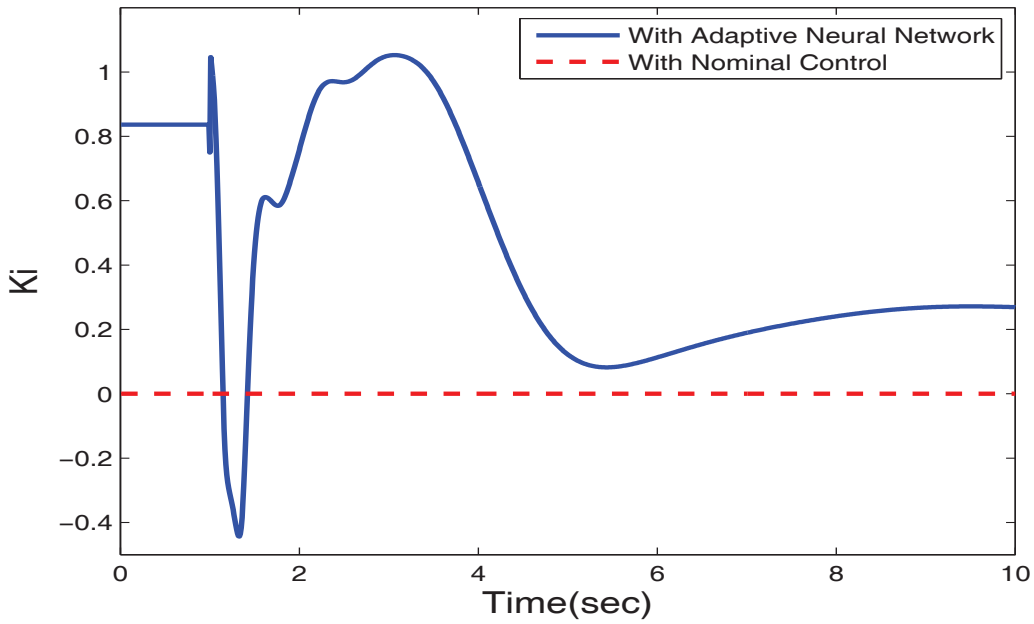

Figure 5.15: Variation of K_I with a step change in wind speed from 12m/s to 11m/s at t=1sec while K_I=0 for nominal control

5.4 Test Case II

An step change in wind speed from $12m/s$ to $14m/s$ is applied to the system as shown in figure 5.16. As compared to the previous the case an upward change in wind speed is applied. This is just to ensure that the system is capable enough of making all sorts of adjustments with sudden changes in wind speeds. Initially the system was operating at 0.902 p.u at 12 m/s. The disturbance is applied at time t=1 sec. A new mechanical power reference is set according to the change in the wind speed. The pitch controller will try to achieve to this new power settings by adjusting the pitch. It can be observed from figure 5.17 that the electrical power is able to track to the mechanical power very smoothly in the case of the adaptive neural network. With an increase in mechanical power, the generator speed also increases but settles in about 6 seconds as is clear from figures 5.18 and 5.19. The system states including the stator and the rotor currents, the terminal voltage and the DC link capacitor voltage show similar responses as illustrated from figures 5.20-5.23.

The controller gains as in figures 5.24 and 5.25 are adapted to changes in the system states by the adaptive neural network until the system stabilises. These optimum gains provide a high level of damping resulting in minimum transients. The nominal control again provides less damping and has a degraded performance as compared to the pitch controller based on adaptive neural network.

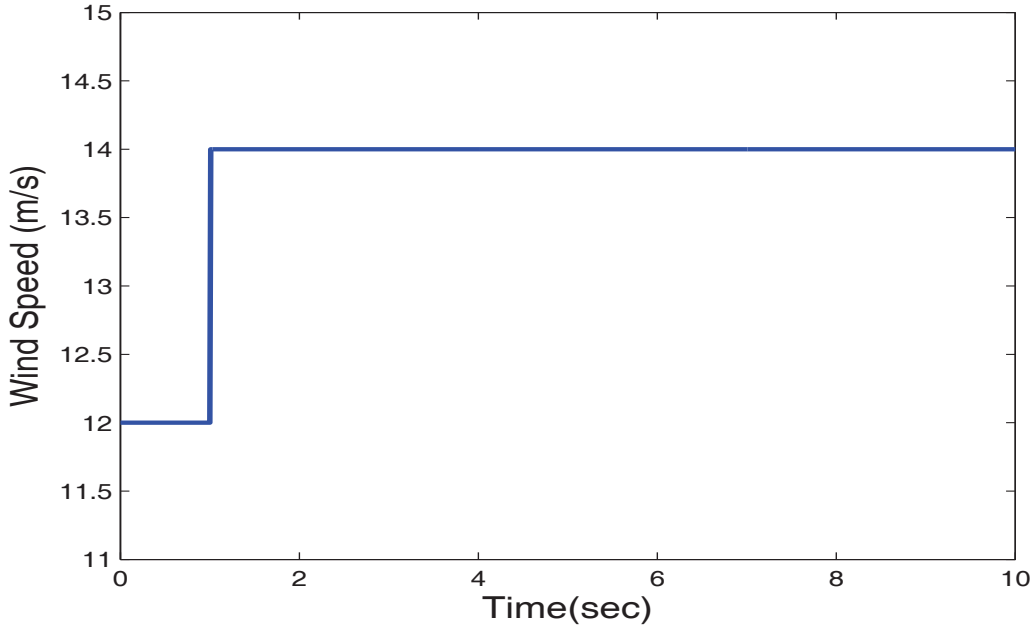

Figure 5.16: Test case wind speed

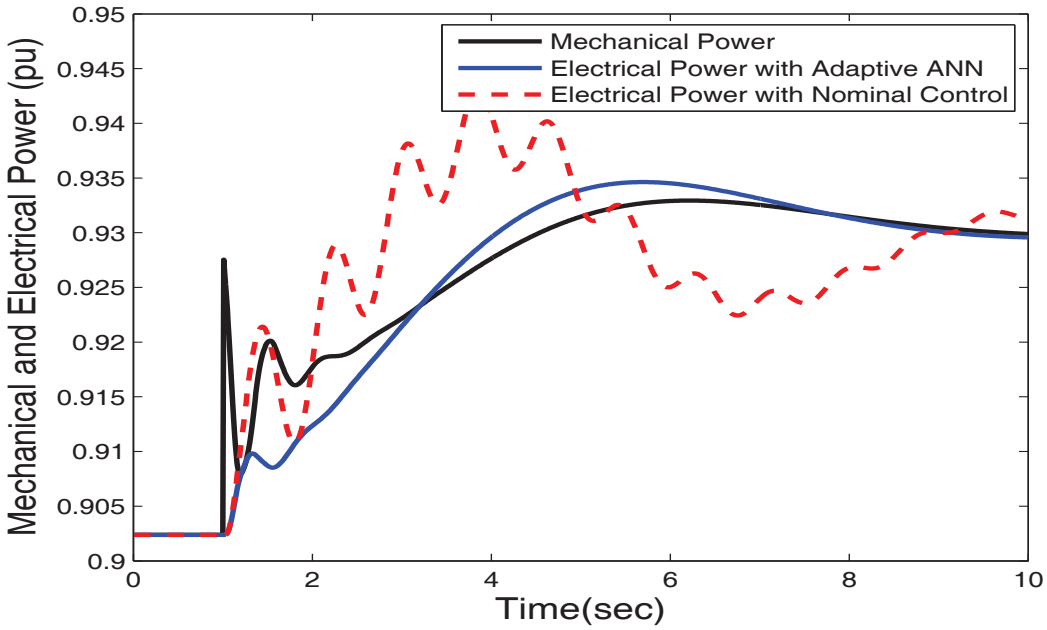

Figure 5.17: Output power with a step change in wind speed from 12m/s to 14m/s at t=1sec (a) With adaptive neural network and (b) Nominal control scenario

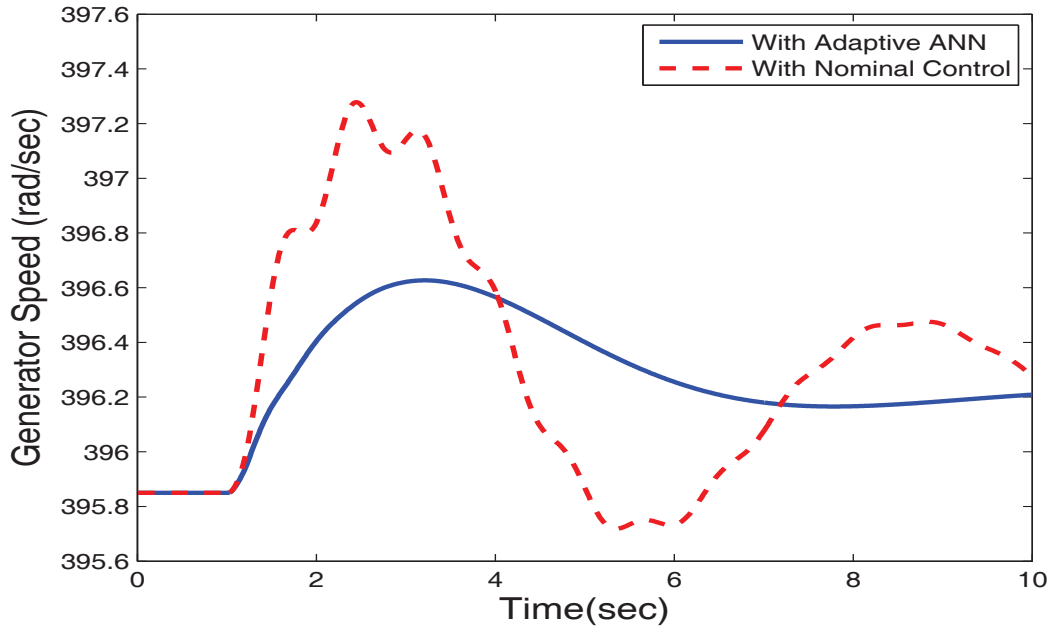

Figure 5.18: Generator speed with a step change in wind speed from 12m/s to 14m/s at t=1sec (a) With adaptive neural network and (b) Nominal control scenario

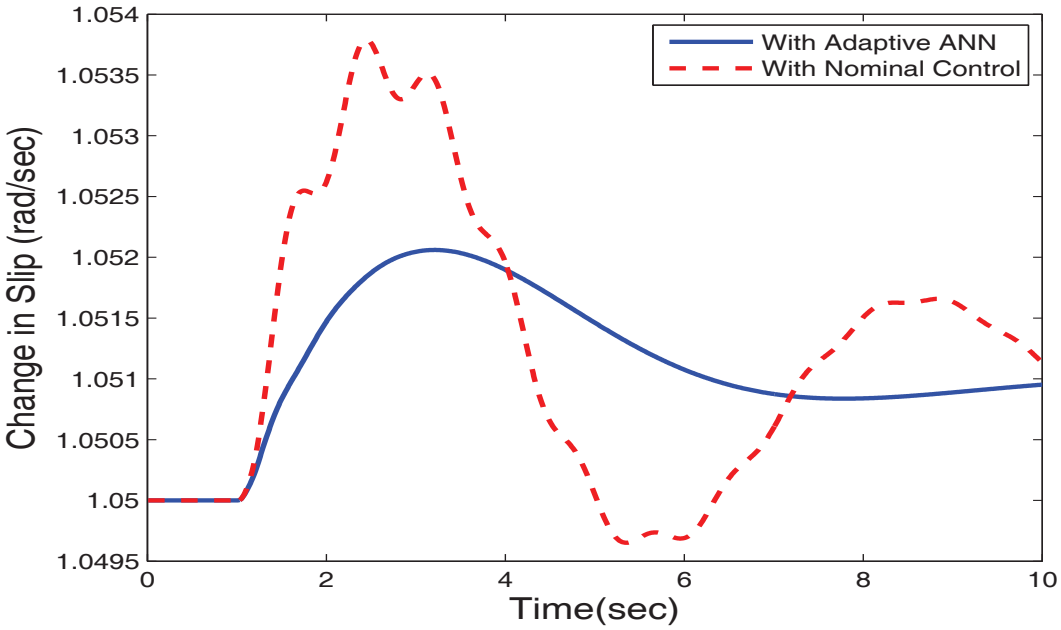

Figure 5.19: Change in slip with a step change in wind speed from 12m/s to 14m/s at t=1sec (a) With adaptive neural network and (b) Nominal control scenario

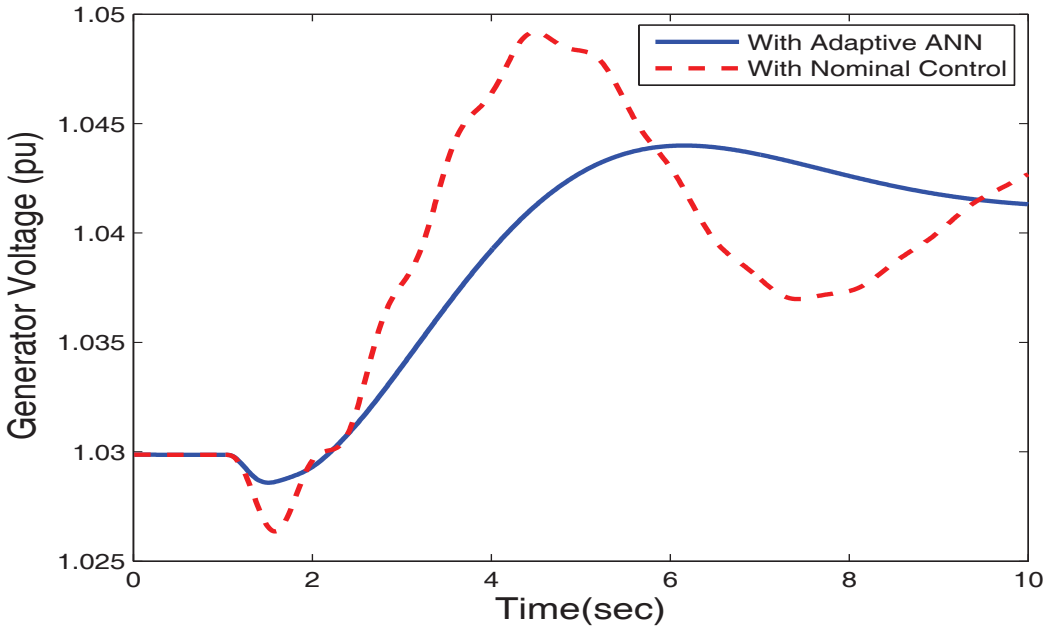

Figure 5.20: Terminal voltage with a step change in wind speed from 12m/s to 14m/s at t=1sec (a) With adaptive neural network and (b) Nominal control scenario

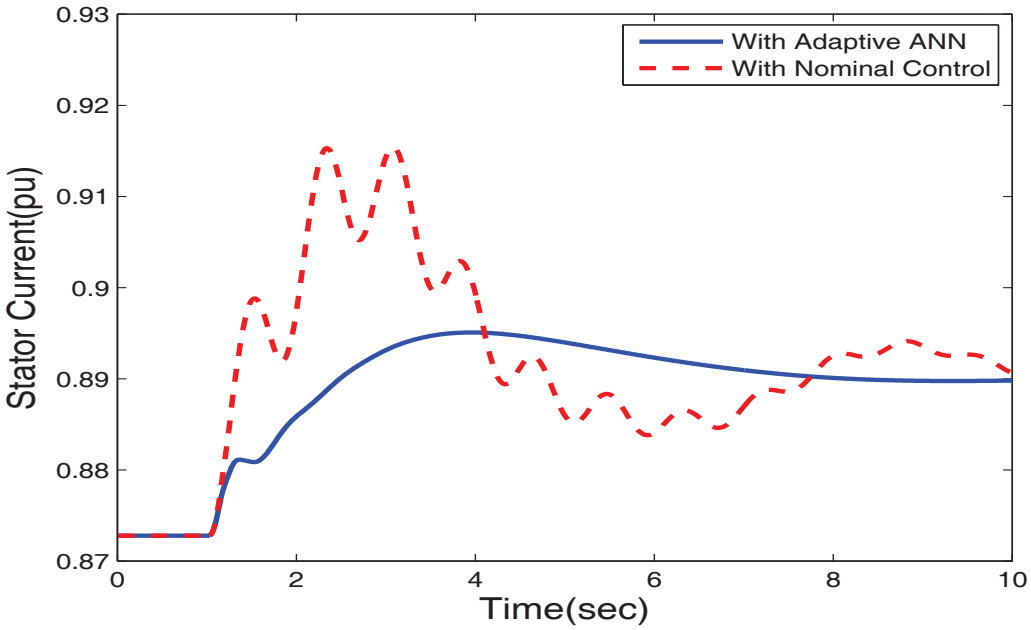

Figure 5.21: Response of stator current with a step change in wind speed from 12m/s to 14m/s at t=1sec (a) With adaptive neural network and (b) Nominal control scenario

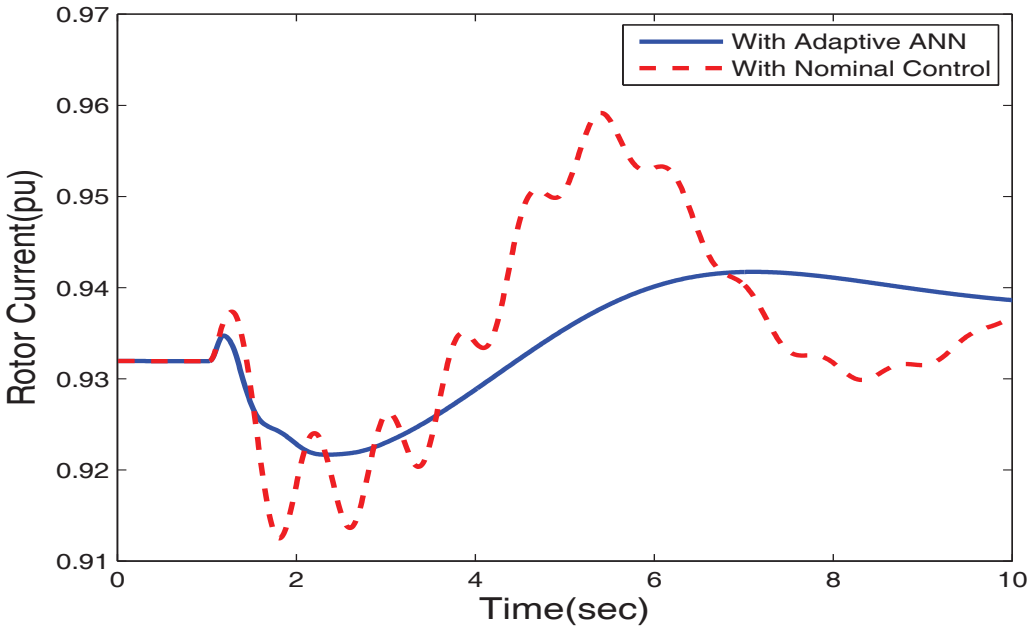

Figure 5.22: Response of rotor current with a step change in wind speed from 12m/s to 14m/s at t=1sec (a) With adaptive neural network and (b) Nominal control scenario

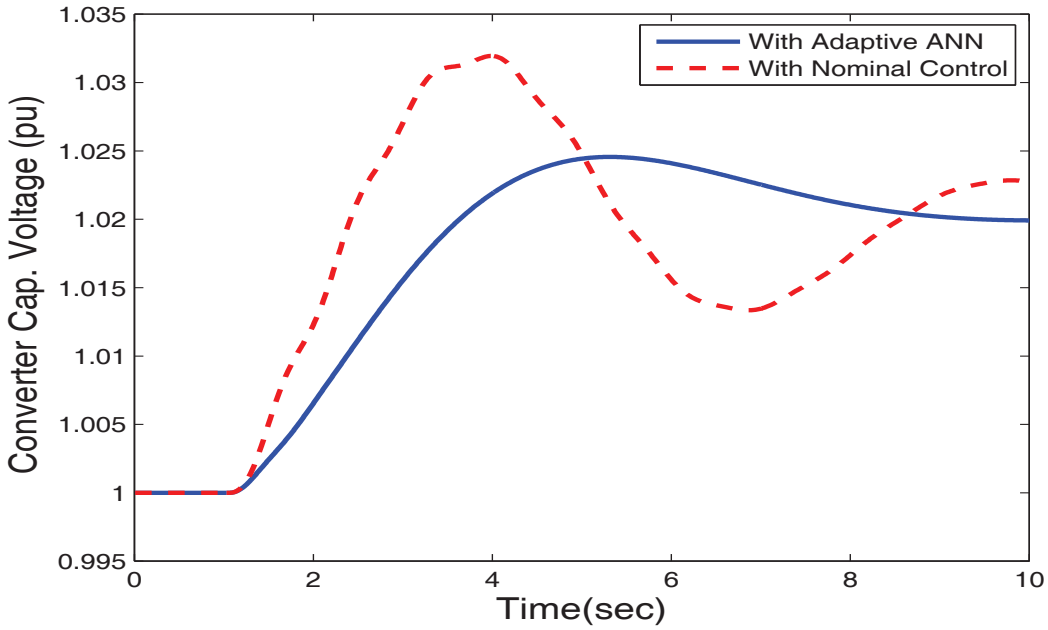

Figure 5.23: DC link voltage with a step change in wind speed from 12m/s to 14m/s at t=1sec (a) With adaptive neural network and (b) Nominal control scenario

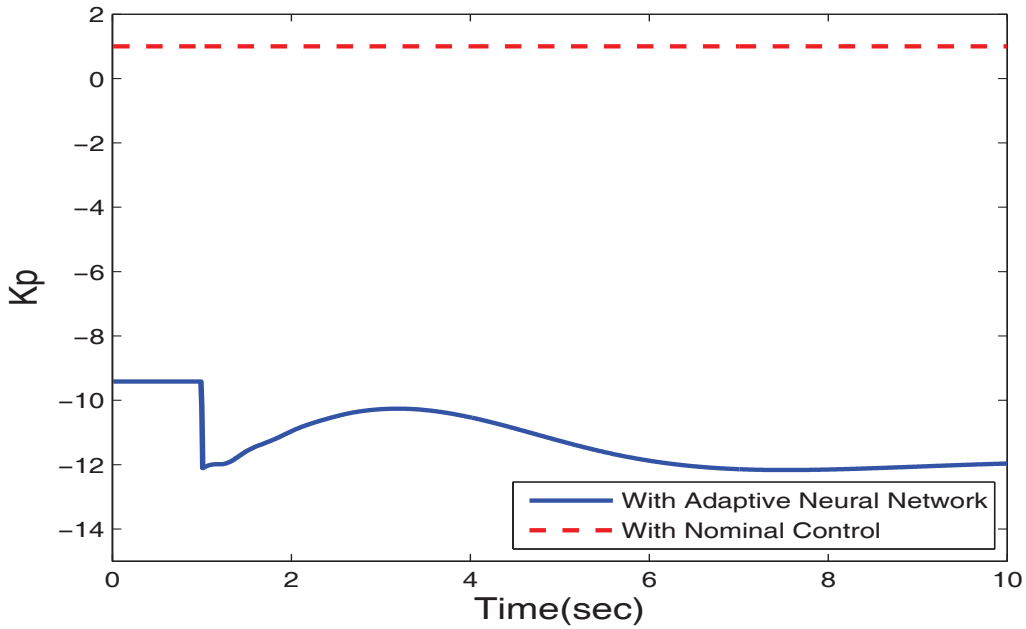

Figure 5.24: Variation of K_P with a step change in wind speed from 12m/s to 14m/s at t=1sec while K_P=1 for nominal control

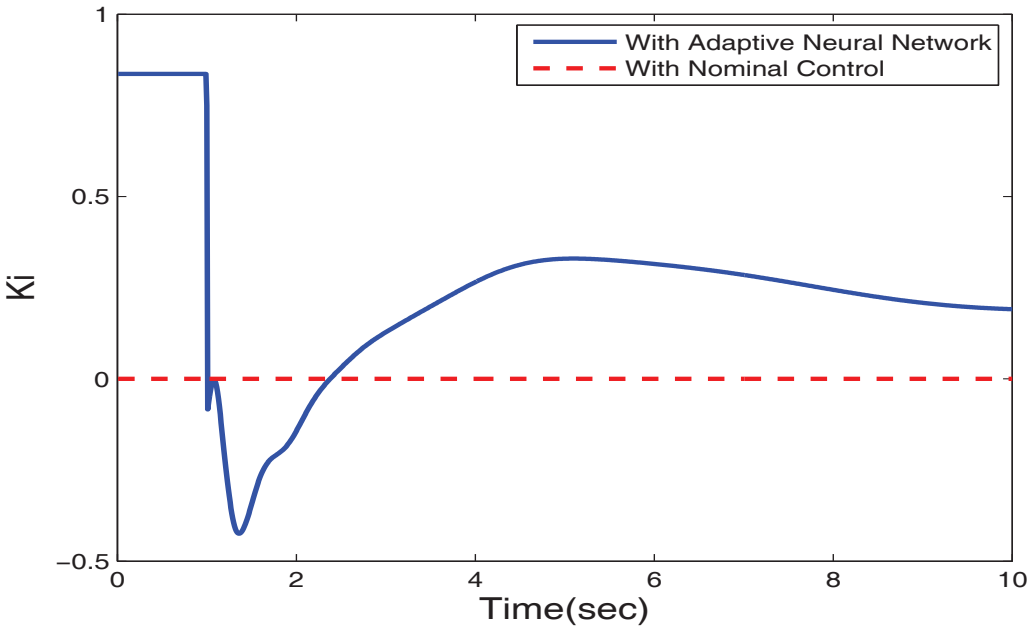

Figure 5.25: Variation of K_I with a step change in wind speed from 12m/s to 14m/s at t=1sec while K_I=0 for nominal control

5.5 Test Case III

In this particular case, a sinusoidal wind speed disturbance is applied to the system as shown in figure 5.26. Test cases I and II represented unrealistic changes in wind speeds. To demonstrate a higher practical value for this case, white noise has been added to the wind speed. The white noise will allow an impure sine wave to be generated and hence imparts randomness in the wind speed. The signal to noise ratio (SNR) for the white noise is set to be at 25 dB. This value was chosen as a SNR value much below 30 dB will distort the shape of the sine wave significantly.

The variation in mechanical power is shown in figure 5.27. The output electrical power also shows a sinusoidal response. The pitch angle variation is illustrated in figure 5.34. It is observed that with the wind speed varying sinusoidally, the pitch angle has the same response. It is also noted that as the pitch angle decreases, the mechanical power increases but the increase in electrical power takes place after a time delay because of the actuator that is connected between the pitch controller and the wind turbine. The increase in mechanical power can be explained in terms of the amount opening of the turbine blades. A decrease in pitch angle means that more wind power is allowed to pass through and hence more aerodynamic power is available for the generator.

The generator speed and variation in generator slip as in figures 5.28 and 5.29 also show a sinusoidal response after the disturbance, which is expected. From the terminal voltage response as illustrated in figure 5.30, it can be concluded that although the disturbance applied was sinusoidal, the voltage does not dip significantly and remains

within 5% of the initial value. The rest of the system states including the stator and rotor currents and DC link capacitor voltage shown in figures 5.31-5.33 show a relative sinusoidal response to the disturbance.

The controller gains are shown in figures 5.35 and 5.36. As the system states change, the gains are also updated by the adaptive neural network. As expected, the gains also show a sinusoidal response as they are updated. The slight glitches in the response are because of the white noise that has been added to the wind speed.

It is concluded that the adaptive neural network based pitch controller is capable of damping the transients in this case of wind speed variation, much better as compared to the nominal control.

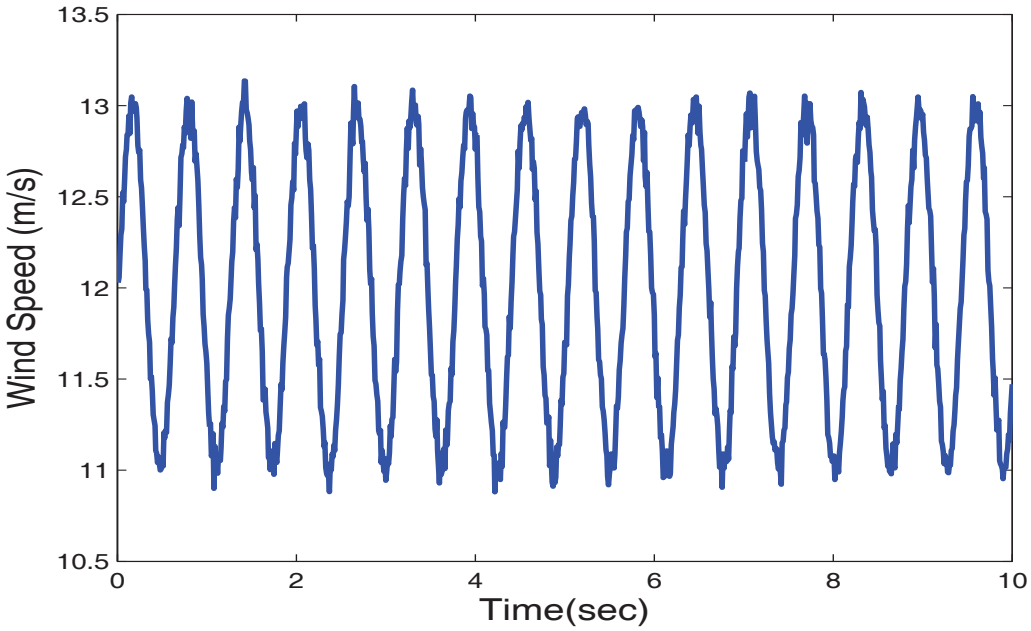

Figure 5.26: Test case wind speed

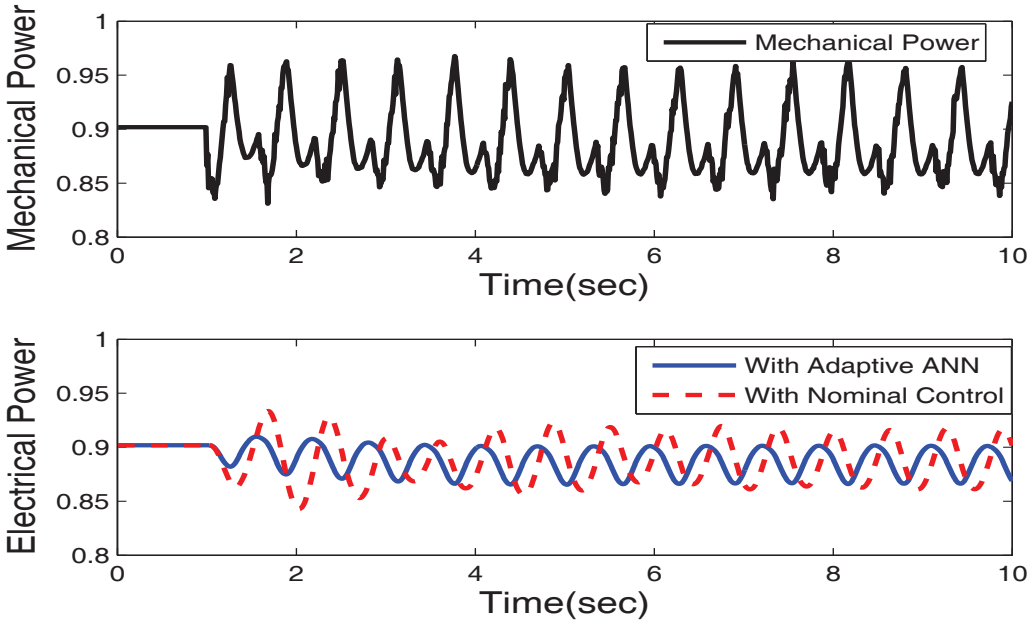

Figure 5.27: Output power with a sinusoidal change in wind speed at t=1sec (a) With adaptive neural network and (b) Nominal control scenario

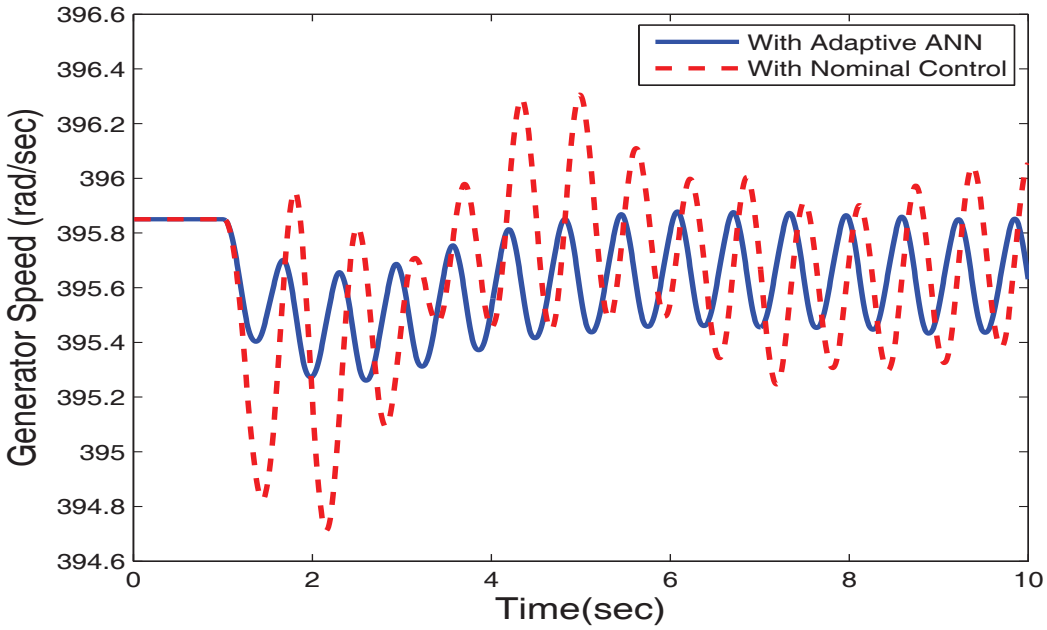

Figure 5.28: Generator speed with a sinusoidal change in wind speed at t=1sec (a) With adaptive neural network and (b) Nominal control scenario

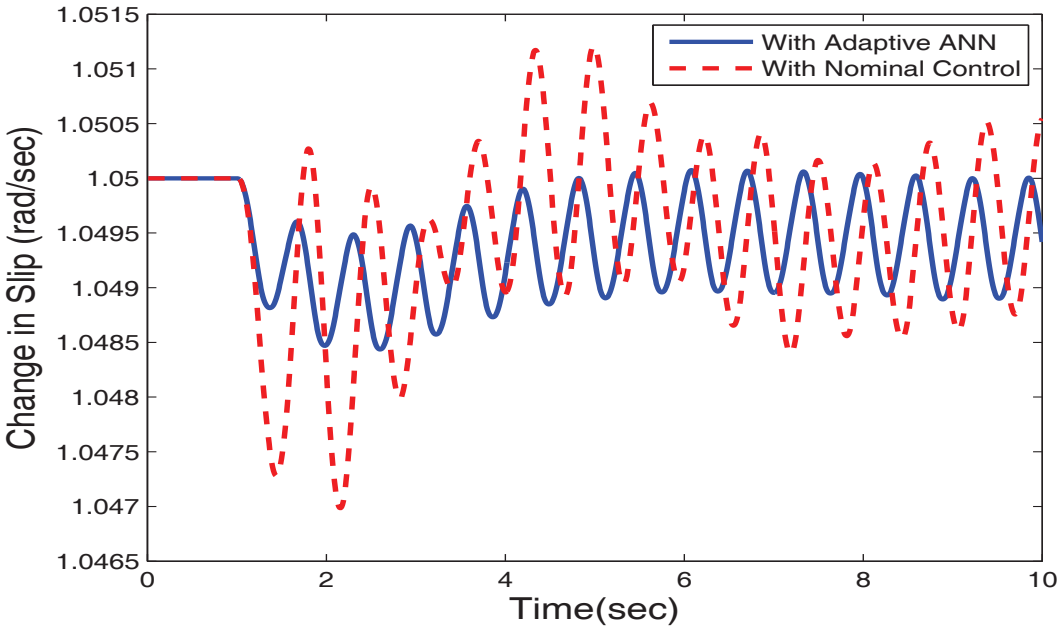

Figure 5.29: Change in slip with a sinusoidal change in wind speed at t=1sec (a) With adaptive neural network and (b) Nominal control scenario

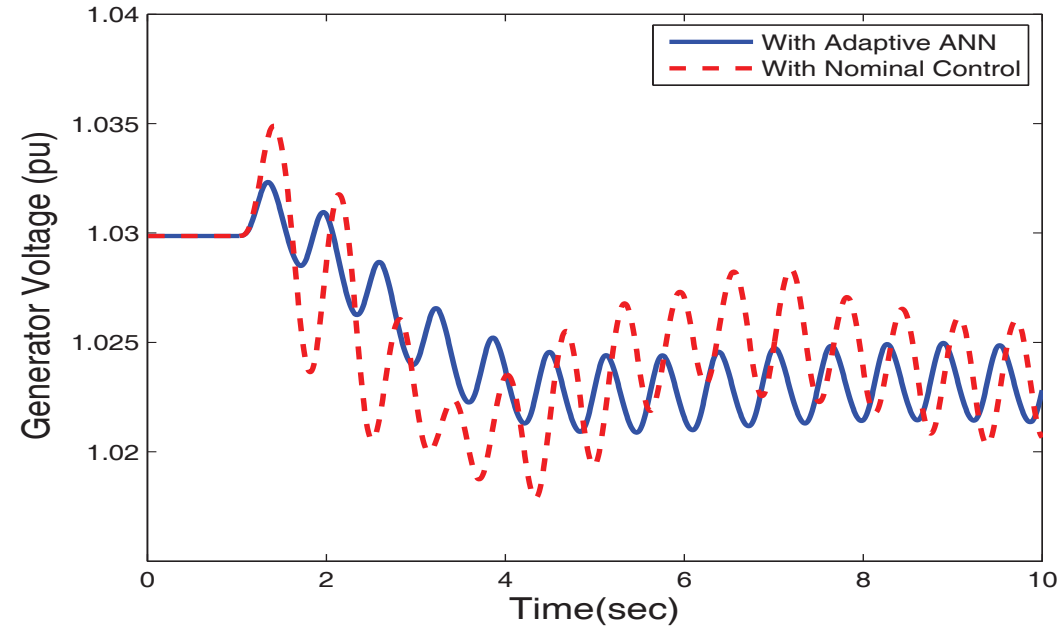

Figure 5.30: Terminal voltage with a sinusoidal change in wind speed at t=1sec (a) With adaptive neural network and (b) Nominal control scenario

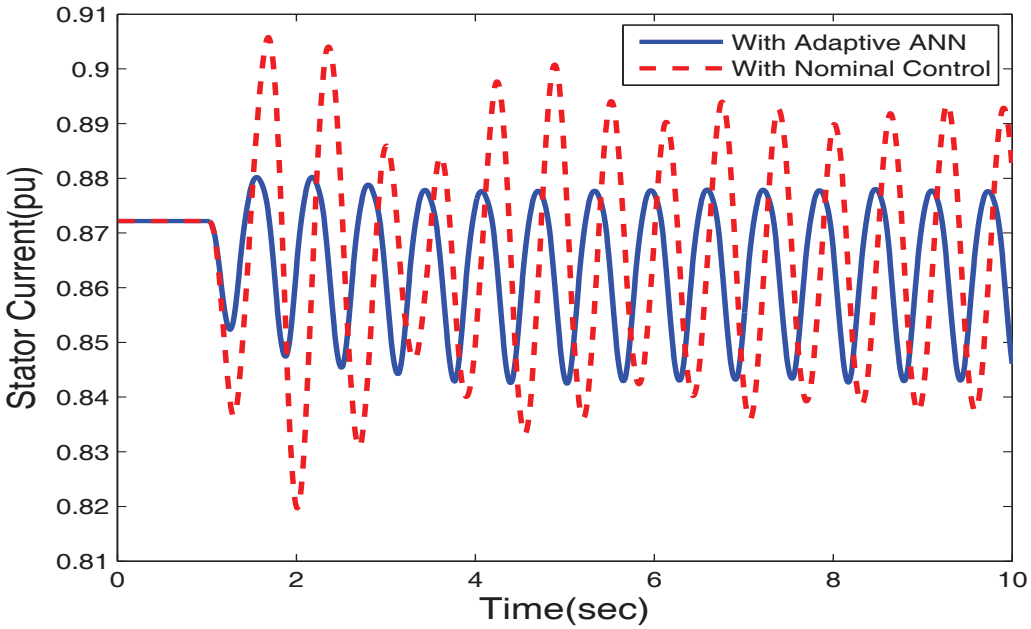

Figure 5.31: Response of stator current with a sinusoidal change in wind speed at t=1sec (a) With adaptive neural network and (b) Nominal control scenario

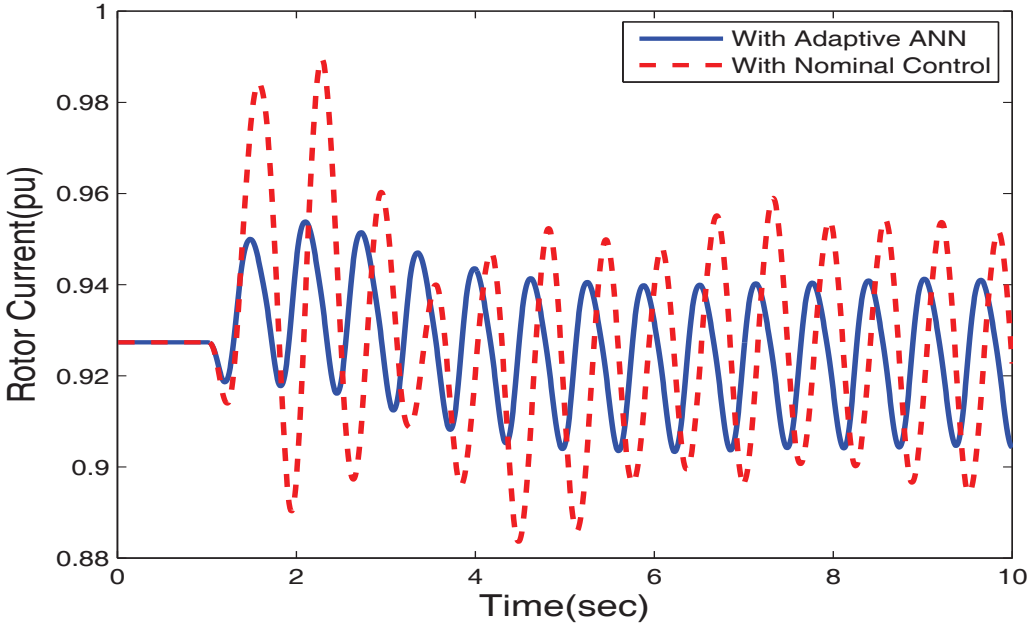

Figure 5.32: Response of rotor current with a sinusoidal change in wind speed at t=1sec (a) With adaptive neural network and (b) Nominal control scenario

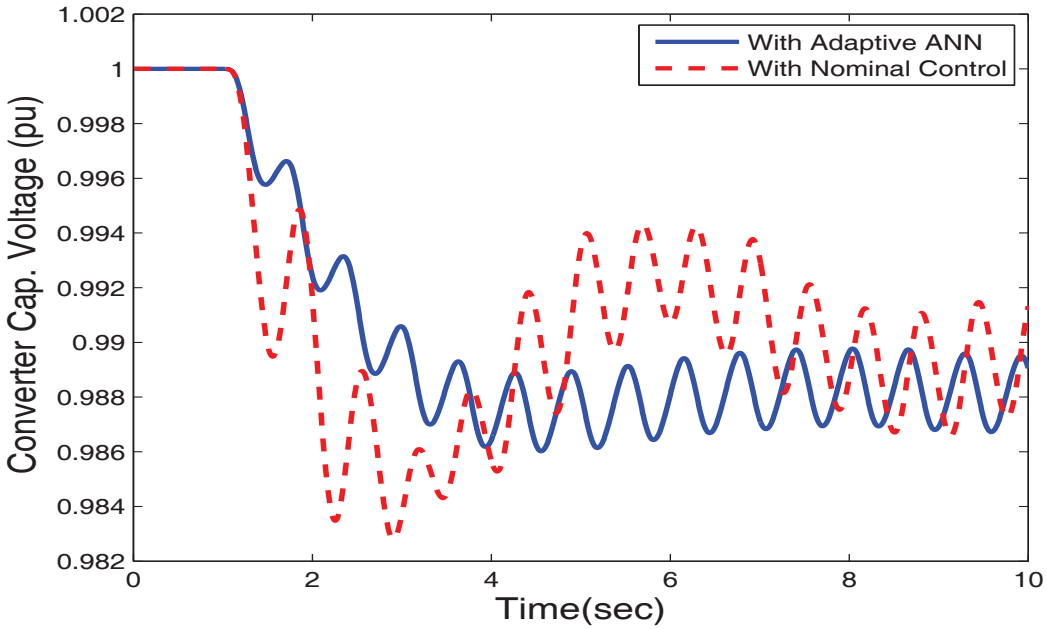

Figure 5.33: DC link capacitor voltage with a sinusoidal change in wind speed at t=1sec (a) With adaptive neural network and (b) Nominal control scenario

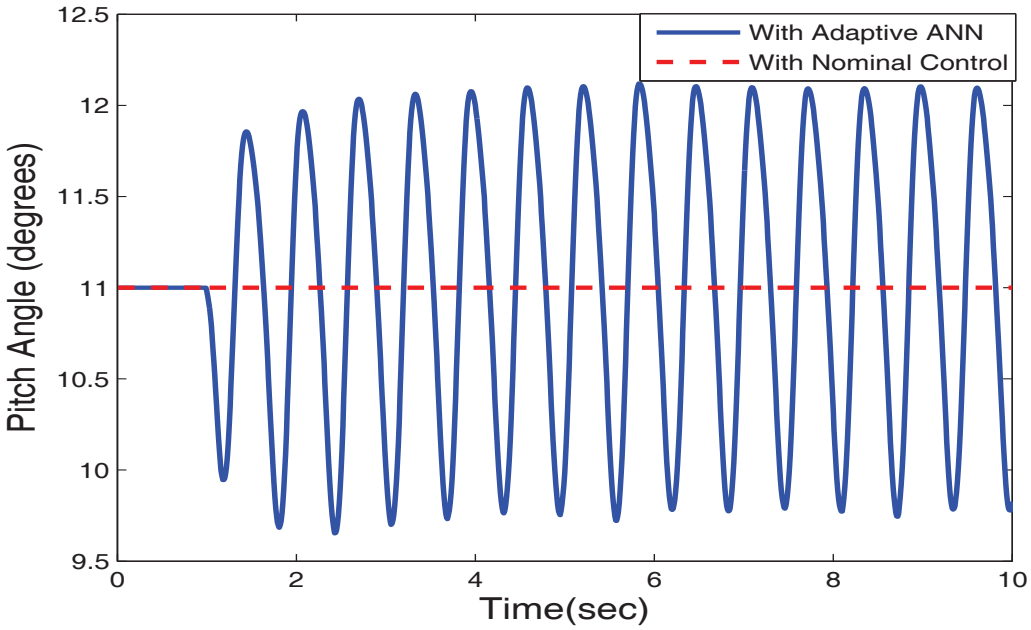

Figure 5.34: Pitch angle variation with a sinusoidal change in wind speed at t=1sec while $\beta = 11^0$ in nominal control scenario

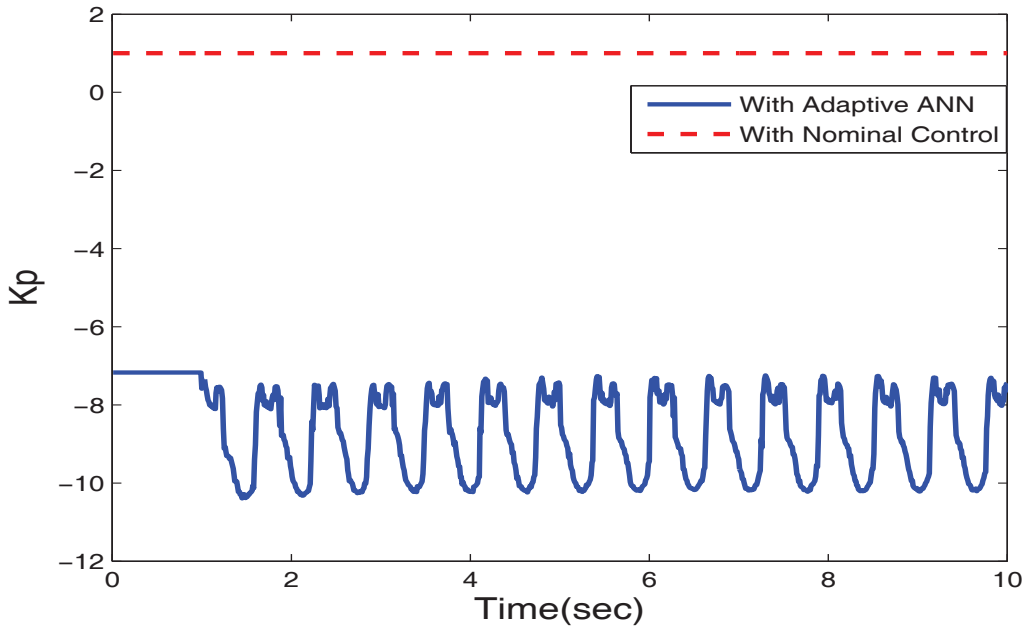

Figure 5.35: Variation of K_P with a sinusoidal change in wind speed at t=1sec while $K_P = 1$ in nominal control scenario

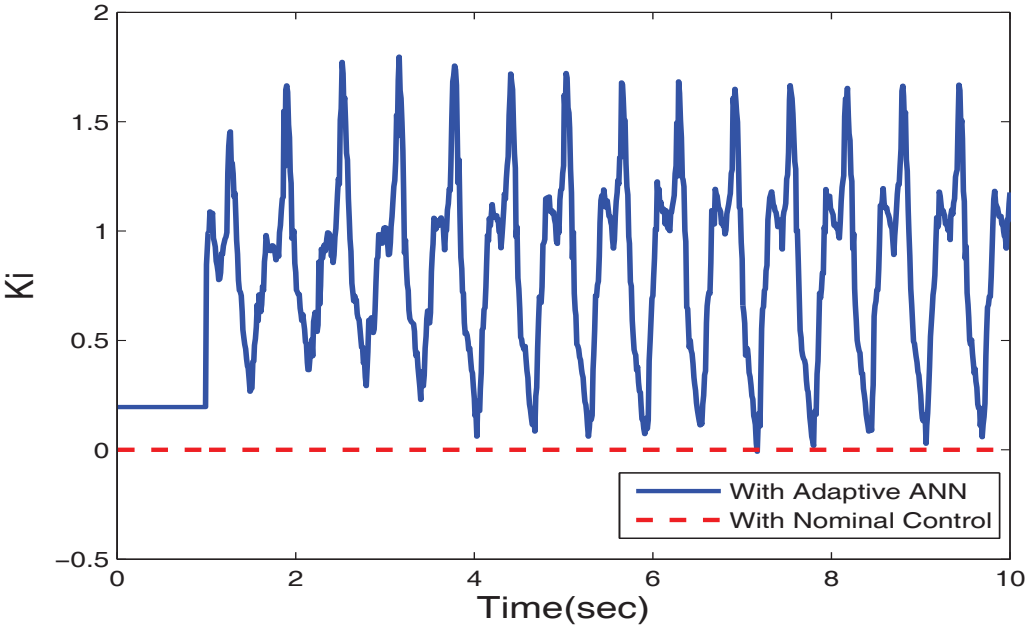

Figure 5.36: Variation of K_I with a sinusoidal change in wind speed at t=1sec while $K_I = 0$ in nominal control scenario

5.6 Test Case IV

To test the algorithm random wind data from KFUPM beach front was collected for the month of October 2010 and plotted as shown in figure 5.37. The data that is usually collected is after 10 minutes time stamp. The wind speeds were also scaled so as to meet the system requirements. For simulation work, this data is scaled to 10 seconds. This data is applied as a disturbance to the system at time t=1 sec. With the wind speeds changing rapidly, it is imperative to check that the system does not get unstable with such a disturbance.

The variation in mechanical and electrical power is shown in figure 5.38. As the pitch angle relative to the wind speed changes illustrated in figure 5.45 changes, the mechanical power also varies accordingly. From the electrical power plot, it is clear that the output power tracks the mechanical power that is available from the wind. It is also observed that contrary to the rapid changes in mechanical power, the electrical power supplied by the wind generator is smooth with least transients with an adaptive neural network based pitch controller.

The pitch angle variation can be compared with the wind speed data. The primary purpose of the pitch controller is to reduce the pitch angle when the wind speed goes below the rated wind speed and vise verse. Comparing figure 5.37 with 5.45 it is concluded that the pitch controller is performing the same task.

A controlled response of the generator speed, terminal voltage, stator and rotor currents and the DC link capacitor voltage is also observed from figures 5.40-5.44, with the adaptive neural network based pitch controller. The generator speed varies

between the mean of the wind speed data. The terminal voltage, shown in figure 5.41, demonstrates that the voltage remains within 5% of the initial value even with the random changes in wind speeds.

The controller parameters are updated regularly with changes in wind speeds and system states. This is clear from figures 5.46 and 5.47. This continuous update of gains allow for increased damping of the states. The nominal control is unable to cope with random change in wind speeds and hence it is observed that the transients are not damped and provides a poor response as compared to the adaptive neural network based controller.

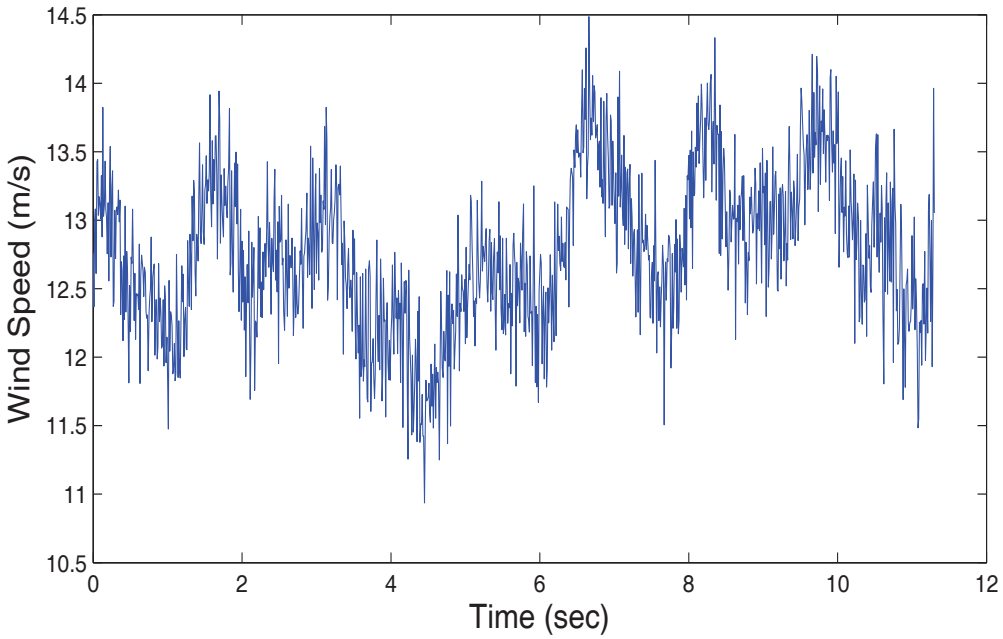

Figure 5.37: Scaled wind speeds as taken from KFUPM beach front

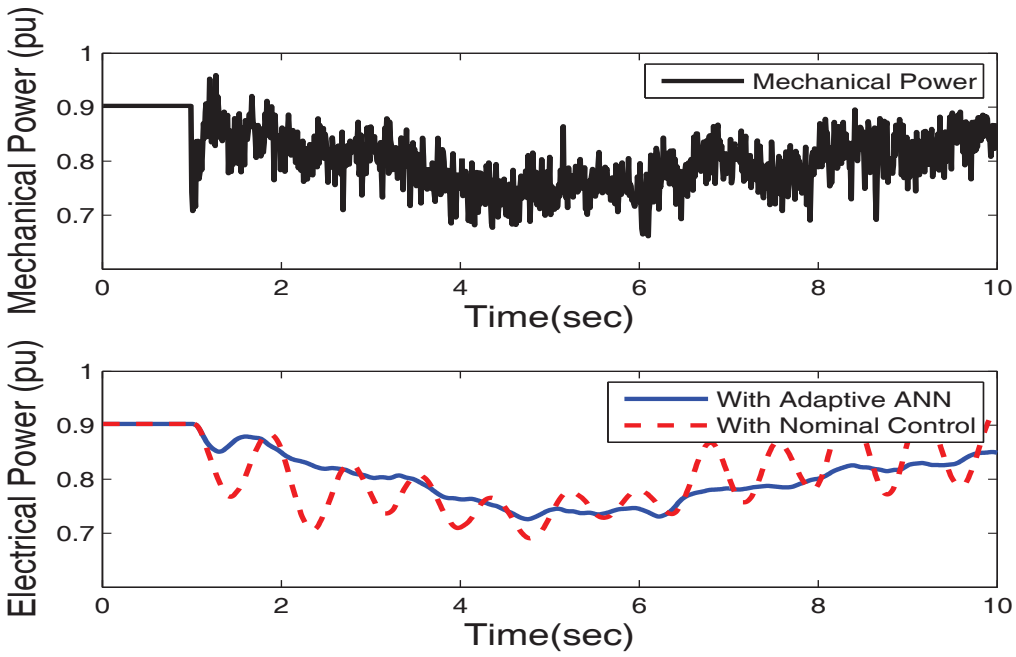

Figure 5.38: Mechanical power available from wind and the resultant electrical power from (a) With adaptive neural network and (b) Nominal control scenario

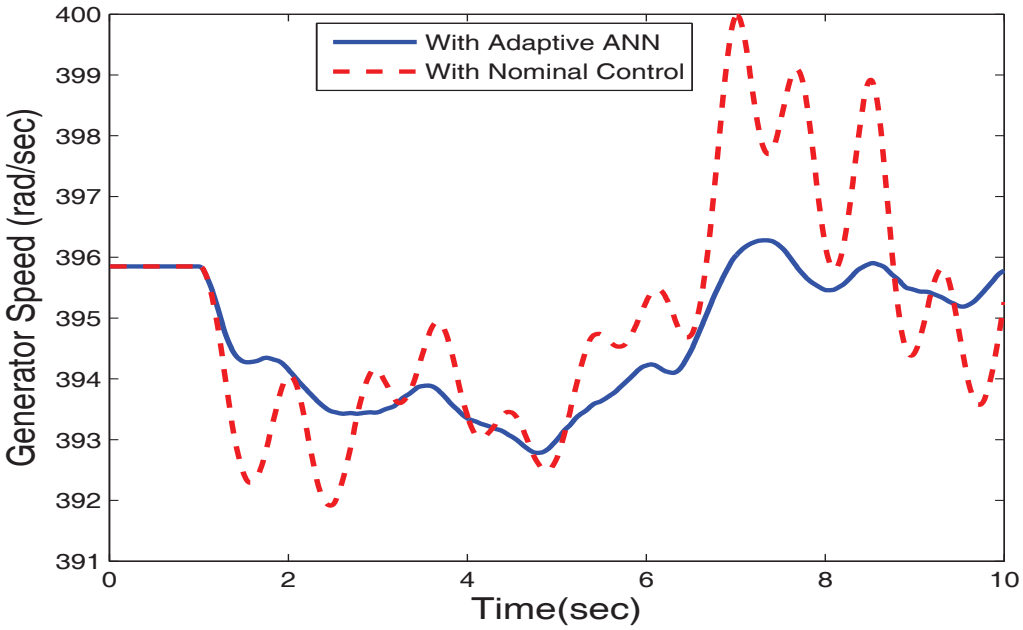

Figure 5.39: Generator speed with real wind data in (a) With adaptive neural network and (b) Nominal control scenario

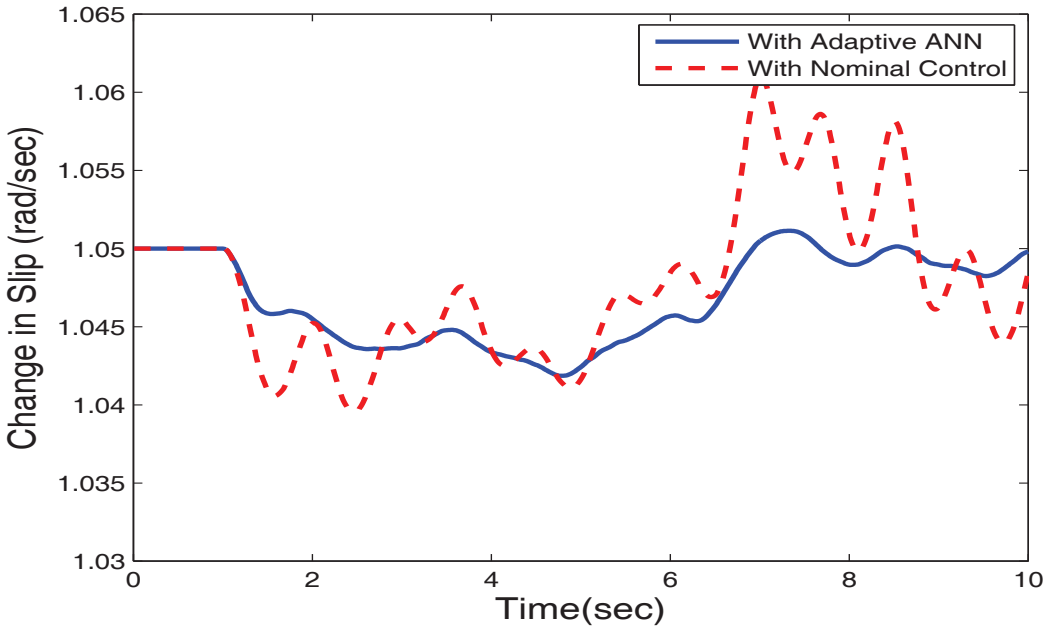

Figure 5.40: Change in slip with real wind data in (a) With adaptive neural network and (b) Nominal control scenario

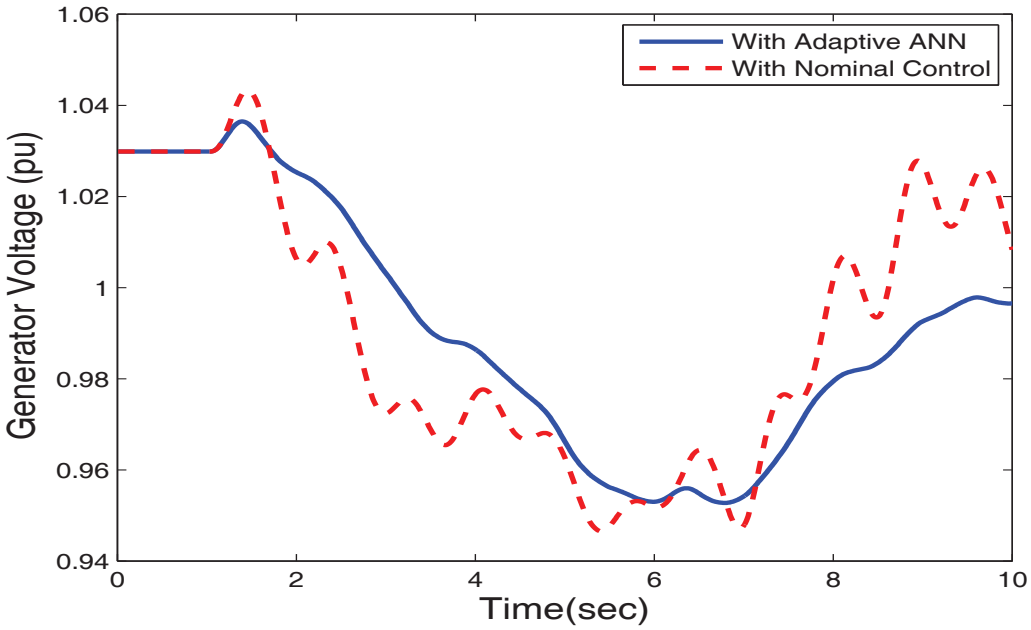

Figure 5.41: Variation in terminal voltage with real wind data (a) With adaptive neural network and (b) Nominal control scenario

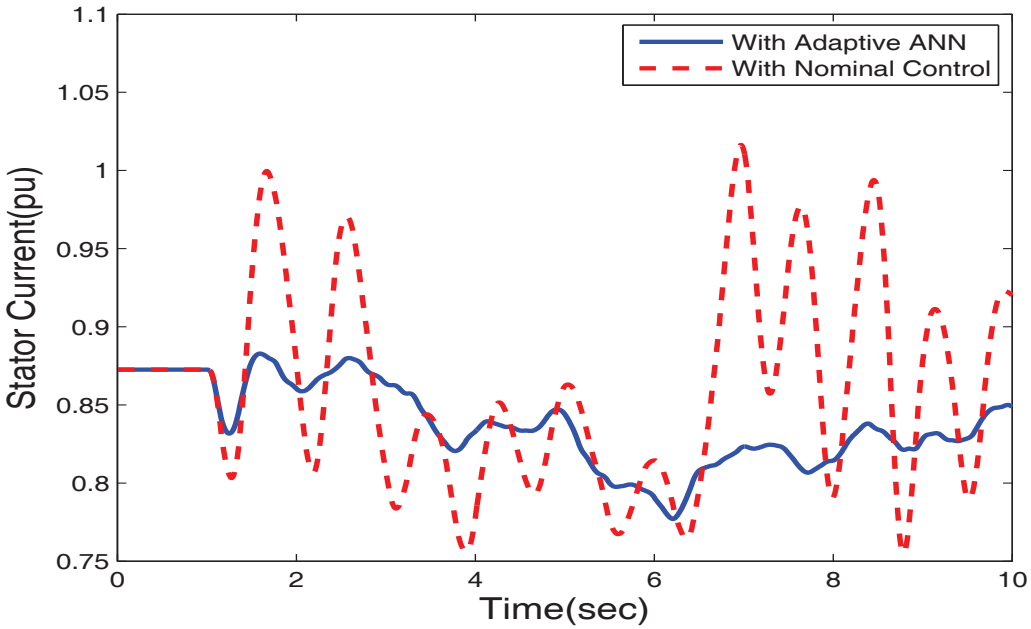

Figure 5.42: Response of stator current with real wind data in (a) With adaptive neural and (b) Nominal control scenario network

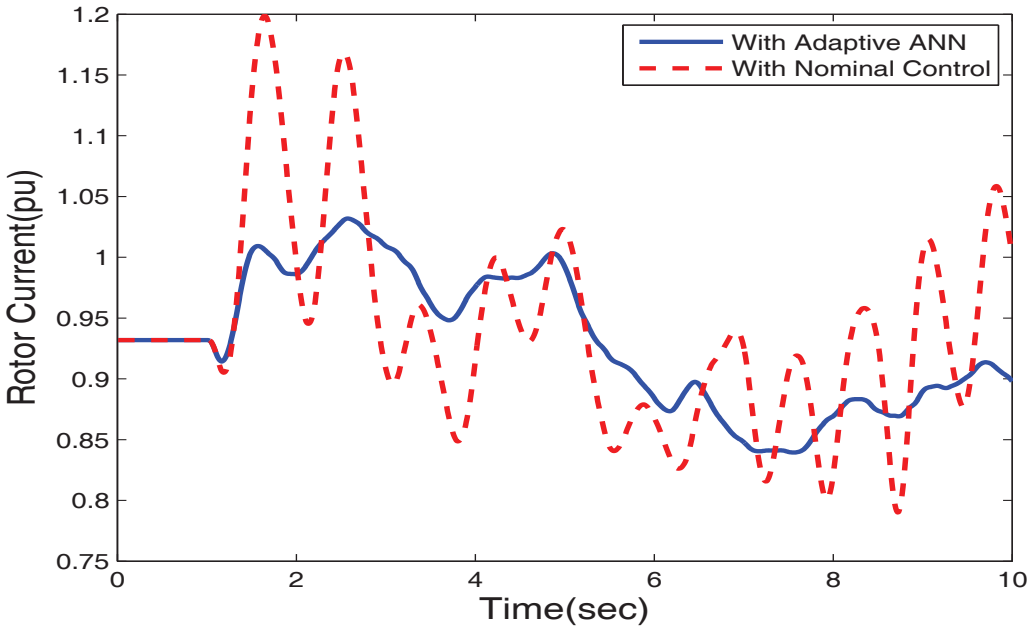

Figure 5.43: Response of rotor current with real wind data in (a) With adaptive neural network and (b) Nominal control scenario

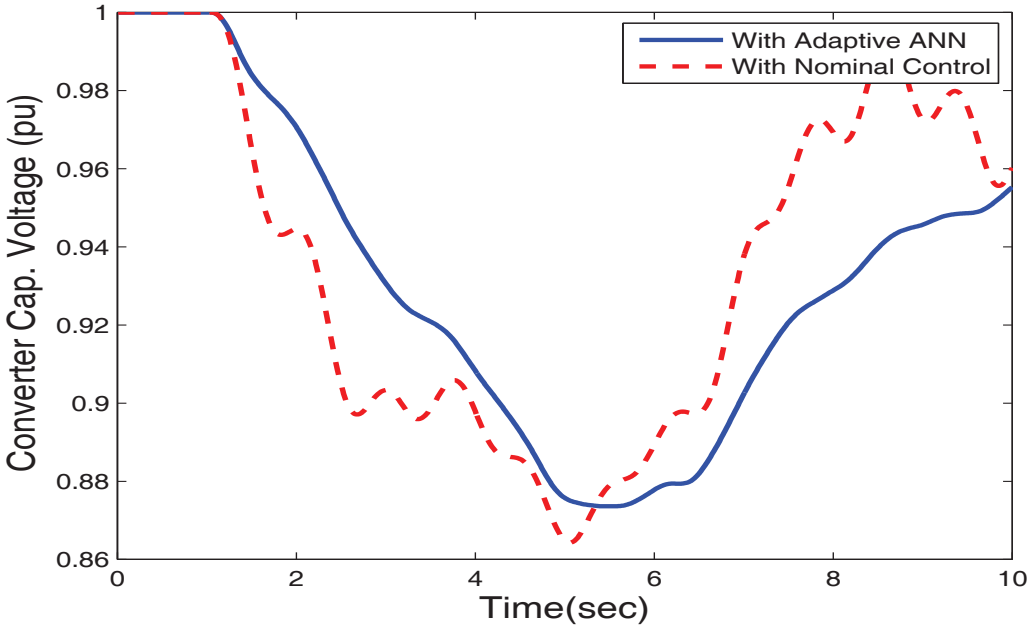

Figure 5.44: Response of rotor current with real wind data in (a) With adaptive neural network and (b) Nominal control scenario

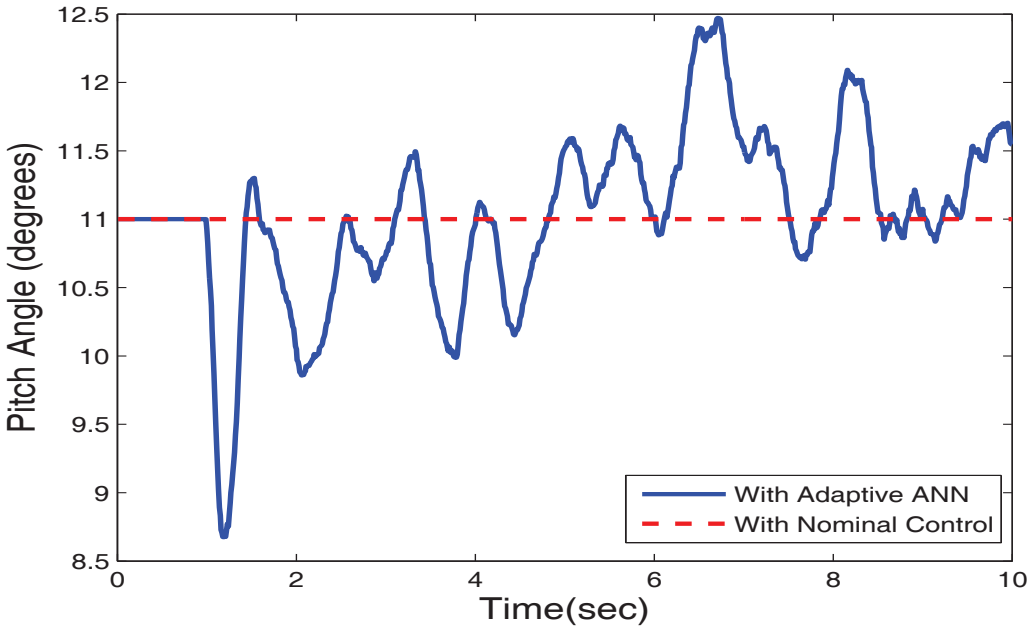

Figure 5.45: Variation of pitch angle β while $\beta = 11^0$ in nominal control scenario

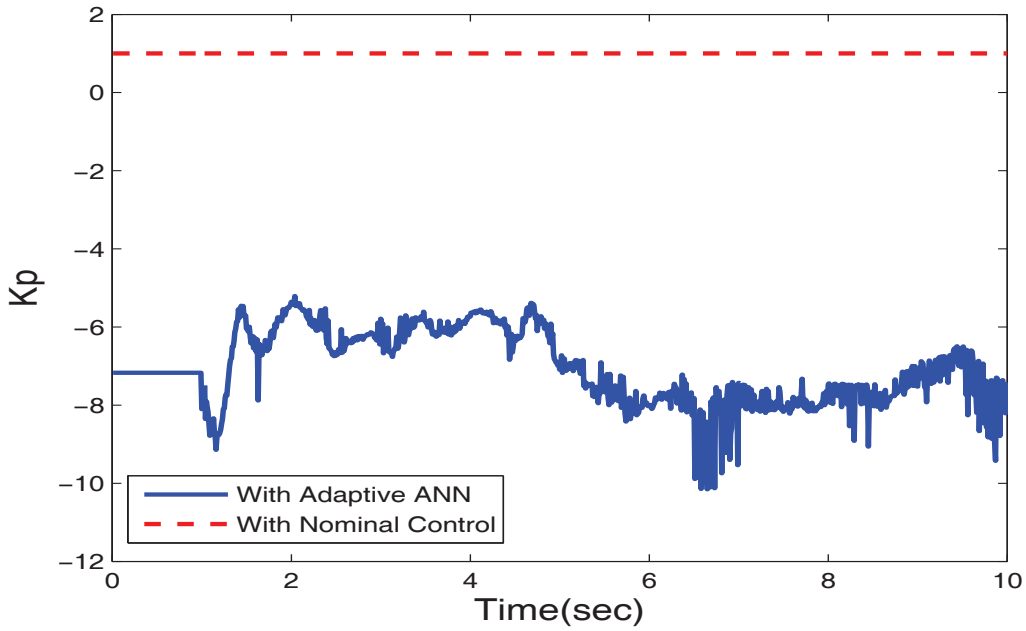

Figure 5.46: Variation of K_P while $K_P = 1$ in nominal control scenario

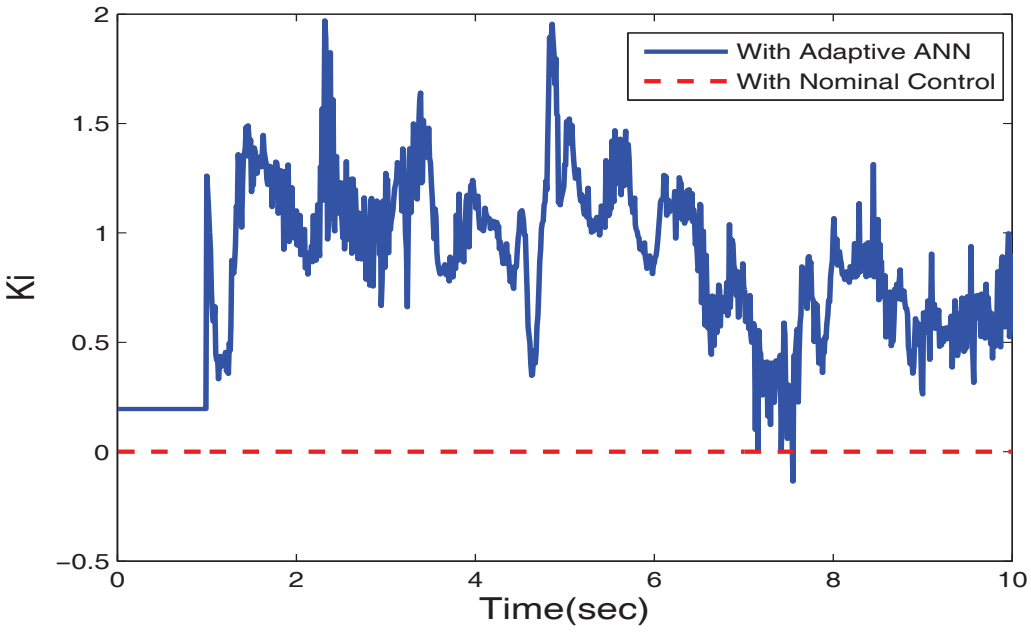

Figure 5.47: Variation of K_I while $K_I = 0$ in nominal control scenario

CHAPTER 6

CONCLUSION AND FUTURE WORK

6.1 Conclusion

A smart pitch control strategy, which adaptively tunes the controller parameters, is presented in this thesis. The strategy involves generation of the controller gains for the range of wind speeds through a differential evolution technique, training the control parameters through a back propagation neural network and adaptively tuning the network weights for random wind speeds and variable operating scenarios.

A complete dynamic model of DFIG system equipped with converter circuitry and pitch control system is developed. The model consists of the generator, wind turbine, aerodynamic and the converter systems. The pitch controller parameters were optimized using differential evolution intelligent technique, which made use of an eigenvalue based objective function to obtain the optimized values. The back

propagation neural network was trained using a large data set of varying wind speed conditions. The self tuning adaptive neural network updates the control parameters in response to variable system operating regimes.

System stability has been investigated from the eigenvalue analysis which shows that with nominal control the system is under damped while with pitch controller the system has sufficient damping to reduce the transients in the system states. Several cases have been studied, including a case with real wind data.

From the simulation results, it is observed that the pitch controlled system employed enables the electrical power to track the mechanical power from wind by varying the pitch angle of the blades. The adaptive neural network based pitch controller generates the necessary control to keep the system stable with minimum transients. The controls generated by the adaptive ANN controller are optimum controls from differential evolution algorithm for each wind speed disturbance and operating conditions. The adaptive ANN controller was compared with nominal control scenario, which is unable reduce the system transients and also incapable to allow the electrical power to track the mechanical power available from wind.

6.2 Future Work

There are several issues that are still to be addressed in the thesis subject:

- The pitch controller designed in this thesis, tries to achieve the reference mechanical power from wind but other maximum power point tracking (MPPT) configurations making use of converter controls for the generator can be incorporated to increase the efficiency of the system.

- Due to the stochastic nature of wind, pitch controllers designed through linear quadratic gaussian (LQG) methodology can also be studied. The LQG method will generate the necessary control by making use of an adaptive Kalman filter. Other techniques may involve, the use of linear quadratic and robust controllers.

- A study can be carried out for wind turbines equipped with pitch control and comparing the generation mix with other generating units in a smart grid environment.

- Instead of neural networks, fuzzy logic controllers can also be incorporated. The membership functions for these controllers can be made according to the system requirements. These membership functions will define the new pitch command depending upon the wind speed disturbance.

APPENDICES

Appendix A

System Data

Mean wind speed (V_w)	12 m/s
Radius of the blades (R)	13.5 m
Density of air (ρ)	1.225 kg/m^2
Turbine intertia (H_t)	2 s
Generator intertia (H_g)	0.5 s
Shaft stiffness (K_s)	0.3 p.u/el.rad
Stator reactance (x_s)	0.09241 p.u
Stator resistance (R_s)	0.00488 p.u
Rotor reactance (x_r)	0.2 p.u
Rotor resistance (R_r)	0.0059 p.u
Mutual inductance (x_m)	3.95379 p.u
Grid side converter circuit resistance (R_a)	0.001 p.u
Grid side converter circuit reactance (L_a)	0.1 p.u
Transmission line resistance (R)	0.02 p.u
Transmission line reactance (X)	0.15 p.u
Capacitor (C)	1.0 p.u
Load (Y_{11})	0.402-j0.0389 p.u

Table 1: System Data

Generator Modeling

The Induction Machine equations in generator convention is given by,

$$\boxed{\begin{aligned}
&\frac{1}{\omega_0}\dot{\Psi}_{ds} - \frac{\omega_e}{\omega_0}\dot{\Psi}_{qs} - R_s i_{ds} = v_{ds} \\
&\frac{1}{\omega_0}\dot{\Psi}_{qs} + \frac{\omega_e}{\omega_0}\dot{\Psi}_{ds} - R_s i_{qs} = v_{qs} \\
&\frac{1}{\omega_0}\dot{\Psi}_{dr} - s\dot{\Psi}_{qr} - R_r i_{dr} = v_{dr} \\
&\frac{1}{\omega_0}\dot{\Psi}_{qr} + s\dot{\Psi}_{dr} - R_r i_{qr} = v_{qr}
\end{aligned}} \tag{A.1}$$

Where,

$$\boxed{\begin{aligned}
\Psi_{ds} &= -x_s i_{ds} - x_m i_{dr} \\
\Psi_{qs} &= -x_s i_{qs} - x_m i_{qr} \\
\Psi_{dr} &= -x_r i_{dr} - x_m i_{ds} \\
\Psi_{qr} &= -x_r i_{qr} - x_m i_{qs}
\end{aligned}} \tag{A.2}$$

Substitute (A.2) in (A.1)

$$-x_s\dot{i}_{ds} - x_m\dot{i}_{dr} + \omega_e\left(x_s i_{qs} + x_m i_{qr}\right) - \omega_0 R_s i_{ds} = \omega_0 v_{ds} \tag{A.3}$$

$$-x_s\dot{i}_{qs} - x_m\dot{i}_{qr} + \omega_e\left(-x_s i_{qs} - x_m i_{dr}\right) - \omega_0 R_s i_{qs} = \omega_0 v_{qs} \tag{A.4}$$

$$-x_r\dot{i}_{dr} - x_m\dot{i}_{ds} + \omega_0 s x_r i_{qr} + \omega_0 s x_m i_{qs} - \omega_0 R_r i_{dr} = \omega_0 v_{dr} \tag{A.5}$$

$$-x_r\dot{i}_{qr} - x_m\dot{i}_{qs} - \omega_0 s x_r i_{dr} - \omega_0 s x_m i_{ds} - \omega_0 R_r i_{qr} = \omega_0 v_{qr} \tag{A.6}$$

Combining (A.3),(A.5) and (A.4),(A.6) gives (A.7) and(A.8)

$$\begin{bmatrix} -x_s & -x_m \\ -x_m & -x_r \end{bmatrix} \begin{bmatrix} \dot{i_{ds}} \\ \dot{i_{dr}} \end{bmatrix} = \begin{bmatrix} \omega_0 R_s & -\omega_e x_s & 0 & -\omega_e x_m \\ 0 & -\omega_0 s x_m & \omega_0 R_r & -\omega_0 s x_r \end{bmatrix} \begin{bmatrix} i_{ds} \\ i_{qs} \\ i_{dr} \\ i_{qr} \end{bmatrix} + \begin{bmatrix} \omega_0 v_{ds} \\ \omega_0 v_{dr} \end{bmatrix} \quad \text{(A.7)}$$

$$\begin{bmatrix} -x_s & -x_m \\ -x_m & -x_r \end{bmatrix} \begin{bmatrix} \dot{i_{qs}} \\ \dot{i_{qr}} \end{bmatrix} = \begin{bmatrix} \omega_e x_s & -\omega_0 R_s & \omega_e x_m & 0 \\ \omega_e s x_m & 0 & \omega_0 s x_r & -\omega_0 R_r \end{bmatrix} \begin{bmatrix} i_{ds} \\ i_{qs} \\ i_{dr} \\ i_{qr} \end{bmatrix} + \begin{bmatrix} \omega_0 v_{qs} \\ \omega_0 v_{qr} \end{bmatrix} \quad \text{(A.8)}$$

Pre-multiplying the inverse of $\begin{bmatrix} -x_s & -x_m \\ -x_m & -x_r \end{bmatrix}$ on both sides of (A.7) and(A.8) gives (A.9) and (A.10),

$$\begin{bmatrix} \dot{i_{ds}} \\ \dot{i_{dr}} \end{bmatrix} = \frac{1}{x_s x_r - {x_m}^2} \begin{bmatrix} -\omega_0 R_s x_r & \omega_0 \left(x_r x_s - s{x_m}^2\right) & \omega_0 R_r x_m & \omega_0 x_m x_r \left(1 - s\right) \\ \omega_0 R_s x_m & \omega_0 x_s x_m \left(s - 1\right) & -\omega_0 x_s R_r & \omega_0 \left(s x_r x_s - {x_m}^2\right) \end{bmatrix} \cdot \begin{bmatrix} i_{ds} \\ i_{qs} \\ i_{dr} \\ i_{qr} \end{bmatrix} + \frac{1}{x_s x_r - {x_m}^2} \begin{bmatrix} -\omega_0 x_r v_{ds} + \omega_0 x_m v_{dr} \\ \omega_0 x_m v_{ds} - \omega_0 x_s v_{dr} \end{bmatrix} \quad \text{(A.9)}$$

$$\begin{bmatrix} \dot{i_{qs}} \\ \dot{i_{qr}} \end{bmatrix} = \frac{1}{x_s x_r - {x_m}^2} \begin{bmatrix} \omega_0 \left(s{x_m}^2 - x_s x_r \right) & -\omega_0 R_s x_r & \omega_0 x_m x_r \left(s-1 \right) & \omega_0 R_r x_m \\ \omega_0 x_s x_m \left(1-s \right) & \omega_0 x_m R_s & \omega_0 \left({x_m}^2 - s x_r x_s \right) & -\omega_0 R_r x_s \end{bmatrix} \cdot \begin{bmatrix} i_{ds} \\ i_{qs} \\ i_{dr} \\ i_{qr} \end{bmatrix} + \frac{1}{x_s x_r - {x_m}^2} \begin{bmatrix} -\omega_0 x_r v_{qs} + \omega_0 x_m v_{qr} \\ \omega_0 x_m v_{qs} - \omega_0 x_s v_{qr} \end{bmatrix} \quad \text{(A.10)}$$

Combining (A.9) and (A.10),

$$\begin{bmatrix} \dot{i_{ds}} \\ \dot{i_{qs}} \\ \dot{i_{dr}} \\ \dot{i_{qr}} \end{bmatrix} = \begin{bmatrix} a(1,1) & a(1,2) & a(1,3) & a(1,4) \\ a(2,1) & a(2,2) & a(2,3) & a(2,4) \\ a(3,1) & a(3,2) & a(3,3) & a(3,4) \\ a(4,1) & a(4,2) & a(4,3) & a(4,4) \end{bmatrix} \begin{bmatrix} i_{ds} \\ i_{qs} \\ i_{dr} \\ i_{qr} \end{bmatrix} + \begin{bmatrix} b(1,1) & 0 & b(1,3) & 0 \\ 0 & b(2,2) & 0 & b(2,4) \\ b(3,1) & 0 & b(3,3) & 0 \\ 0 & b(4,2) & 0 & b(4,4) \end{bmatrix} \begin{bmatrix} v_{ds} \\ v_{qs} \\ v_{dr} \\ v_{qr} \end{bmatrix} \quad \text{(A.11)}$$

Where,

$$
\begin{aligned}
a(1,1) =& \frac{1}{x_s x_r - {x_m}^2} \left(-\omega_0 R_s x_r\right) \\
a(1,2) =& \frac{1}{x_s x_r - {x_m}^2} \left(\omega_0 \left(x_r x_s - s{x_m}^2\right)\right) \\
a(1,3) =& \frac{1}{x_s x_r - {x_m}^2} \left(\omega_0 R_r x_m\right) \\
a(1,4) =& \frac{1}{x_s x_r - {x_m}^2} \left(\omega_0 x_m x_r \left(1-s\right)\right)
\end{aligned}
\tag{A.12}
$$

$$
\begin{aligned}
a(2,1) =& \frac{1}{x_s x_r - {x_m}^2} \left(\omega_0 \left(s{x_m}^2 - x_s x_r\right)\right) \\
a(2,2) =& \frac{1}{x_s x_r - {x_m}^2} \left(-\omega_0 R_s x_r\right) \\
a(2,3) =& \frac{1}{x_s x_r - {x_m}^2} \left(\omega_0 x_m x_r \left(s-1\right)\right) \\
a(2,4) =& \frac{1}{x_s x_r - {x_m}^2} \left(\omega_0 R_r x_m\right)
\end{aligned}
\tag{A.13}
$$

$$
\begin{aligned}
a(3,1) =& \frac{1}{x_s x_r - {x_m}^2} \left(\omega_0 R_s x_m\right) \\
a(3,2) =& \frac{1}{x_s x_r - {x_m}^2} \left(\omega_0 x_s x_m \left(s-1\right)\right) \\
a(3,3) =& \frac{1}{x_s x_r - {x_m}^2} \left(-\omega_0 x_s R_r\right) \\
a(3,4) =& \frac{1}{x_s x_r - {x_m}^2} \left(\omega_0 \left(s x_r x_s - {x_m}^2\right)\right)
\end{aligned}
\tag{A.14}
$$

$$
\begin{aligned}
a(4,1) =& \frac{1}{x_s x_r - {x_m}^2} \left(\omega_0 x_s x_m \left(1 - s\right)\right) \\
a(4,2) =& \frac{1}{x_s x_r - {x_m}^2} \left(\omega_0 x_m R_s\right) \\
a(4,3) =& \frac{1}{x_s x_r - {x_m}^2} \left(\omega_0 \left({x_m}^2 - s x_r x_s\right)\right) \\
a(4,4) =& \frac{1}{x_s x_r - {x_m}^2} \left(-\omega_0 R_r x_s\right)
\end{aligned}
\tag{A.15}
$$

$$
\begin{aligned}
b(1,1) =& \frac{1}{x_s x_r - {x_m}^2} \left(-\omega_0 x_r\right) \\
b(1,3) =& \frac{1}{x_s x_r - {x_m}^2} \left(\omega_0 x_m\right)
\end{aligned}
\tag{A.16}
$$

$$
\begin{aligned}
b(2,2) =& \frac{1}{x_s x_r - {x_m}^2} \left(-\omega_0 x_r\right) \\
b(2,4) =& \frac{1}{x_s x_r - {x_m}^2} \left(\omega_0 x_m\right)
\end{aligned}
\tag{A.17}
$$

$$
\begin{aligned}
b(3,1) =& \frac{1}{x_s x_r - {x_m}^2} \left(\omega_0 x_m\right) \\
b(3,3) =& \frac{1}{x_s x_r - {x_m}^2} \left(-\omega_0 x_s\right)
\end{aligned}
\tag{A.18}
$$

$$
\begin{aligned}
b(4,2) =& \frac{1}{x_s x_r - {x_m}^2} \left(\omega_0 x_m\right) \\
b(4,4) =& \frac{1}{x_s x_r - {x_m}^2} \left(-\omega_0 x_s\right)
\end{aligned}
\tag{A.19}
$$

Initial Conditions:

In order to find the initial conditions of the system, we have to make use of figure1.

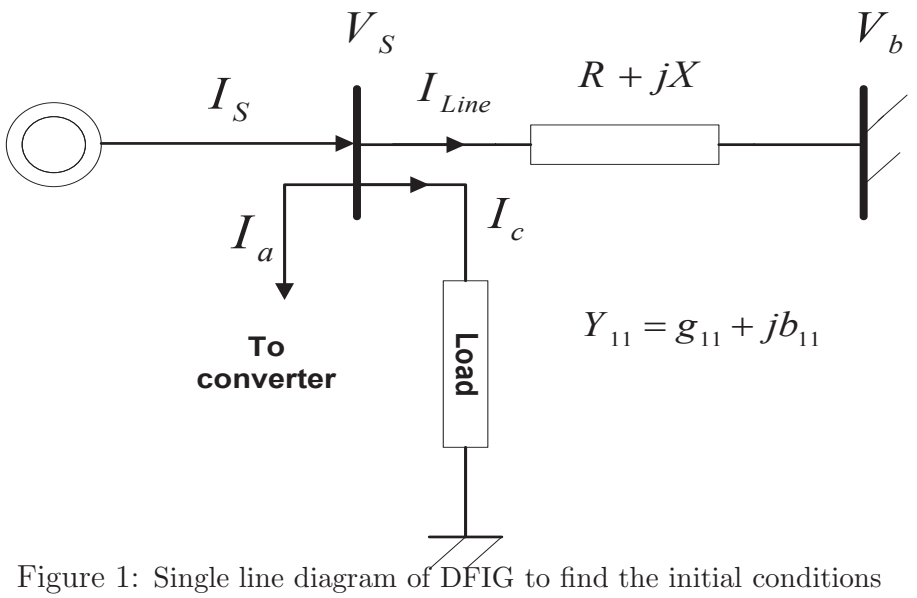

Figure 1: Single line diagram of DFIG to find the initial conditions

$$I_s = I_a + I_c + I_{Line} \tag{A.20}$$

$$I_s - I_a = V_s\, Y_{11} + I_{Line}$$

$$I_s - I_a = V_s\, Y_{11} + [(V_s - V_b)\, Y_{12}]$$

$$\boxed{I_s - I_a = V_s\,[Y_{11} + Y_{12}] - V_b\, Y_{12}} \tag{A.21}$$

Writing the terminal voltage, the stator current and the converter current in its $d - q$

components.

$$V_s = v_{ds} + j v_{qs} \tag{A.22}$$

$$I_s = i_{ds} + j i_{qs} \tag{A.23}$$

$$I_a = i_{ad} + j i_{aq} \tag{A.24}$$

$\Rightarrow$ We can write A.2 as,

$$(v_{ds} + j v_{qs})\,[Y_{11} + Y_{12}] = V_b\,[g_{12} + j b_{12}] + [i_{ds} + j i_{qs} - (i_{ad} + j i_{aq})] \tag{A.25}$$

$$(v_{ds} + j v_{qs})\,[g_{11} + g_{12} + j b_{11} + b_{12}] = V_b\,[g_{12} + j b_{12}] + [i_{ds} + j i_{qs} - (i_{ad} + j i_{aq})] \tag{A.26}$$

Separating the real and imaginary components

$$\boxed{\begin{aligned} (g_{11} + g_{12})\,v_{ds} - (b_{11} + b_{12})\,v_{qs} &= V_b g_{12} + (i_{ds} - i_{ad}) \\ (b_{11} + b_{12})\,v_{ds} + (g_{11} + g_{12})\,v_{qs} &= V_b b_{12} + (i_{qs} - i_{aq}) \end{aligned}} \tag{A.27}$$

Writing in matrix form,

$$\begin{bmatrix} (g_{11} + g_{12}) & -(b_{11} + b_{12}) \\ (b_{11} + b_{12}) & (g_{11} + g_{12}) \end{bmatrix} \begin{bmatrix} v_{ds} \\ v_{qs} \end{bmatrix} = \begin{bmatrix} g_{12} \\ b_{12} \end{bmatrix} V_b + \begin{bmatrix} i_{ds} - i_{ad} \\ i_{qs} - i_{aq} \end{bmatrix} \tag{A.28}$$

$$\boxed{\begin{bmatrix} v_{ds} \\ v_{qs} \end{bmatrix} = \begin{bmatrix} z_{11} & z_{12} \\ z_{21} & z_{22} \end{bmatrix} \begin{bmatrix} g_{12} \\ b_{12} \end{bmatrix} V_b + \begin{bmatrix} z_{11} & z_{12} \\ z_{21} & z_{22} \end{bmatrix} \begin{bmatrix} i_{ds} - i_{ad} \\ i_{qs} - i_{aq} \end{bmatrix}} \tag{A.29}$$

Where impedance matrix, $\begin{bmatrix} z_{11} & z_{12} \\ z_{21} & z_{22} \end{bmatrix}$ is given by the inverse of $\begin{bmatrix} (g_{11} + g_{12}) & -(b_{11} + b_{12}) \\ (b_{11} + b_{12}) & (g_{11} + g_{12}) \end{bmatrix}$. The individual elements of the impedance matrix are found as,

$$z_{11} = \frac{(g_{11} + g_{12})}{(g_{11} + g_{12})^2 + (b_{11} + b_{12})^2} \tag{A.30}$$

$$z_{12} = \frac{(b_{11} + b_{12})}{(g_{11} + g_{12})^2 + (b_{11} + b_{12})^2} \tag{A.31}$$

$$z_{21} = \frac{-(b_{11} + b_{12})}{(g_{11} + g_{12})^2 + (b_{11} + b_{12})^2} \tag{A.32}$$

$$z_{22} = \frac{(g_{11} + g_{12})}{(g_{11} + g_{12})^2 + (b_{11} + b_{12})^2} \tag{A.33}$$

Equating v_{ds},v_{qs},v_{dr} and v_{qr} given by the induction generator model given by,

$$\boxed{\begin{aligned} v_{ds} &= -R_s i_{ds} + x_s i_{qs} + x_m i_{qr} \\ v_{qs} &= -x_{ss} i_{ds} - R_s i_{qs} - X_m i_{dr} \\ v_{dr} &= s x_m i_{qs} - R_r i_{dr} + s x_{rr} i_{qr} \\ v_{qr} &= -s x_m i_{qs} - R_r i_{qr} - s x_{rr} i_{dr} \end{aligned}} \tag{A.34}$$

Substituting the set (A.15) equations in (A.10)

$$\begin{bmatrix} -(R_s + z_{11}) & (x_s + z_{12}) & 0 & x_m \\ -(x_{ss} + z_{21}) & -(R_s + z_{22}) & -x_m & 0 \\ 0 & sx_m & -R_r & sx_{rr} \\ -sx_m & 0 & -sx_{rr} & -R_r \end{bmatrix} \begin{bmatrix} i_{ds} \\ i_{qs} \\ i_{dr} \\ i_{qr} \end{bmatrix} = \begin{bmatrix} z_{11}\, g_{12} + z_{12}\, b_{12} \\ z_{21}\, g_{12} + z_{22}\, b_{12} \\ v_{dr} \\ v_{qr} \end{bmatrix} V_b - \begin{bmatrix} z_{11}\, i_{ad} + z_{12}\, i_{aq} \\ z_{21}\, i_{ad} + z_{22}\, i_{aq} \\ 0 \\ 0 \end{bmatrix} \quad \text{(A.35)}$$

Appendix B

Linearization

The non-linear state equations of the system are linearized around an operating point.

Stator d-axis current (i_{ds}):

$$\boxed{\dot{i_{ds}} = a(1,1)i_{ds} + a(1,2)i_{qs} + a(1,3)i_{dr} + a(1,4)i_{qr} + b(1,1)v_{ds} + b(1,3)v_{dr}} \quad \text{(B.1)}$$

Substituting the constant values we have,

$$\begin{aligned} \dot{i_{ds}} &= \frac{1}{x_s x_r - {x_m}^2}\Big\{\omega R_s x_r i_{ds} + \omega\left(x_s x_r - s{x_m}^2\right) i_{qs} + \omega R_r x_m i_{dr} \\ &\quad + \omega x_r x_m \left(1-s\right) i_{qr} - \left(\omega x_r\right) v_{ds} + \left(\omega x_m\right) v_{dr}\Big\} \end{aligned} \tag{B.2}$$

Linearizing (B.2)

$$\begin{aligned} \left(\dot{i_{ds}} + \Delta\dot{i_{ds}}\right) &= \frac{1}{x_s x_r - {x_m}^2}\Big\{\left(-\omega R_s x_r\right)\left(i_{ds0} + \Delta i_{ds}\right) + \omega\left(x_s x_r - \left(s_0 + \Delta s\right){x_m}^2\right)\cdot \\ &\quad \left(i_{qs0} + \Delta i_{qs}\right) + \left(\omega R_r x_m\right)\left(i_{dr0} + \Delta i_{dr}\right) + \\ &\quad \left(\omega x_r x_m\right)\left(1 - \left(s_0 + \Delta s\right)\right)\left(i_{qr0} + \Delta i_{qr}\right) - \left(\omega x_r\right)\left(v_{ds0} + \Delta v_{ds}\right) \\ &\quad + \left(\omega x_m\right)\left(v_{dr0} + \Delta v_{dr}\right)\Big\} \end{aligned} \tag{B.3}$$

$$\begin{aligned} \left(\dot{i_{ds}} + \Delta\dot{i_{ds}}\right) &= \frac{1}{x_s x_r - {x_m}^2}\Big\{\left(\omega R_s x_r\right) i_{ds0} - \left(\omega R_s x_r\right)\Delta i_{ds} + \left(\omega x_s x_r\right) i_{qs0} \\ &\quad + \left(\omega x_s x_r\right)\Delta i_{qs} + \left(-\omega s_0 {x_m}^2\right) i_{qs0} + \left(-\omega s_0 {x_m}^2\right)\Delta i_{qs} \\ &\quad - \left(\omega {x_m}^2 i_{qs0}\right)\Delta s + \left(\omega R_r x_m\right) i_{dr0} + \left(\omega R_r x_m\right)\Delta i_{dr} \\ &\quad \left(\omega x_r x_m\right)\left(i_{qr0} + \Delta i_{qr} - s_0 i_{qr0} - s_0 \Delta i_{qr} - \Delta s i_{qr0}\right) \\ &\quad - \left(\omega x_r\right)\left(v_{ds} + \Delta v_{ds}\right) + \left(\omega x_m\right)\left(v_{dr} + \Delta v_{dr}\right)\Big\} \end{aligned}$$

$$\boxed{\begin{aligned}\Delta\dot{i}_{ds} = \frac{1}{x_s x_r - {x_m}^2}\Big\{ & \left(-\omega R_s x_r\right)\Delta i_{ds} + \left(\omega x_s x_r - \omega s_0 {x_m}^2\right)\Delta i_{qs} \\ & - \left({x_m}^2 \omega i_{qs0} - \omega x_r x_m i_{qr0}\right)\Delta\omega_g + \left(\omega x_r x_m - \omega x_r x_m s_0\right)\Delta i_{qr} \\ & + \left(\omega x_r\right) z_{11}\Delta i_{ad} + \left(\omega x_r\right) z_{12}\Delta i_{aq} + \left(\omega x_m\right)\left(m_2 \cos\alpha_2\right)\Delta V_c \\ & + \left(\omega x_r\right) z_{11}\Delta i_{dg} + \left(\omega x_r\right) z_{12}\Delta i_{qg}\Big\}\end{aligned}} \tag{B.4}$$

Stator q-axis current (i_{qs}):

$$\boxed{\dot{i_{qs}} = a(2,1)i_{ds} + a(2,2)i_{qs} + a(2,3)i_{dr} + a(2,4)i_{qr} + b(2,2)v_{qs} + b(2,4)v_{qr}} \tag{B.5}$$

Substituting the constant values we have,

$$\begin{aligned}\dot{i_{qs}} = & \frac{1}{x_s x_r - {x_m}^2}\Big\{\omega\left(s{x_m}^2 - x_r x_s\right) i_{ds} - \left(\omega R_s x_r\right) i_{qs} \\ & + \left(\omega x_r x_m\left(s-1\right)\right) i_{dr} + \left(\omega R_r x_m\right) i_{qr} - \left(\omega x_r\right) v_{qs} \\ & + \left(\omega x_m\right) v_{qr}\Big\}\end{aligned} \tag{B.6}$$

Linearizing (B.7)

$$\begin{aligned}\left(\dot{i_{qs}} + \Delta\dot{i}_{qs}\right) = & \frac{1}{x_s x_r - {x_m}^2}\Big\{\omega\left(\left(s_0 + \Delta s\right){x_m}^2 - x_r x_s\right)\left(i_{ds0} + \Delta i_{ds}\right) - \left(\omega R_s x_r\right)\cdot \\ & \left(i_{qs0} + \Delta i_{qs}\right) + \left(\omega x_r x_m\left(\left(s_0 + \Delta s\right) - 1\right)\right)\left(i_{dr0} + \Delta i_{dr}\right) \\ & + \left(\omega R_r x_m\right)\left(i_{qr0} + \Delta i_{qr}\right) - \left(\omega x_r\right)\left(v_{qs0} + \Delta v_{qs}\right) \\ & + \left(\omega x_m\right)\left(v_{qr0} + \Delta v_{qr}\right)\Big\}\end{aligned} \tag{B.7}$$

$$\begin{aligned}\left(\dot{i_{qs}} + \Delta\dot{i_{qs}}\right) &= \frac{1}{x_s x_r - {x_m}^2}\Big\{\omega\left(s_0 {x_m}^2 - x_r x_s\right) i_{ds0} + \omega\left(s_0 {x_m}^2 - x_r x_s\right)\Delta i_{ds} \\ &\quad + \left(\omega {x_m}^2 i_{ds0}\right)\Delta s - \left(\omega R_s x_r\right) i_{qs0} - \left(\omega R_s x_r\right)\Delta i_{qs} \\ &\quad + \left(\omega x_r x_m\left(s_0 - 1\right)\right) i_{dr} + \left(\omega x_r x_m\left(s_0 - 1\right)\right)\Delta i_{dr} \\ &\quad + \left(\omega x_r x_m i_{dr0}\right)\Delta s + \left(\omega R_r x_m\right) i_{qr0} + \left(\omega R_r x_m\right)\Delta i_{qr} \\ &\quad - \left(\omega x_r\right) v_{qs} - \left(\omega x_r\right)\Delta v_{qs} + \left(\omega x_m\right) v_{qr} + \left(\omega x_m\right)\Delta v_{qr}\Big\} \end{aligned} \tag{B.8}$$

$$\begin{aligned}\Delta\dot{i_{qs}} = \frac{1}{x_s x_r - {x_m}^2}\Big\{&\omega\left(s_0 {x_m}^2 - x_r x_s\right)\Delta i_{ds} - \left(\omega R_s x_r\right)\Delta i_{qs} \\ &+ \left(\omega {x_m}^2 i_{ds0} + \omega x_r x_m i_{dr0}\right)\Delta\omega_g + \left(\omega x_r x_m\left(s_0 - 1\right)\right)\Delta i_{dr} \\ &+ \left(\omega R_r x_m\right)\Delta i_{qr} - \left(\omega x_r\right) z_{21}\Delta i_{ds} - \left(\omega x_r\right) z_{22}\Delta i_{qs} \\ &+ \left(\omega x_r\right) z_{21}\Delta i_{ad} + \left(\omega x_r\right) z_{22}\Delta i_{aq} + \left(\omega x_m\right)\left(m_2 \sin\alpha_2\right)\Delta V_c\Big\}\end{aligned} \tag{B.9}$$

Rotor d-axis current (i_{dr}):

$$\dot{i_{dr}} = a(3,1) i_{ds} + a(3,2) i_{qs} + a(3,3) i_{dr} + a(3,4) i_{qr} + b(3,1) v_{ds} + b(3,3) v_{dr} \tag{B.10}$$

Substituting the constant values we have,

$$\begin{aligned}\dot{i_{dr}} &= \frac{1}{x_s x_r - {x_m}^2}\Big\{\left(\omega R_s x_m\right) i_{ds} + \left(\omega x_m x_s\left(s_0 - 1\right)\right) i_{qs} - \left(\omega R_r X_s\right) i_{dr} \\ &\quad + \left(\omega\left(s_0 x_r x_s - {x_m}^2\right)\right) i_{qr} + \left(\omega x_m\right) v_{ds} - \left(\omega x_s\right) v_{dr}\Big\}\end{aligned} \tag{B.11}$$

Linearizing (B.12)

$$\begin{aligned}\left(\dot{i_{dr}} + \Delta\dot{i_{dr}}\right) &= \frac{1}{x_s x_r - {x_m}^2}\Big\{ \left(\omega R_s x_m\right)\left(i_{ds} + \Delta i_{ds}\right) + \left(\omega x_m x_s\left(\left(s_0 + \Delta s\right) - 1\right)\right) \\ &\quad \left(i_{qs} + \Delta i_{qs}\right) - \left(\omega R_r x_s\right)\left(i_{dr} + \Delta i_{dr}\right) \\ &\quad + \left(\omega\left(\left(s_0 x_r x_s\right) + \Delta s\left(x_r x_s\right) - {x_m}^2\right)\right)\left(i_{qr} + \Delta i_{qr}\right) \\ &\quad + \left(\omega x_m\right)\left(v_{ds0} + \Delta v_{ds}\right) - \left(\omega x_s\right)\left(v_{dr0} + \Delta v_{dr}\right)\Big\} \end{aligned} \tag{B.12}$$

$$\begin{aligned}\left(\dot{i_{dr}} + \Delta\dot{i_{dr}}\right) &= \frac{1}{x_s x_r - {x_m}^2}\Big\{ \left(\omega R_s x_m\right) i_{ds0} + \left(\omega R_s x_m\right)\Delta i_{ds} \\ &\quad + \left(\omega x_m x_s\left(s_0 - 1\right)\right) i_{qs0} + \left(\omega x_m x_s\left(s_0 - 1\right)\right)\Delta i_{qs} \\ &\quad + \left(\omega x_m x_s i_{qs0}\right)\Delta s - \left(\omega R_r x_s\right) i_{dr0} - \left(\omega x_r x_s\right)\Delta i_{dr} \\ &\quad + \left(\omega\left(s_0 x_r x_s - {x_m}^2\right)\right) i_{qr0} + \left(\omega\left(s_0 x_r x_s - {x_m}^2\right)\right)\Delta i_{qr} \\ &\quad + \left(\omega x_r x_s i_{qr0}\right)\Delta s + \left(\omega x_m\right) v_{ds0} + \left(\omega x_m\right)\Delta v_{ds} \\ &\quad - \left(\omega x_s\right) v_{dr0} - \left(\omega x_s\right)\Delta v_{dr}\Big\} \end{aligned} \tag{B.13}$$

$$\begin{aligned}\Delta\dot{i}_{dr} = \frac{1}{x_s x_r - {x_m}^2}\Big\{ &\left(\omega R_s x_m\right)\Delta i_{ds} + \left(\omega x_m x_s\left(s_0 - 1\right)\right)\Delta i_{qs} \\ &- \left(\omega R_r x_s\right)\Delta i_{dr} + \left(\omega\left(s_0 x_r x_s - {x_m}^2\right)\right)\Delta i_{qr} \\ &+ \left(\omega x_m x_s i_{qs0} + \omega x_r x_s i_{qr0}\right)\Delta\omega_g + \left(\omega x_m\right) z_{11}\Delta i_{ds} \\ &+ \left(\omega x_m\right) z_{12}\Delta i_{qs} + \left(\omega x_s\right) z_{11}\Delta i_{ad} + \left(\omega x_s\right) z_{12}\Delta i_{aq} \\ &- \left(\omega x_s m_2 \cos\alpha_2\right)\Delta V_c\Big\} \end{aligned} \tag{B.14}$$

Rotor q-axis current (i_{qr}):

$$\boxed{\dot{i_{qr}} = a(4,1)i_{ds} + a(4,2)i_{qs} + a(4,3)i_{dr} + a(4,4)i_{qr} + b(4,2)v_{qs} + b(4,4)v_{qr}} \quad \text{(B.15)}$$

Substituting the constant values we have,

$$\begin{aligned} \dot{i_{qr}} &= \frac{1}{x_s x_r - {x_m}^2}\Big\{ \left(\omega x_s x_m \left(1-s\right)\right) i_{ds} + \left(\omega R_s x_m\right) i_{qs} + \left(\omega \left({x_m}^2 - s x_r x_s\right)\right) i_{dr} \\ &\quad - \left(\omega R_r x_s\right) i_{qr} + \left(\omega x_m\right) v_{qs} - \left(\omega x_s\right) v_{qr} \Big\} \end{aligned} \quad \text{(B.16)}$$

Linearizing (B.17)

$$\begin{aligned} \left(\dot{i_{qr}} + \Delta\dot{i_{qr}}\right) &= \frac{1}{x_s x_r - {x_m}^2}\Big\{ \left(\omega x_s x_m \left(1-\left(s_0+\Delta s\right)\right)\right)\left(i_{ds0}+\Delta i_{ds}\right) \\ &\quad + \left(\omega R_s x_m\right)\left(i_{qs0}+\Delta i_{qs}\right) + \left(\omega \left({x_m}^2 - \left(s_0+s\right) x_r x_s\right)\right)\left(i_{dr0}+\Delta i_{dr}\right) \\ &\quad - \left(\omega R_r x_s\right)\left(i_{qr0}+\Delta i_{qr}\right) + \left(\omega x_m\right)\left(v qs + \Delta v_{qs}\right) \\ &\quad - \left(\omega x_s\right)\left(v_{qr}+\Delta v_{qr}\right) \Big\} \end{aligned} \quad \text{(B.17)}$$

$$\begin{aligned} \left(\dot{i_{qr}} + \Delta\dot{i_{qr}}\right) &= \frac{1}{x_s x_r - {x_m}^2}\Big\{ \left(\omega x_s x_m \left(1-s_0\right)\right) i_{ds0} + \left(\omega x_s x_m \left(1-s_0\right)\right)\Delta i_{ds} \\ &\quad - \left(\omega x_s x_m i_{ds0}\right)\Delta s + \left(\omega R_s x_m\right) i_{ds0} + \left(\omega R_s x_m\right)\Delta i_{ds} \\ &\quad + \left(\omega \left({x_m}^2 - s_0 x_r x_s\right)\right)\Delta i_{dr} - \left(\omega x_r x_s i_{dr0}\right)\Delta s \\ &\quad - \left(\omega R_r x_s\right) i_{qr0} - \left(\omega R_r x_s\right)\Delta i_{qr} + \left(\omega x_m\right) v_{qs0} \\ &\quad + \left(\omega x_m\right)\Delta v_{qs} - \left(\omega x_s\right) v_{qr0} - \left(\omega x_s\right)\Delta v_{qr} \Big\} \end{aligned} \quad \text{(B.18)}$$

$$\boxed{\begin{aligned}\Delta\dot{i}_{qr} = \frac{1}{x_s x_r - {x_m}^2}\Big\{ & \left(\omega x_s x_m \left(1 - s_0\right)\right)\Delta i_{ds} + \left(\omega R_s x_m\right)\Delta i_{qs} \\ & + \left(\omega\left({x_m}^2 - s_0 x_r x_s\right)\right)\Delta i_{dr} - \left(\omega R_r x_s\right)\Delta i_{qr} \\ & - \left(\omega x_s x_m i_{ds0} + \omega\left(x_r x_s\right) i_{dr0}\right)\Delta\omega_g - \left(\omega x_m\right) z_{21}\Delta i_{ad} \\ & - \left(\omega x_m\right) z_{22}\Delta i_{aq} - \left(\omega x_s m_2 \sin\alpha_2\right)\Delta V_c\Big\}\end{aligned}} \tag{B.19}$$

Mechanical Power (P_m):

Mechanical Power P_m is given by,

$$\boxed{P_m = \frac{1}{2}\rho\pi R^2 V_w^3 C_p\left(\lambda,\beta\right)} \tag{B.20}$$

Power Coefficient $C_p\left(\lambda,\beta\right)$ is given by,

$$\boxed{\begin{aligned} C_p\left(\lambda,\beta\right) &= 0.5176\left[\frac{116}{\lambda_i - 0} - 0.4\beta - 5\right]\mathrm{e}^{\frac{-21}{\lambda_i}} + 0.0068\lambda \\ \frac{1}{\lambda_i} &= \frac{1}{\lambda + 0.08\beta} - \frac{0.035}{\beta^3 + 1}\end{aligned}} \tag{B.21}$$

Substituting λ_i in $C_p\left(\lambda,\beta\right)$ expression,

$$C_p\left(\lambda,\beta\right) = 0.5176\left[\frac{116}{\lambda + 0.08\beta} - \frac{4.06}{\beta^3 + 1}\right]\mathrm{e}^{\left[-\frac{21}{\lambda + 0.08\beta} + \frac{0.735}{\beta^3 + 1}\right]} + 0.0068\lambda \tag{B.22}$$

Replacing λ with: equation $\boxed{\lambda = \frac{\omega_t R}{V}}$ equation in (B.23)

$$C_p\left(\lambda,\beta\right) = 0.5176\left[\frac{116}{\frac{\omega_t R}{V}+0.08\beta} - \frac{4.06}{\beta^3+1}\right] \mathrm{e}^{\left[-\frac{21}{\frac{\omega_t R}{V}+0.08\beta}+\frac{0.735}{\beta^3+1}\right]} + 0.0068\frac{\omega_t R}{V} \quad \text{(B.23)}$$

Taking partial derivative w.r.t. ω_T

$$\begin{aligned}\frac{\partial C_p\left(\lambda,\beta\right)}{\partial \omega_t} = 0.5176\Bigg\{ & \left[116\left(\frac{\omega_t R}{V}+0.08\beta\right)^{-1} - \frac{4.06}{\beta^3+1}\right] \\ & \cdot \mathrm{e}^{\left[-21\left(\frac{\omega_t R}{V}+0.08\beta\right)^{-1}+0.735\left(\beta^3+1\right)^{-1}\right]} \cdot \left(\frac{21}{\frac{\omega_t R}{V}} \cdot \frac{R}{V}\right)\Bigg\} \\ & + 0.5176\Bigg\{\mathrm{e}^{\left[-21\left(\frac{\omega_t R}{V}+0.08\beta\right)^{-1}+0.735\left(\beta^3+1\right)^{-1}\right]} \cdot \\ & - 116\left(\left(\frac{\omega_t R}{V}+0.08\beta\right)^{-2} \cdot \frac{R}{V}\right)\Bigg\}\end{aligned} \quad \text{(B.24)}$$

Taking partial derivative w.r.t. β

$$\begin{aligned}\frac{\partial C_p\left(\lambda,\beta\right)}{\partial \beta} = 0.5176\Bigg\{ & \left[\frac{116}{\left(\frac{\omega_{t0} R}{V}+0.08\beta_0\right)} - \frac{0.035}{\left(\beta_0^3+1\right)} - 0.4\beta_0 - 5\right] \cdot \\ & \mathrm{e}^{-21\left[\left(\frac{\omega_{t0} R}{V}+0.08\beta_0\right)^{-1}-0.035\left(\beta_0^3+1\right)^{-1}\right]} \cdot \\ & \left[1.68\left(\frac{\omega_{t0} R}{V}+0.08\beta_0\right)^{-2} - 2.205\beta_0^2\left(\beta_0^3+1\right)^{-2}\right]\Bigg\} \\ & + 0.5176\left[\mathrm{e}^{-21\left(\frac{\omega_{t0} R}{V}+0.08\beta_0\right)^{-1}-0.035\left(\beta_0^3+1\right)^{-1}}\right] \cdot \\ & 166\left[\left(-0.08\left(\frac{\omega_{t0} R}{V}+0.08\beta_0\right)^{-2} + \frac{0.105\beta_0^2}{\left(\beta_0^3+1\right)^2}\right) - 0.4\right]\end{aligned} \quad \text{(B.25)}$$

Linearizing (B.21)

$$\boxed{\begin{aligned}\Delta P_m =& \frac{\partial C_p\left(\lambda,\beta\right)}{\partial \omega_T}\Delta\omega_t + \frac{\partial C_p\left(\lambda,\beta\right)}{\partial \beta}\Delta\beta \\ =& \mathcal{K}_1\Delta\omega_t + \mathcal{K}_2\Delta\beta\end{aligned}} \tag{B.26}$$

Turbine speed (ω_t):

$$\boxed{\dot{\omega}_t = \frac{P_m - K_s\theta_s}{2H_t}} \tag{B.27}$$

Linearizing (B.28)

$$\left(\dot{\omega}_t + \Delta\dot{\omega}_t\right) = \frac{\left(P_m + \Delta P_m\right) - K_s\left(\theta_s + \Delta\theta_s\right)}{2H_t} \tag{B.28}$$

$$\Delta\dot{\omega}_t = \frac{\Delta P_m - K_s\Delta\theta_s}{2H_t} \tag{B.29}$$

Substituting P_m from (B.27) in (B.30)

$$\boxed{\Delta\dot{\omega}_t = \frac{1}{2H_t}\left(\mathcal{K}_1\Delta\omega_t + \mathcal{K}_2\Delta\beta - K_s\Delta\theta_s\right)} \tag{B.30}$$

Generator Speed (w_g):

$$\boxed{\dot{\omega_g} = \frac{K_s\theta_s - P_e}{2H_g}} \tag{B.31}$$

Substituting P_e as,

$$\boxed{P_e = x_m i_{ds} i_{qr} - x_m i_{qs} i_{dr}} \tag{B.32}$$

$$\begin{aligned}(\dot{\omega_g} + \Delta\dot{\omega_g}) = \ & \tfrac{1}{2H_g}\Big\{K_s\left(\theta_s + \Delta\theta_S\right) - \{x_m\left(i_{ds0} + \Delta i_{ds}\right)\left(i_{qr0} + \Delta i_{qr}\right) \\ & -x_m\left(i_{qs0} + \Delta i_{qs}\right)\left(i_{dr0} + \Delta i_{dr}\right)\}\Big\}\end{aligned} \tag{B.33}$$

$$\boxed{\begin{aligned}\Delta\dot{\omega_g} = & \frac{1}{2H_g}\Big\{K_s\Delta\theta_s - x_m i_{qr0}\Delta i_{ds} + x_m i_{dr0}\Delta i_{qs} \\ & - x_m i_{ds0}\Delta i_{qr} + x_m i_{qs0}\Delta i_{dr}\Big\}\end{aligned}} \tag{B.34}$$

Shaft torsional twist (θ_s):

$$\boxed{\dot{\theta}_s = \omega_e\left(\omega_t - \omega_g\right)} \tag{B.35}$$

Linearizing (B.37):

$$\boxed{\Delta\dot{\theta}_s = \omega_e\left(\Delta\omega_t - \Delta\omega_g\right)} \tag{B.36}$$

Capacitor voltage (V_c):

$$\boxed{\begin{aligned}\dot{V}_c = & \frac{1}{C}\Big[\left(m_1\cos\alpha_1\right)i_{ad} + \left(m_1\sin\alpha_1\right)i_{aq} + \left(m_2\cos\alpha_2\right)i_{dr} \\ & + \left(m_2\sin\alpha_2\right)i_{qr}\Big]\end{aligned}} \tag{B.37}$$

Linearizing (B.44):

$$\begin{aligned}\left(\dot{V}_c + \Delta\dot{V}_c\right) = \; & \tfrac{1}{C}\Big[\left(m_1\cos\alpha_1\right)\left(i_{ad0}+\Delta i_{ad}\right)+\left(m_1\sin\alpha_1\right)\left(i_{aq0}+\Delta i_{aq}\right) \\ & +\left(m_2\cos\alpha_2\right)\left(i_{dr0}+\Delta i_{dr}\right)+\left(m_2\sin\alpha_2\right)\left(i_{qr0}+\Delta i_{qr}\right)\Big] \end{aligned} \tag{B.38}$$

$$\boxed{\begin{aligned}\Delta\dot{V}_c = & \frac{1}{C}\Big[\left(m_1\cos\alpha_1\right)\Delta i_{ad}+\left(m_1\sin\alpha_1\right)\Delta i_{aq}+\left(m_2\cos\alpha_2\right)\Delta i_{dr} \\ & +\left(m_2\sin\alpha_2\right)\Delta i_{qr}\Big]\end{aligned}} \tag{B.39}$$

Converter d-axis current (i_{ad}):

$$\boxed{\dot{i_{ad}} = \frac{\omega_e}{x_a}\left[-R_a\, i_{ad}+x_a\, i_{aq}\right]+\frac{\omega_e}{x_a}\left[v_{ds}-m_1\, V_c\cos\alpha_1\right]} \tag{B.40}$$

Linearizing (B.38):

$$\begin{aligned}\left(\dot{i_{ad}}+\Delta\dot{i_{ad}}\right) = \; & \frac{\omega_e}{x_a}\Big[-R_a\left(i_{ad0}+\Delta i_{ad}\right)+x_a\left(i_{aq0}+\Delta i_{aq}\right)\Big] \\ & +\frac{\omega_e}{x_a}\Big[\left(z_{11}\, g_{12}+z_{12}\, b_{12}\right)V_b+z_{11}\left(i_{ds0}+\Delta i_{ds}\right) \\ & +z_{12}\left(i_{qs0}+\Delta i_{qs}\right)-z_{11}\left(i_{ad0}+\Delta i_{ad}\right) \\ & -z_{12}\left(i_{aq0}+\Delta i_{aq}\right)-\left(m_1\, V_c\cos\alpha_1\right)\Big]\end{aligned} \tag{B.41}$$

$$\boxed{\begin{aligned}\Delta\dot{i_{ad}} = & \frac{\omega_e}{x_a}z_{11}\Delta i_{ds}+\frac{\omega_e}{x_a}z_{12}\Delta i_{qs}-\frac{\omega_e}{x_a}\left(R_a+z_{11}\right)\Delta i_{ad} \\ & +\left(\omega_e-\frac{\omega_e}{x_a}z_{12}\right)\Delta i_{aq}-\frac{\omega_e}{x_a}m_1\cos\alpha_1\Delta V_c\end{aligned}} \tag{B.42}$$

Converter q-axis current (i_{aq}):

$$\boxed{\dot{i_{aq}} = \frac{\omega_e}{x_a}\left[-R_a\, i_{aq} - x_a\, i_{ad}\right] + \frac{\omega_e}{x_a}\left[v_{qs} - m_1\, V_c \sin\alpha_1\right]} \tag{B.43}$$

Linearizing (B.41):

$$\begin{aligned}\left(\dot{i_{aq}} + \Delta\dot{i_{aq}}\right) \;=\; & \frac{\omega_e}{x_a}\Big[- R_a\left(i_{aq0} + \Delta i_{aq}\right) - x_a\left(i_{ad0} + \Delta i_{ad}\right)\Big] \\ & + \frac{\omega_e}{x_a}\Big[\left(z_{21}\, g_{12} + z_{22}\, b_{12}\right) V_b + z_{21}\left(i_{ds0} + \Delta i_{ds}\right) \\ & + z_{22}\left(i_{qs0} + \Delta i_{qs}\right) - z_{21}\left(i_{ad0} + \Delta i_{ad}\right) \\ & - z_{22}\left(i_{aq0} + \Delta i_{aq}\right) - \left(m_1\, V_c \sin\alpha_1\right)\Big]\end{aligned} \tag{B.44}$$

$$\boxed{\begin{aligned}\Delta\dot{i_{aq}} =& \frac{\omega_e}{x_a} z_{21}\Delta i_{ds} + \frac{\omega_e}{x_a} z_{22}\Delta i_{qs} - \frac{\omega_e}{x_a}\left(R_a + z_{22}\right)\Delta i_{aq} \\ & + \left(-\omega_e - \frac{\omega_e}{x_a} z_{21}\right)\Delta i_{ad} - \frac{\omega_e}{x_a} m_1 \sin\alpha_1 \Delta V_c\end{aligned}} \tag{B.45}$$

Power Feedback Equations:

From figure 3.4 equation for the integrating block giving β_i can be written as,

$$\boxed{\dot{\beta}_i = K_I \left(P_e - P_{e,ref}\right)} \tag{B.46}$$

Linearizing (B.47):

$$\left(\dot{\beta}_i + \Delta\dot{\beta}_i\right) = K_I\Big\{ \left(P_e + \Delta P_e\right) - P_{e,ref}\Big\} \tag{B.47}$$

$$\Delta\dot{\beta}_i = K_I \Delta P_e \tag{B.48}$$

Substituting P_e as,

$$\boxed{P_e = x_m i_{ds} i_{qr} - x_m i_{qs} i_{dr}} \tag{B.49}$$

(B.49) can be written as,

$$\boxed{\Delta\dot{\beta}_i = K_I\Big[x_m i_{qr0}\Delta i_{ds} - x_m i_{dr0}\Delta i_{qs} - x_m i_{qs0}\Delta i_{dr} + x_m i_{ds0}\Delta i_{qr}\Big]} \tag{B.50}$$

The overall control equation giving β from figure 3.4 can be written as,

$$\boxed{\dot{\beta} = K_a\left(K_P\left(P_e - P_{e,ref}\right) + \beta_i\right) - K_a\beta_i} \tag{B.51}$$

Linearizing (B.52):

$$\left(\dot{\beta}+\Delta\dot{\beta}\right)+K_a\left(\beta+\Delta\beta\right)=K_a\Big\{K_P\left(P_e+\Delta P_e-P_{e,ref}\right)+\left(\beta_i+\Delta\beta_i\right)\Big\} \tag{B.52}$$

$$\Delta\dot{\beta}=K_aK_P\Delta P_e+K_a\Delta\beta_i-K_a\Delta\beta \tag{B.53}$$

Substituting P_e as in (B.50), linearizing it and then substituting in (B.54)

$$\begin{aligned}\Delta\dot{\beta}=&K_aK_P\left(x_m i_{qr0}\Delta i_{ds}-x_m i_{dr0}\Delta i_{qs}-x_m i_{qs0}\Delta i_{dr}+x_m i_{ds0}\Delta i_{qr}\right)\\&+K_a\Delta\beta_i-K_a\Delta\beta\end{aligned} \tag{B.54}$$

The overall closed loop matrix A_c for the system model can written as in (B.56)

$$\begin{bmatrix} \Delta\dot{i}_{ds} \\ \Delta\dot{i}_{qs} \\ \Delta\dot{i}_{dr} \\ \Delta\dot{i}_{qr} \\ \Delta\dot{\omega}_t \\ \Delta\dot{\omega}_g \\ \Delta\dot{\theta}_s \\ \Delta\dot{i}_{ad} \\ \Delta\dot{i}_{aq} \\ \Delta\dot{V}_c \\ \Delta\dot{\beta}_i \\ \Delta\dot{\beta} \end{bmatrix} = \begin{bmatrix} a_{(1,1)} & a_{(1,2)} & a_{(1,3)} & a_{(1,4)} & 0 & a_{(1,6)} & 0 & a_{(1,8)} & a_{(1,9)} & a_{(1,10)} & 0 & 0 \\ a_{(2,1)} & a_{(2,2)} & a_{(2,3)} & a_{(2,4)} & 0 & a_{(2,6)} & 0 & a_{(2,8)} & a_{(2,9)} & a_{(2,10)} & 0 & 0 \\ a_{(3,1)} & a_{(3,2)} & a_{(3,3)} & a_{(3,4)} & 0 & a_{(3,6)} & 0 & a_{(3,8)} & a_{(3,9)} & a_{(3,10)} & 0 & 0 \\ a_{(4,1)} & a_{(4,2)} & a_{(4,3)} & a_{(4,4)} & 0 & a_{(4,6)} & 0 & a_{(4,8)} & a_{(4,9)} & a_{(4,10)} & 0 & 0 \\ 0 & 0 & 0 & 0 & a_{(5,5)} & 0 & a_{(5,7)} & 0 & 0 & 0 & 0 & a_{(5,12)} \\ a_{(6,1)} & a_{(6,2)} & a_{(6,3)} & a_{(6,4)} & 0 & 0 & a_{(6,7)} & 0 & 0 & 0 & 0 & 0 \\ 0 & 0 & 0 & 0 & a_{(7,5)} & a_{(7,6)} & 0 & 0 & 0 & 0 & 0 & 0 \\ a_{(8,1)} & a_{(8,2)} & 0 & 0 & 0 & 0 & 0 & a_{(8,8)} & a_{(8,9)} & a_{(8,10)} & 0 & 0 \\ a_{(9,1)} & a_{(9,2)} & 0 & 0 & 0 & 0 & 0 & a_{(9,8)} & a_{(9,9)} & a_{(9,10)} & 0 & 0 \\ 0 & 0 & a_{(10,3)} & a_{(10,4)} & 0 & 0 & 0 & a_{(10,8)} & a_{(10,9)} & 0 & 0 & 0 \\ a_{(11,1)} & a_{(11,2)} & a_{(11,3)} & a_{(11,4)} & 0 & 0 & 0 & 0 & 0 & 0 & 0 & 0 \\ a_{(12,1)} & a_{(12,2)} & a_{(12,3)} & a_{(12,4)} & 0 & 0 & 0 & 0 & 0 & 0 & a_{(12,11)} & a_{(12,12)} \end{bmatrix} \begin{bmatrix} \Delta i_{ds} \\ \Delta i_{qs} \\ \Delta i_{dr} \\ \Delta i_{qr} \\ \Delta\omega_t \\ \Delta\omega_g \\ \Delta\theta_s \\ \Delta i_{ad} \\ \Delta i_{aq} \\ \Delta V_c \\ \Delta\beta_i \\ \Delta\beta \end{bmatrix}$$

Where,

$$
\begin{aligned}
a_{(1,1)} &= a(1,1) + z_{11} b(1,1) \\
a_{(1,2)} &= a(1,2) + z_{12} b(1,1) \\
a_{(1,3)} &= a(1,3) \\
a_{(1,4)} &= a(1,4) \\
a_{(1,6)} &= -\frac{1}{x_s x_r - {x_m}^2} \left({x_m}^2 \omega i_{qs0} - \omega x_r x_m i_{qr0} \right) \\
a_{(1,8)} &= -z_{11} b(1,1) \\
a_{(1,9)} &= -z_{12} b(1,1) \\
a_{(1,10)} &= \left(m_2 \cos \alpha_2 \right) b(1,3)
\end{aligned}
\tag{B.55}
$$

$$
\begin{aligned}
a_{(2,1)} &= a(2,1) + z_{21} b(2,2) \\
a_{(2,2)} &= a(2,2) + z_{22} b(2,2) \\
a_{(2,3)} &= a(2,3) \\
a_{(2,4)} &= a(2,4) \\
a_{(2,6)} &= \frac{1}{x_s x_r - {x_m}^2} \left(\omega {x_m}^2 i_{ds0} + \omega x_r x_m i_{dr0} \right) \\
a_{(2,8)} &= -z_{21} b(2,2) \\
a_{(2,9)} &= -z_{22} b(2,2) \\
a_{(2,10)} &= \left(m_2 \sin \alpha_2 \right) b(2,4)
\end{aligned}
\tag{B.56}
$$

$$
\begin{aligned}
a_{(3,1)} =& a(3,1) + z_{11} b(3,1) \\
a_{(3,2)} =& a(3,2) + z_{12} b(3,1) \\
a_{(3,3)} =& a(3,3) \\
a_{(3,4)} =& a(3,4) \\
a_{(3,6)} =& \frac{1}{x_s x_r - {x_m}^2} \left(\omega x_m x_s i_{qs0} + \omega x_r x_s i_{qr0} \right) \\
a_{(3,8)} =& - z_{11} b(3,1) \\
a_{(3,9)} =& - z_{12} b(3,1) \\
a_{(3,10)} =& \left(m_2 \cos \alpha_2 \right) b(3,3)
\end{aligned}
\tag{B.57}
$$

$$
\begin{aligned}
a_{(4,1)} =& a(4,1) + z_{21} b(4,2) \\
a_{(4,2)} =& a(4,2) + z_{22} b(4,2) \\
a_{(4,3)} =& a(4,3) \\
a_{(4,4)} =& a(4,4) \\
a_{(4,6)} =& - \frac{1}{x_s x_r - {x_m}^2} \left(\omega x_s x_m i_{ds0} + \omega \left(x_r x_s \right) i_{dr0} \right) \\
a_{(4,8)} =& - z_{21} b(4,2) \\
a_{(4,9)} =& - z_{22} b(4,2) \\
a_{(4,10)} =& \left(m_2 \sin \alpha_2 \right) b(4,4)
\end{aligned}
\tag{B.58}
$$

$$
\begin{aligned}
a_{(5,5)} =& \frac{1}{2H_t}\mathcal{K}_1 \\
a_{(5,7)} =& -\frac{1}{2H_t}K_s \\
a_{(5,12)} =& \frac{1}{2H_t}\mathcal{K}_2
\end{aligned}
\tag{B.59}
$$

$$
\begin{aligned}
a_{(6,1)} =& -\frac{1}{2H_g}X_m i_{qr0} \\
a_{(6,2)} =& \frac{1}{2H_g}X_m i_{dr0} \\
a_{(6,3)} =& \frac{1}{2H_g}X_m i_{qs0} \\
a_{(6,4)} =& -\frac{1}{2H_g}X_m i_{ds0} \\
a_{(6,7)} =& \frac{1}{2H_g}K_s
\end{aligned}
\tag{B.60}
$$

$$
\begin{aligned}
a_{(7,5)} =& \omega_e \\
a_{(7,6)} =& -\omega_e
\end{aligned}
\tag{B.61}
$$

$$
\begin{aligned}
a_{(8,1)} =& \frac{\omega_e}{x_a} z_{11} \\
a_{(8,2)} =& \frac{\omega_e}{x_a} z_{12} \\
a_{(8,8)} =& -\frac{\omega_e}{x_a} \left(R_a + z_{11}\right) \\
a_{(8,9)} =& \omega_e \left(1 - \frac{1}{x_a} z_{12}\right) \\
a_{(8,10)} =& -\frac{\omega_e}{x_a} m_1 \cos\alpha_1
\end{aligned}
\tag{B.62}
$$

$$
\begin{aligned}
a_{(9,1)} =& \frac{\omega_e}{x_a} z_{21} \\
a_{(9,2)} =& \frac{\omega_e}{x_a} z_{22} \\
a_{(9,8)} =& -\omega_e \left(1 + \frac{1}{x_a} z_{21}\right) \\
a_{(9,9)} =& -\frac{\omega_e}{x_a} \left(R_a + z_{22}\right) \\
a_{(9,10)} =& -\frac{\omega_e}{x_a} m_1 \sin\alpha_1
\end{aligned}
\tag{B.63}
$$

$$
\begin{aligned}
a_{(10,3)} =& \frac{1}{C} \left(m_2 \cos\alpha_2\right) \\
a_{(10,4)} =& \frac{1}{C} \left(m_2 \sin\alpha_2\right) \\
a_{(10,8)} =& \frac{1}{C} \left(m_1 \cos\alpha_1\right) \\
a_{(10,9)} =& \frac{1}{C} \left(m_1 \sin\alpha_1\right)
\end{aligned}
\tag{B.64}
$$

$$
\begin{aligned}
a_{(11,1)} &= K_I x_m i_{qr0} \\
a_{(11,2)} &= -\,K_I x_m i_{dr0} \\
a_{(11,3)} &= -\,K_I x_m i_{qs0} \\
a_{(11,4)} &= K_I x_m i_{ds0}
\end{aligned}
\tag{B.65}
$$

$$
\begin{aligned}
a_{(12,1)} &= K_a K_P x_m i_{qr0} \\
a_{(12,2)} &= -\,K_a K_P x_m i_{dr0} \\
a_{(12,3)} &= -\,K_a K_P x_m i_{qs0} \\
a_{(12,4)} &= K_a K_P x_m i_{ds0} \\
a_{(12,11)} &= K_a \\
a_{(12,12)} &= -\,K_a
\end{aligned}
\tag{B.66}
$$

NOMENCLATURE

Abbreviations

WECS	Wind Energy Conversion System
PMSG	Permanent Magnet Synchronous Generator
DFIG	Doubly Fed Induction Generator
VSWT	Variable Speed Wind Turbines
PI	Proportional Integral
HAWT	Horizontal Axis Wind Turbine
VAWT	Vertical Axis Wind Turbine
DE	Differential Evolution
ANN	Artificial Neural Network
LMS	Least Mean Square

Symbols

I_s	Stator current
I_a	Converter current
I_c	Load current
I_{Line}	Transmission line current
V_s	Stator coltage
Y_{11}	Admittance of load

g_{11}	Conductance of load
b_{11}	Susceptance of load
Y_{12}	Admittance of transmission line
g_{12}	Conductance of transmission line
b_{12}	Susceptance of transmission line
V_b	Infinite bus voltage
v_{ds}	d-axis stator voltage
v_{qs}	q-axis stator voltage
i_{ds}	d-axis stator current
i_{qs}	q-axis stator current
i_{ad}	d-axis converter current
i_{aq}	q-axis converter current
z_{11}	First entry of impedance matrix
z_{12}	Second entry of impedance matrix
z_{21}	Third entry of impedance matrix
z_{22}	Fourth entry of impedance matrix
R_s	Stator resistance
X_s	Stator reactance
X_m	Mutual reactance
R_r	Rotor resistance
i_{dr}	d-axis rotor current
i_{qr}	q-axis rotor current
v_{dr}	d-axis rotor voltage
v_{qr}	q-axis rotor voltage
s	Slip
Ψ_{ds}	d-axis stator flux linkage
Ψ_{qs}	q-axis stator flux linkage

Ψ_{dr}	d-axis rotor flux linkage
Ψ_{qr}	q-axis rotor flux linkage
ω_e	Synchronous speed
ω_g	Rotor speed
V_c	Capacitor voltage
P_m	Mechanical power
ρ	Density of air
R	Radius of wind turbine
V_w	Wind speed
C_p	Power coefficient
λ	Tip speed ratio
β	Pitch angle
ω_T	Turbine speed
$\mathcal{K}_1$	Linearization constant
$\mathcal{K}_2$	Linearization constant
K_s	Shaft stiffness
θ_s	Torsional angle
H_t	Turbine inertia
P_e	Electrical power
H_g	Generator inertia
m_1	Modulation index of rotor side converter
m_2	Modulation index of grid side converter
α_1	Firing angle of rotor side converter
α_2	Firing angle of grid side converter
C	Capacitor
R_a	Converter resistance
X_a	Converter reactance

β_i	Pitch state from integrating block
K_I	Integral gain
$P_{e,ref}$	Reference power
K_P	Proportional gain
K_a	Actuator gain
i_{dr0}	Initial value of d-axis rotor current
i_{qr0}	Initial value of q-axis rotor current
v_{dr0}	Initial value of d-axis rotor voltage
v_{qr0}	Initial value of q-axis rotor voltage
v_{ds0}	Initial value of d-axis stator voltage
v_{qs0}	Initial value of q-axis stator voltage
i_{ds0}	Initial value of d-axis stator current
i_{qs0}	Initial value of q-axis stator current
i_{ad0}	Initial value of d-axis converter current
i_{aq}	Initial value of q-axis converter current
β_0	Initial value of pitch
ω_{t0}	Initial value of turbine speed
Δ	Perturbed State around the operating point
A_c	Closed Loop A matrix
Z	State matrix
G	Generation
X_n^i	Candidate solutions
D	Problem dimension for DE
NP	Population size
$\mathcal{F}$	Mutation factor
$\mathcal{CR}$	Crossover factor
V_i^G	Mutated vector

z_{lk}	Output from neuron j from layer l
w_{lkj}	Weight between neuron j and neuron k
X_i	Training input vector
T	Target vector
N_t	Number of neurons in layer l
L	Number of layers
W_t	Weight matrix
$E(W)$	Sum of square error function
∇	Gradient vector
μ	Learning parameter
ϵ	Instantaneous linear error
J	Objective function
ζ	Damping ratio
ζ_0	Set value of damping ratio
P_{AC}	AC power
P_{DC}	DC power
E_{da}	d-axis grid side converter voltage
E_{qa}	q-axis grid side converter voltage

Bibliography

[1] Lucy Y. Pao and Kathryn E. Johnson, "A Tutorial on the Dynamics and Control of Wind Turbines and Wind Farms," in *American Control Conference , USA*, 2009, pp. 2076–2089.

[2] Vladislav Akhmatov, *Induction Generators for Wind Power*, 2005 edition.

[3] Justin Wilkes and Jacopo Moccia, "Wind in power: 2010 European statistics," Tech. Rep. February, European Wind Energy Association, 2010.

[4] M.E. Haque, M. Negnevitsky, and K.M. Muttaqi, "A Novel Control Strategy for a Variable-Speed Wind Turbine With a Permanent-Magnet Synchronous Generator," *IEEE Transactions on Industry Applications*, vol. 46, no. 1, pp. 331–339, 2010.

[5] Deng Qiu-ling, L. I. U. Gou-rong, and Xiao Feng, "Control of Variable-speed Permanent Magnet Synchronous Generators Wind Generation System," in *International Conference on Electrical Machines and Systems, ICEMS*, 2008, pp. 2454–2458.

[6] Cristian Busca, Ana-irina Stan, Tiberiu Stanciu, and Daniel Ioan Stroe, "Control of Permanent Magnet Synchronous Generator for Large Wind Turbines," in *International Symposium on Industrial Electronics (ISIE)*, 2010, pp. 3871–3876.

[7] Shun Miyabukuro, Masashi Takiguchi, and Rion Takahashi, "Modeling and Simulation of Wind Turbine Fed Interior Permanent Magnet Synchronous Generator," in *18th International Conference on Electrical Machines, ICEM*, 2008, number 4, pp. 1–6.

[8] Ming Yin, Gengyin Li, and Ming Zhou, "Modeling of the Wind Turbine with a Permanent Magnet Synchronous Generator for Integration," in *Power Engineering Society General Meeting*, 2007, pp. 1–6.

[9] M. G. Molina, A. G. Sanchez, and A. M. Rizzato Lede, "Dynamic Modeling of Wind Farms with Variable- Speed Direct-Driven PMSG Wind Turbines," in *Transmission and Distribution Conference and Exposition: Latin America (T&D-LA), IEEE/PES*, 2010, pp. 816–823.

[10] I .D. Margaris and N. D. Hatziargyriou, "Direct Drive Synchronous Generator Wind Turbine Models for Power System Studies," in *7th Mediterranean Conference and Exhibition on Power Generation, Transmission, Distribution and Energy Conversion*, 2010, number November, pp. 1–7.

[11] Liyong Yang, Zhigang Chen, Peie Yuan, and Zhenguo Chang, "A novel fuzzy logic and anti-windup PI controller for a rectifier with direct driven permanent magnet synchronous generator," *2009 2nd International Conference on Power*

Electronics and Intelligent Transportation System (PEITS), pp. 422–426, Dec. 2009.

[12] Fujin Deng and Zhe Chen, "Low-Voltage Ride-Through of Variable Speed Wind Turbines with Permanent Magnet Synchronous Generator," in *35th Annual Conference of IEEE Industrial Electronics, ECON.*, 2009, number 2, pp. 621–626.

[13] Rajveer Mittal, K. S. Sandhu, and D. K. Jain, "Fault Ride- through Capability of Grid Connected Variable Speed Permanent Magnet Synchronous Generator for Wind Energy Conversion System," in *Electrical Power & Energy Conference (EPEC), IEEE*, 2009, pp. 1–6.

[14] L. Holdsworth, X. G. Wu, J. B. Ekanayake, and N. Jenkins, "Comparison of fixed speed and doubly-fed induction wind turbines during power system disturbances," *IEEE Proceedings of Generation, Transmission, Distribution*, vol. 150, no. 3, pp. 343–352, 2003.

[15] A.H.M.A. Rahim and I.O. Habiballah, "DFIG rotor voltage control for system dynamic performance enhancement," *Electric Power Systems Research*, vol. 81, no. 2, pp. 503–509, Feb. 2011.

[16] H. Geng and G. Yang, "Robust pitch controller for output power levelling of variable-speed variable-pitch wind turbine generator systems," *IET Renewable Power Generation*, vol. 3, no. July 2008, pp. 168– 179, 2009.

[17] Xingjia Yao, Changchun Guo, and Zuoxia Xing, "Pitch regulated LQG controller design for variable speed wind turbine," in *2009 International Conference on Mechatronics and Automation*, Aug. 2009, pp. 845–849.

[18] Endusa Billy Muhando, Tomonobu Senjyu, and Eitaro Omine, "Full State Feedback Digital Control of WECS with State Estimation by Stochastic Modeling Design," in *Power and Energy Society General Meeting - Conversion and Delivery of Electrical Energy in the 21st Century*, 2008, pp. 1–8.

[19] A. Bati and S. Leabi, "NN Self-Tuning Pitch Angle Controller of Wind Power Generation Unit," in *IEEE PES Power Systems Conference and Exposition*, 2006, pp. 2019–2029.

[20] M. Narayana and G. Putrus, "Optimal Control of Wind Turbine Using Neural Networks," in *UPEC 2010*, 2010, pp. 8–12.

[21] Y. L. Abdel-Magid and M .A. Abido, "Optimal Multiobjective Design of Robust Power System Stabilizers Using Genetic Algorithms," *IEEE Transactions on Power Systems*, vol. 18, no. 3, pp. 1125–1132, 2003.

[22] L .J. Cai and I. Erlich, "Simultaneous Coordinated Tuning of PSS and FACTS Controller for Damping Power System Oscillations in Multi-Machine Systems," in *IEEE Bologna Power Tech Conference*, 2003.

[23] Vladislav Akhmatov, *Induction generators for wind power*, Multi-Science Pub, 2007.

[24] S. Heier, *Grid Integration of Wind Energy Conversion Systems*, John Wiley and Sons Ltd, 2007.

[25] "Wind Energy, the facts," `http://www.wind-energy-the-facts.org`.

[26] Vladislav Akhmatov, "Variable-Speed Wind Turbines with Doubly-Fed Induction Generators, Part I: Modelling in Dynamic Simulation Tools," *Wind Engineering*, vol. 26, no. 2, pp. 85–108, 2002.

[27] Xianyou Yang, Bin Duan, Zhanglong Jing, and Guoqi Chen, "Research on pitch-controlled wind turbine system based on bladed," , no. 50677058, pp. 1–6, Apr. 2009.

[28] Morten H Hansen, Anca Hansen, Torben J Larsen, Stig Ø ye, Poul Sø rensen, and Peter Fuglsang, *Control design for a pitch-regulated, variable speed wind turbine*, vol. 1500, 2005.

[29] Bin Wu, Yongqiang Lang, Navid Zargari, and Samir Kaouro, *Power conversion and control of wind energy systems*, IEEE Press Series on Power Engineering, 1st edition, 2011.

[30] Bunlung Neammanee and Somporn Sirisumrannukul, "Control strategies for variable speed fixed pitch wind turbines," in *Wind Power*, S.M Muyeen, Ed., pp. 209–232. IEEE Press Series on Power Engineering, 2010.

[31] Z. L. Dou, M. Z. Cheng, Z. B. Ling, and X. Cai, "An Adjustable Pitch Control System in a Large Wind Turbine Based on a Fuzzy-PID Controller," in *In-*

ternational Symposium on Power Electronics, Electric Drives, Automation and Motion, 2010, pp. 391–395.

[32] Wei Qiao, Ronald G. Harley, and Ganesh K. Venayagamoorthy, "Dynamic modeling of wind farms with fixed speed wind turbine generators," *Power Engineering Society General Meeting*, pp. 1–8, 2007.

[33] Eftichios Koutroulis and Kostas Kalaitzakis, "Design of a maximum power tracking System for wind energy conversion applications," *IEEE Transactions on Industrial Electronics*, vol. 53, no. 2, pp. 486–494, 2006.

[34] P. Bauer, S.W.H. De Haan, C.R. Meyl, and J.T.G. Pierik, "Evaluation of electrical systems for offshore windfarms," *Conference Record of the 2000 IEEE Industry Applications Conference. Thirty-Fifth IAS Annual Meeting and World Conference on Industrial Applications of Electrical Energy (Cat. No.00CH37129)*, pp. 1416–1423, 2000.

[35] Mohamed Mansour, M N Mansouri, and M F Mmimouni, "Study and Control of a Variable-Speed Wind- Energy System Connected to the Grid," *International Journal of renewable Energy Research*, vol. 1, no. 2, pp. 96–104, 2011.

[36] Hitoshi Takaai, Yuichi Chida, Kimi Sakurai, and Takashi Isobe, "Pitch angle control of wind turbine generator using less conservative robust control," *2009 IEEE International Conference on Control Applications*, pp. 542–547, July 2009.

[37] Jianzhong Zhang, Ming Cheng, Zhe Chen, and Xiaofan Fu, "Pitch angle control for variable speed wind turbines," in *2008 Third International Conference on*

Electric Utility Deregulation and Restructuring and Power Technologies, Apr. 2008, number April, pp. 2691–2696.

[38] Anca D. Hansen, Poul Sø rensen, Florin Iov, and Frede Blaabjerg, "Control of variable speed wind turbines with doubly-fed induction generators," *Wind Engineering*, vol. 28, no. 4, pp. 411–432, 2004.

[39] Tomonobu Senjyu, Ryosei Sakamoto, Naomitsu Urasaki, Hiroki Higa, Katsumi Uezato, and Toshihisa Funabashi, "Output Power Control of Wind Turbine Generator by Pitch Angle Control using Minimum Variance Control," *International Conference on Power System Technology*, vol. 124, no. 12, pp. 1455–1462, 2004.

[40] H. Siguerdidjane L. Lupu, B. Boukhezzar, "Pitch and torque control strategy for variable speed wind turbines," in *European Wind Energy Conference Proceedings*, 2006.

[41] Marcelo Godoy Sim, Bimal K. Bose, and Ronald J. Spiegel, "Design and Performance Evaluation of Wind Generation System," *IEEE Transactions on Industry Applications*, vol. 33, no. 4, pp. 956–965, 1997.

[42] Peter Vas, *Artificial-Intelligence-Based Electrical Machines and Drives: Application of Fuzzy, Neural, Fuzzy-neural, and Genetic-Algorithm-based Techniques*, Oxford University Press, 1999 edition.

[43] I. A. Isaac, D. Cabrera, H. Pizarro, D. Giraldo, J. W. Gonzalez, and H. Biechl, "Fuzzy Logic Based Parameter Estimator for Variable Speed Wind Generators PI Pitch Control," 2010.

[44] C. A. M. Amandola and D. P. Gonzaga, "Fuzzy-Logic Control System of a Variable-Speed Variable-Pitch Wind-Turbine and a Double-Fed Induction Generator," in *Seventh International Conference on Intelligent Systems Design and Applications (ISDA 2007)*, Oct. 2007, number Point D, pp. 252–257.

[45] Marcelo Godoy Simoes, Bimal K. Bose, and Ronald J. Spiegel, "Fuzzy Logic Based Intelligent Control of a Variable Speed Cage Machine Wind Generation System," *IEEE Transactions on Power Electronics*, vol. 12, no. 1, pp. 87–95, 1997.

[46] Feng Gao, Daping Xu, and Yuegang Lv, "Pitch-control for large-scale wind turbines based on feed forward Fuzzy-PI," *2008 7th World Congress on Intelligent Control and Automation*, pp. 2277–2282, 2008.

[47] Mitsuo Hirata and Yumi Hasegawa, "High Bandwidth Design of Track-Following Control System of Hard Disk Drive Using H-infinity Control Theory," in *16th IEEE International Conference on Control Applications, Singapore*, 2007, number October, pp. 1–3.

[48] R. Rocha and L.S.M. Filho, "A Multivariable H-infinity Control for Wind Energy Conversion System," vol. 4, no. 5, pp. 222–227, Oct. 1972.

[49] Toshiaki Kaneko, Tomonobu Senjyu, Atsushi Yona, Manoj Datta, Toshihisa Funabashi, and Chul-Hwan Kim, "Output Power Coordination Control for Wind Farm in Small Power System," *2007 International Conference on Intelligent Systems Applications to Power Systems*, pp. 1–6, Nov. 2007.

[50] Ryosei Sakamoto, Tomonobu Senjyu, Naomitsu Urasaki, and Toshihisa Funabashi, "Output Power Leveling of Wind Turbine Generators Using Pitch Angle Control for All Operating Regions in Wind Farm," *ISAP*, vol. 2, no. 1, pp. 367–372, 2005.

[51] T. Senjyu, R. Sakamoto, N. Urasaki, T. Funabashi, H. Fujita, and H. Sekine, "Output Power Leveling of Wind Turbine Generator for All Operating Regions by Pitch Angle Control," *IEEE Transactions on Energy Conversion*, vol. 21, no. 2, pp. 467–475, June 2006.

[52] D. W. Clarke, C. Mohtadi, and O. S. Tuffs, "Generalized predictive control Part I. The basic algorithm," *Automatica*, vol. 23, no. 2, pp. 137–148, 1987.

[53] D. W. Clarke, C. Mohtadi, and O. S. Tuffs, "Generalized predictive control Part II. Extensions and interpretations," *Automatica*, vol. 23, no. 2, pp. 149–160, 1987.

[54] Michio Sugeno, *Fuzzy Logic*, Nikkan Kogyo Shimbun, Ltd, 1988.

[55] S. K. Leabi, *NN Self-Tuning Pitch Angle Controller Of Wind Power Generation*, Ph.D. thesis, University Of Technology, Iraq-Baghdad, 2006.

[56] Whei-min Lin and Chih-ming Hong, "A New Elman Neural Network-Based Control Algorithm for Adjustable-Pitch Variable-Speed Wind-Energy Conversion Systems," *IEEE Transactions on Power Electronics*, vol. 26, no. 2, pp. 473–481, 2011.

[57] Ahmed A. A. Esmin, Germano Lambert-Torres, and Antônio C. Zambroni De Souza, "A Hybrid Particle Swarm Optimization Applied to Loss Power Mini-

mization," *IEEE Transactions on Power Systems*, vol. 20, no. 2, pp. 859–866, 2005.

[58] Jacob Robinson and Yahya Rahmat-Samii, "Particle Swarm Optimization in Electromagnetics," *IEEE Transactions on Antennas and Propogation*, vol. 52, no. 2, pp. 397–407, 2004.

[59] J. L. Elman, "Finding Structure in Time," *Cognitive Science*, vol. 14, no. 2, pp. 179–211, 1990.

[60] R Gianto and T.T Nguyen, "Neural networks for adaptive control coordination of PSSs and FACTS devices in multimachine power system," *Generation, Transmission and Distribution, IET*, vol. 2, no. 3, pp. 355–372, 2008.

[61] Maryam Jamela Ismail, Rosdiazli Ibrahim, and Idris Ismail, "Adaptive Neural Network Prediction Model for Energy Consumption," in *3rd International Conference Computer Research and Development (ICCRD)*, 2011, pp. 109–113.

[62] Faa Jeng Lin, Po-hung Shen, and Ying Shieh Kung, "Adaptive Wavelet Neural Network Control for Linear Synchronous Motor Servo Drive," *IEEE Transactions on magnetics*, vol. 41, no. 12, pp. 4401–4412, 2005.

[63] S .S. Ge, C. C. Hang, and T. Zhang, "Adaptive neural network control of nonlinear systems by state and output feedback," *IEEE transactions on systems, man, and cybernetics. Part B, Cybernetics : a publication of the IEEE Systems, Man, and Cybernetics Society*, vol. 29, no. 6, pp. 818–28, Jan. 1999.

[64] Jin Sung Kim, Jonghyun Jeon, and Hoon Heo, "Design of adaptive PID for pitch control of large wind turbine generator," in *Control And Instrumentation*, 2011, number 1.

[65] M. Sedighizadeh and M. Kalantar, "Adaptive PID control of wind energy conversion systems using wavenets," in *39th International Universities Power Engineering Conference*, 2004, number 1, pp. 299–303.

[66] Jimo Park, Goeun Kim, Jinsung Kim, Sanggun Na, and Hoon Heo, "Simulation of reverse osmosis plant using RCGA based PID controller," in *ICROS-SICE International Joint Conference 2009*, 2009, vol. 1000, pp. 2972–2976.

[67] Zuoxia Xing, Qinwei Li, Xianbin Su, and Hengyi Guo, "Application of BP Neural Network for Wind Turbines," in *Second International Conference on Intelligent Computation Technology and Automation*, 2009, pp. 42–44.

[68] J.T. Guan, *The control technology of mechanical, electrical and hydraulic*, Tongji University Press, Shanghai, 2003.

[69] B. Boukhezzar and H. Siguerdidjane, "Nonlinear control of variable speed wind turbines for power regulation," in *Proceedings of 2005 IEEE Conference on Control Applications, 2005. CCA 2005.*, 2005, number 2, pp. 114–119.

[70] C. Pournaras, A. Soldatos S. Papathanassiou, and A. Kladas, "Robust controller for Variable Speed Stall Regulated Wind Turbines," pp. 7–12.

[71] C. L. Bottasso, A. Croce, and B. Savini, "Performance comparison of control schemes for variable-speed wind turbines," *Journal of Physics: Conference Series*, vol. 75, pp. 012079, July 2007.

[72] H. J. Ferreau, G. Lorini, and M. Diehl, "Fast Nonlinear Model Predictive Control of Gasoline Engines," in *October*, 2006, number 4, pp. 2754–2759.

[73] D.Q Dang, Y. Wang, and W. Cai, "Nonlinear Model Predictive control (NMPC) of fixed pitch variable speed wind turbine," *2008 IEEE International Conference on Sustainable Energy Technologies*, vol. 2, no. 2, pp. 29–33, Nov. 2008.

[74] P. Borne, G. Dauphin-Tanguy, J. P. Richard, F. Rotella, and I. Zambettakia, "Commande et Optimization des Processuers," in *Technip*, 1990.

[75] Nadhira Khezami, Xavier Guillaud, and Naceur Benhadj Braiek, "Multimodel LQ controller design for variable speed and variable pitch wind turbines at high wind speeds," in *6th International Multi-Conference on systems, Signals and Devices*, 2009, number 2, pp. 6–11.

[76] Z. Kardous, N.Benhadj Braeik, and A. Al Kamel, "On the multimodel stabilization control of uncertain systems Part 2," *International Journal of Problems of Non-Linear Analysis in Engineering Systems*, vol. 13, no. 1, pp. 76–87, 2007.

[77] Z. Kardous, N. Benhadj Braiek, and A. Al Kamel, "On the multimodel stabilization control of uncertain systems Part 1," *International Scientific IFNA-ANS Journal: Problems on Nonlinear Analysis in Engineering Systems*, vol. 12, pp. 60–71, 2006.

[78] J.G Slootweg, H. Polinder, and W.L Kling, "Dynamic Modelling of a Wind Turbine with Doubly Fed Induction Generator," pp. 644–649, 2001.

[79] Libao Shi, Zheng Xu, Jin Hao, and Yixin Ni, "Modelling Analysis of Transient Penetration of Grid-connected Wind Farms of DFIG Type," *Wind Energy*, vol. 10, pp. 303–320, 2007.

[80] Istvan Erlich, Jörg Kretschmann, Jens Fortmann, Stephan Mueller-Engelhardt, and Holger Wrede, "Modeling of Wind Turbines Based on Doubly-Fed Induction Generators for Power System Stability Studies," *IEEE Transactions on Power Systems*, vol. 22, no. 3, pp. 909–919, 2007.

[81] F. Mei and B. Pal, "Modal Analysis of Grid-Connected Doubly Fed Induction Generators," *IEEE Transactions on Power Systems*, vol. 22, no. 3, pp. 728–736, 2007.

[82] F. Wu, X. Zhang, K. Godfrey, and P. Ju, "Small signal stability analysis and optimal control of a wind turbine with doubly fed induction generator," *IET Genration, Transmission, Distribution*, vol. 1, no. 5, pp. 751–760, 2007.

[83] J.G. Slootweg and W.L. Kling, "The impact of large scale wind power generation on power system oscillations," *Electric Power System Research*, vol. 67, no. 1, pp. 9–20, 2003.

[84] R Pena, J.C. Clare, and G.M. Asher, "Doubly fed induction generator using back-to-back PWM converters and its application to variable-speed wind-energy

generation," *IEE Proceedings - Electric Power Applications*, vol. 143, no. 3, pp. 231, 1996.

[85] Wei Qiao, Xiang Gong, and Liyan Qu, "Output Maximization Control for DFIG Wind Turbines without Using Wind and Shaft Speed Measurements," in *IEEE Energy Conversion Congress and Exposition*, 2009, pp. 404–410.

[86] Arantxa Tapia, Gerardo Tapia, and J. Xabier Ostolaza, "Modeling and Control of a Wind Turbine Driven Doubly Fed Induction Generator," *IEEE Transactions on Energy Conversion*, vol. 18, no. 2, pp. 194–204, 2003.

[87] P. C. Krause, O. Wasynczuk, and S. D. Sudhoff, *Analysis of Electric Machinery and Drive Systems*, IEEE press, 2002.

[88] S. R. Spea, A. A. Abou El Ela, and M. A. Abido, "Multi-objective differential evolution algorithm for environmental-economic power dispatch problem," *2010 IEEE International Energy Conference*, pp. 841–846, Dec. 2010.

[89] M A Abido and N.A Al-Ali, "Multi-Objective Differential Evolution for Optimal Power Flow," in *International Conference on Power Engineering, Energy and Electrical Drives, POWERENG*, 2009, pp. 101–106.

[90] A. H. Al-Mohammad, M.A. Abido, and M.M. Mansour, "Optimal PMU Placement for Power System Observability Using Differential Evolution," in *11th International Conference on Intelligent Systems Design and Applications (ISDA)*, 2011, pp. 277–282.

[91] B. Widrow and M.a. Lehr, "30 years of adaptive neural networks: perceptron, Madaline, and backpropagation," *Proceedings of the IEEE*, vol. 78, no. 9, pp. 1415–1442, 1990.

List of Publications

- S.A. Raza & A.H.M.A. Rahim, "Smart Pitch Control Strategy for Wind Generation System Using Differential Evolution and Neural Network", *International Conference on Power and Energy System,* ICPES, Hong Kong, 2012.

Vita

- Syed Ahmed Raza
- Pakistani
- Born on 1^{st} July 1986 in Islamabad.
- Permanent Address: H.No. 1062, St. 6, I-10/2, Islamabad
- Contact: +923326809686, +966547524290
- Received Bachelors in Electrical Engineering degree from National University of Science and Technology, School of Electrical Enginnering and Computer Sciences (NUST-SEECS) in 2009.
- Recepient of Rector's Gold Medal for best overall final year project in bachelors program.
- Joined masters program in King Fahd University of Petroleum and Minerals, Electrical Department in Feb'2010.
- Email: ah_raza@hotmail.com